SIMPLE ASTRODYNAMICS
for
SPACECRAFT ATTITUDE CONTROL ENGINEERS

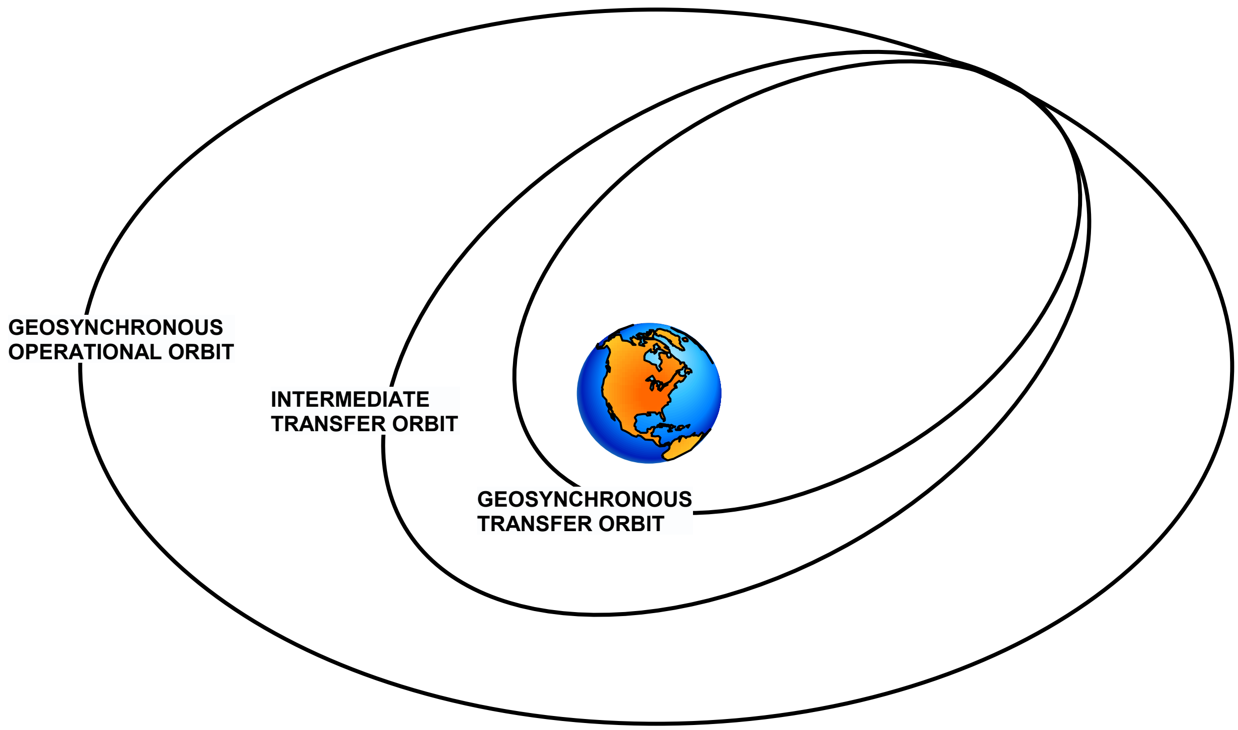

John Smay
January 17, 1995

Table of Contents

Simple Astrodynamics for Spacecraft Attitude Control Engineers

1.0 Classical Keplerian Orbital Element Definitions

The position over time of body in orbit about a central body is described by six independent variables such as position and velocity $\mathbf{x}(t)$, $\dot{\mathbf{x}}(t)$ at a given time. There are numerous equivalent sets. What is known as the classical orbital elements (a, e, i, Ω, ω, M) relate conveniently to the inertial orientation and geometric shape of the orbit. These are defined by;

a = semimajor axis = $(r_p + r_a)/2 = r_p r_a/p = p/(1 - e^2)$

e = eccentricity = $(r_a - r_p)/(r_a + r_p) = 1 - r_p/a = r_a/a - 1$

i = inclination

Ω = longitude of ascending node

ω = argument of perigee

$M = (2\pi/P)(t - T)$ = mean anomaly

Rather than M, we shall deal with true anomaly v, which is equivalent to M through eccentric anomaly E and Keplers Equation, i.e.,

$$M = E - e\sin E \tag{1.1}$$

$$\sin E = [\sqrt{1 - e^2}\sin v]/[1 + e\cos v]; \;\; \cos E = [\cos v + e]/[1 + e\cos v] \tag{1.2a}$$

$$\tan v = [\sqrt{1 - e^2}\sin E]/[\cos E - e] \tag{1.2b}$$

Figures l.1, reconstructed from Ref. 1, show the orbital elements. Inclination and eccentricity are frequently treated as vectors directed from the central body to the ascending node and perigee respectively with the conventional definitions

$$\mathbf{i} = \mathbf{e}_i^T i[\cos\Omega, \sin\Omega, 0]^T = \mathbf{e}_o^T i[1, 0, 0]^T \;, \tag{1.3}$$

and

$$\mathbf{e} = \mathbf{e}_o^T e[\cos\omega, \sin\omega, 0]^T = \mathbf{e}_1^T e[1, 0, 0]^T \;, \tag{1.4}$$

where the vector bases $\mathbf{e}_i$, $\mathbf{e}_o$, and $\mathbf{e}_1$ are specifically described below.

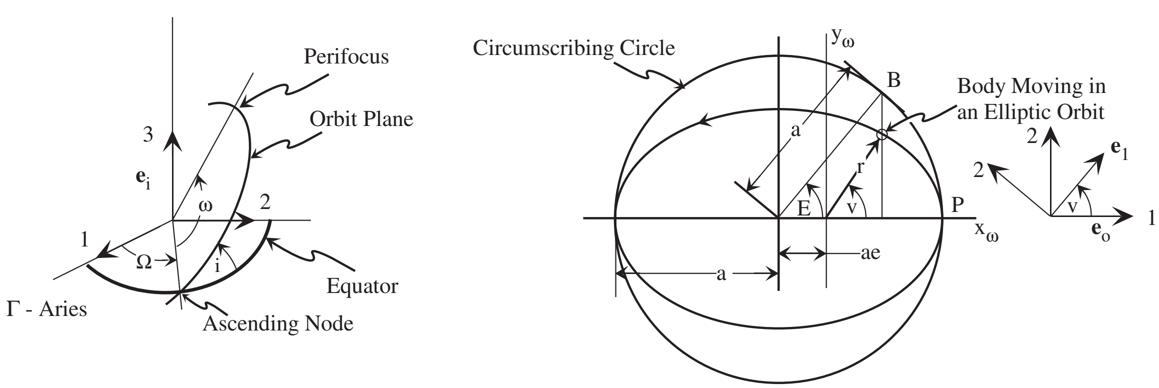

Figure 1.1 Definition of Orbital Elements and Related Parameters.

2.0 Coordinate Definitions

Orthogonal Vector Bases and Rotation Matrices

In this section we describe the vector notation used in this document and define a number of standard vector bases. We shall attempt to consistently use these throughout the following sections. We denote a gibbsian vector basis 'a' by the symbol $\mathbf{e}_a$ and, in the style of Likens, a vector having scalar components $v = [v_1, v_2, v_3]^T$ is written

$$\mathbf{v} = \mathbf{e}_a^T v = \mathbf{e}_a^T [v_1, v_2, v_3]^T \; . \tag{2.1}$$

The following rotation matrices define the symbols $A_i(\,)$ and are correct for transformation of vector scalar components *from* an initial coordinate system, say $\mathbf{e}_a$ *to* a second system $\mathbf{e}_b$ displaced by a positive right handed rotation about the i-axis.

$$A_1(\xi_1) = \begin{bmatrix} 1 & 0 & 0 \\ 0 & \cos\xi_1 & \sin\xi_1 \\ 0 & -\sin\xi_1 & \cos\xi_1 \end{bmatrix};\; A_2(\xi_2) = \begin{bmatrix} \cos\xi_2 & 0 & -\sin\xi_2 \\ 0 & 1 & 0 \\ \sin\xi_2 & 0 & \cos\xi_2 \end{bmatrix};\; A_3(\xi_3) = \begin{bmatrix} \cos\xi_3 & \sin\xi_3 & 0 \\ -\sin\xi_3 & \cos\xi_3 & 0 \\ 0 & 0 & 1 \end{bmatrix}. \tag{2.2}$$

Hence we write

$$\mathbf{e}_b = A_i(\xi_i)\mathbf{e}_a \;;\; \mathbf{e}_b^T = [A_i(\xi_i)\mathbf{e}_a]^T = \mathbf{e}_a^T A_i(\xi_i)^T = \mathbf{e}_a^T A_i(\xi_i)^{-1} = \mathbf{e}_a^T A_i(-\xi_i)\;, \tag{2.3}$$

and transform the components of $\mathbf{v}$ from $\mathbf{e}_a$ to $\mathbf{e}_b$ as

$$\mathbf{v} = \mathbf{e}_a^T v = [A_i(\xi_i)\mathbf{e}_b]^T v = \mathbf{e}_b^T A_i(\xi_i)^T v = \mathbf{e}_b^T A_i(\xi_i)^{-1} v = \mathbf{e}_b^T A_i(-\xi_i) v \; . \tag{2.4}$$

With these conventions coordinate system accounting and transformation becomes a simple application of the recipe.

2.1 *Inertial - Heliocentric and Earth Centered Inertial*

First let $\mathbf{e}_h$ denote an inertial ecliptic (heliocentric) vector basis with 3-axis North and normal to the ecliptic, 1-axis directed from the Sun toward Aries, i.e., Earth to Sun at the vernal equinox. We denote the obliquity of the ecliptic as $\phi_h = -23.44384^o$ and the Earth-centered-inertial (ECI) basis $\mathbf{e}_i$ is

$$\mathbf{e}_i = A_1(\phi_h)\mathbf{e}_h \; . \tag{2.5}$$

2.2 *Earth Fixed - Equatorial*

An earth fixed basis $\mathbf{e}_e$ with 3-axis north is defined as

$$\mathbf{e}_e = A_3(\theta_g(t))\mathbf{e}_i = A_3(\Omega_e t - \lambda)\mathbf{e}_i \tag{2.6a}$$

where $\theta_g(t)$, the sidereal time, is the right ascension of the Greenwich meridian from Aries.

Earth Fixed - Local Horizontal

Denote east longitude and north latitude of the local point by λ, γ respectively. Then a local horizontal basis with 1-axis vertical, 3-axis local horizontal north, and is determined as

$$\mathbf{e}_{lh} = A_2(-\gamma)A_3(\lambda)\mathbf{e}_e = A_2(-\gamma)A_3(\lambda + \theta_g(t))\mathbf{e}_i \; . \tag{2.6b}$$

2.3 *Orbit Coordinates* [1]

Next, an orbital basis for an earth orbiting body, $\mathbf{e}_o$ is defined with 3-axis North and 1-axis earth directed from the perigee of the orbit. This basis is sequentially rotated through longitude of the ascending node Ω, inclination i, and argument of perigee ω, respectively about the 3, 1, and 3-axes from $\mathbf{e}_i$ as

$$\mathbf{e}_o = A_3(\omega)A_1(i)A_3(\Omega)\mathbf{e}_i \; . \tag{2.7}$$

Finally, a vector basis $\mathbf{e}_1$ with 3-axis North and 1-axis directed from the orbiting body to the earth is defined using the true anomaly angle, v, as

$$\mathbf{e}_1 = A_3(v)\mathbf{e}_o = A_3(v)A_3(\omega)A_1(i)A_3(\Omega)\mathbf{e}_i = A_3(v)A_3(\omega)A_1(i)A_3(\Omega)A_3^T(\theta_g(t))\mathbf{e}_e \tag{2.8a}$$

$$= \begin{bmatrix} \cos(v+\omega)\cos(\Omega-\theta_g) - \sin(v+\omega)\cos i\sin(\Omega-\theta_g) & \cos(v+\omega)\sin(\Omega-\theta_g) + \sin(v+\omega)\cos i\cos(\Omega-\theta_g) & \sin(v+\omega)\sin i \\ -\sin(v+\omega)\cos(\Omega-\theta_g) - \cos(v+\omega)\cos i\sin(\Omega-\theta_g) & -\sin(v+\omega)\sin(\Omega-\theta_g) + \cos(v+\omega)\cos i\cos(\Omega-\theta_g) & \cos(v+\omega)\sin i \\ \sin i\sin(\Omega-\theta_g) & -\sin i\cos(\Omega-\theta_g) & \cos i \end{bmatrix}\mathbf{e}_e \; .$$

For geosynchronous orbits, $\omega = 0$, $v = \Omega_e t = \theta_g - \Omega$, and

$$\mathbf{e}_1 \rightarrow A_3(\Omega_e t) A_1(i) A_3^T(\Omega_e t)\mathbf{e}_e \tag{2.8b}$$

$$= \begin{bmatrix} \cos(\Omega_e t)\cos(\Omega_e t) + \sin(\Omega_e t)\cos i \sin(\Omega_e t) & -\cos(\Omega_e t)\sin(\Omega_e t) + \sin(\Omega_e t)\cos i \cos(\Omega_e t) & \sin(\Omega_e t)\sin i \\ -\sin(\Omega_e t)\cos(\Omega_e t) + \cos(\Omega_e t)\cos i \sin(\Omega_e t) & \sin(\Omega_e t)\sin(\Omega_e t) + \cos(\Omega_e t)\cos i \cos(\Omega_e t) & \cos(\Omega_e t)\sin i \\ -\sin i \sin(\Omega_e t) & -\sin i \cos(\Omega_e t) & \cos i \end{bmatrix} \mathbf{e}_e$$

$$= \begin{bmatrix} 1 - \sin^2(\Omega_e t)(1 - \cos i) & -\sin(\Omega_e t)\cos(\Omega_e t)(1 - \cos i) & \sin(\Omega_e t)\sin i \\ -\sin(\Omega_e t)\cos(\Omega_e t)(1 - \cos i) & 1 - \cos^2(\Omega_e t)(1 - \cos i) & \cos(\Omega_e t)\sin i \\ -\sin i \sin(\Omega_e t) & -\sin i \cos(\Omega_e t) & \cos i \end{bmatrix} \mathbf{e}_e \,.$$

2.4 _Right Ascension/Declination_

This system is frequently used to locate inertial directions such as stars or the direction of the spin axis of a spin stabilized spacecraft. α and δ are the right ascension and declination angles respectively and

$$\mathbf{e}_c = A_2(\delta) A_3(\alpha)\mathbf{e}_i \;;\; \text{Equatorial} \tag{2.9a}$$

$$\mathbf{e}_{\hat{c}} = A_2(\delta) A_3(\alpha)\mathbf{e}_h \;;\; \text{Ecliptic .} \tag{2.9b}$$

2.5 _Spacecraft Attitude Coordinates (Body Fixed Basis)_

Spacecraft attitude is typically expressed by the orientation of a body fixed basis $\mathbf{e}_b$ with respect to a nominal or desired attitude. The orbital basis $\mathbf{e}_1$ is a good starting reference, having 1-axis directed from earth center to the orbiting spacecraft and 3-axis North. Let $\mathbf{e}_a$ denote the nominal attitude basis. For many Hughes commercial spacecraft of the spin stabilized vintage, a nominal attitude basis with 3-axis North, 1-axis along the orbit velocity and 2-axis completing the right-handed triad directed from the spacecraft toward earth given by

$$\mathbf{e}_a = A_3(-90^o)\mathbf{e}_1 = A_s \mathbf{e}_1 = \begin{bmatrix} 0 & -1 & 0 \\ 1 & 0 & 0 \\ 0 & 0 & 1 \end{bmatrix} \mathbf{e}_1 \,. \tag{2.10}$$

For body-stabilized spacecraft the industry standard is 1-axis (roll) along the velocity vector, 2-axis (pitch) anti orbit normal (South), and 3-axis (yaw) earth directed, which has heritage with aircraft attitude coordinates. Then

$$\mathbf{e}_a = A_1(-90^o)\mathbf{e}_1 A_3(90^o)\mathbf{e}_1 = A_b \mathbf{e}_1 = \begin{bmatrix} 0 & 1 & 0 \\ 0 & 0 & -1 \\ -1 & 0 & 0 \end{bmatrix} \mathbf{e}_1 \,. \tag{2.11}$$

This represents nominal attitude and is coincident with a body fixed basis $\mathbf{e}_b$ in the absence of attitude displacements. Then we represent true attitude by a sequential displacement about yaw, ϕ_3, pitch, ϕ_2, and roll, ϕ_1 about the 3, 2, and 1-axes, as

$$\mathbf{e}_b = A_a(\phi_1, \phi_2, \phi_3)\mathbf{e}_a = A_1(\phi_1) A_2(\phi_2) A_3(\phi_3)\mathbf{e}_a = \begin{bmatrix} 1 & 0 & 0 \\ 0 & \cos\phi_1 & \sin\phi_1 \\ 0 & -\sin\phi_1 & \cos\phi_1 \end{bmatrix} \begin{bmatrix} \cos\phi_2 & 0 & -\sin\phi_2 \\ 0 & 1 & 0 \\ \sin\phi_2 & 0 & \cos\phi_2 \end{bmatrix} \begin{bmatrix} \cos\phi_3 & \sin\phi_3 & 0 \\ -\sin\phi_3 & \cos\phi_3 & 0 \\ 0 & 0 & 1 \end{bmatrix} \mathbf{e}_a$$

$$= \begin{bmatrix} \cos\phi_2 & 0 & -\sin\phi_2 \\ \sin\phi_1 \sin\phi_2 & \cos\phi_1 & \sin\phi_1 \cos\phi_2 \\ \cos\phi_1 \sin\phi_2 & -\sin\phi_1 & \cos\phi_1 \cos\phi_2 \end{bmatrix} \begin{bmatrix} \cos\phi_3 & \sin\phi_3 & 0 \\ -\sin\phi_3 & \cos\phi_3 & 0 \\ 0 & 0 & 1 \end{bmatrix} \mathbf{e}_a \tag{2.12}$$

$$= \begin{bmatrix} \cos\phi_2 \cos\phi_3 & \cos\phi_2 \sin\phi_3 & -\sin\phi_2 \\ \sin\phi_1 \sin\phi_2 \cos\phi_3 - \cos\phi_1 \sin\phi_3 & \sin\phi_1 \sin\phi_2 \sin\phi_3 + \cos\phi_1 \cos\phi_3 & \sin\phi_1 \cos\phi_2 \\ \cos\phi_1 \sin\phi_2 \cos\phi_3 + \sin\phi_1 \sin\phi_3 & \cos\phi_1 \sin\phi_2 \sin\phi_3 - \sin\phi_1 \cos\phi_3 & \cos\phi_1 \cos\phi_2 \end{bmatrix} \mathbf{e}_a$$

$$\approx \begin{bmatrix} 1 & 0 & -\phi_2 \\ 0 & 1 & \phi_1 \\ \phi_2 & -\phi_1 & 1 \end{bmatrix} \begin{bmatrix} \cos\phi_3 & \sin\phi_3 & 0 \\ -\sin\phi_3 & \cos\phi_3 & 0 \\ 0 & 0 & 1 \end{bmatrix} \mathbf{e}_a \approx \begin{bmatrix} 1 & \phi_3 & -\phi_2 \\ -\phi_3 & 1 & \phi_1 \\ \phi_2 & -\phi_1 & 1 \end{bmatrix} \mathbf{e}_a \,.$$

2.6 *Transformation From Geosynchronous Inclined to Geostationary Orbital Coordinates*

Using $\mathbf{e}_i$ the ECI basis with 1-axis at Aries and 3-axis North, an orbital basis with 1-axis anti-nadir and 3-axis North is obtained as

$$\mathbf{e}_1 = A_3(v)A_3(\omega)A_1(i)A_3(\Omega)\mathbf{e}_i \ , \tag{2.13}$$

and for an ideal geostationary orbit a like basis denoted $\hat{\mathbf{e}}_g$ is obtained as

$$\hat{\mathbf{e}}_g = A_3(v_g)A_3(\omega)A_1(i)A_3(\Omega)\mathbf{e}_i = A_3(v_g)A_3(0)A_1(0)A_3(0)\mathbf{e}_i = A_3(v_g)\mathbf{e}_i \ . \tag{2.14}$$

Hence an inclined orbit basis is related to the ideal geostationary basis as

$$\mathbf{e}_1 = A_3(v)A_3(\omega)A_1(i)A_3(\Omega)A_3^T(v_g)\hat{\mathbf{e}}_g \ . \tag{2.15}$$

For the geosynchronous case we can take $\omega = 0$, and choose a phase in the true anomaly such that $v = \Omega - v_g = \Omega_e t$. Then using 2.8a from the Sect 2.3, this evaluates to

$$\mathbf{e}_1 = A\hat{\mathbf{e}}_g = \begin{bmatrix} 1 - \sin^2(\Omega_e t)(1-\cos i) & -\sin(\Omega_e t)\cos(\Omega_e t)(1-\cos i) & \sin(\Omega_e t)\sin i \\ -\sin(\Omega_e t)\cos(\Omega_e t)(1-\cos i) & 1-\cos^2(\Omega_e t)(1-\cos i) & \cos(\Omega_e t)\sin i \\ -\sin i \sin(\Omega_e t) & -\sin i\cos(\Omega_e t) & \cos i \end{bmatrix}\hat{\mathbf{e}}_g \ . \tag{2.16}$$

A simple sketch of the coordinates systems described above will show that $\hat{\mathbf{e}}_g$ is not in the standard roll-pitch-yaw orientation we have described for $\mathbf{e}_b$ and $\mathbf{e}_g$, but rather

$$\mathbf{e}_2 = A_b\mathbf{e}_1 = A_1(-90^o)A_3(90^o)\mathbf{e}_1 = \begin{bmatrix} 1 & 0 & 0 \\ 0 & 0 & -1 \\ 0 & 1 & 0 \end{bmatrix}\begin{bmatrix} 0 & 1 & 0 \\ -1 & 0 & 0 \\ 0 & 0 & 1 \end{bmatrix}\mathbf{e}_1 = \begin{bmatrix} 0 & 1 & 0 \\ 0 & 0 & -1 \\ -1 & 0 & 0 \end{bmatrix}\mathbf{e}_1 \tag{2.17}$$

and likewise

$$\mathbf{e}_g = A_b\hat{\mathbf{e}}_g \tag{2.18}$$

which leads finally to

$$\mathbf{e}_2 = A_bAA_b^T\mathbf{e}_g = \mathbf{C}\mathbf{e}_g = \begin{bmatrix} 1-\cos^2(\Omega_e t)(1-\cos i) & -\cos(\Omega_e t)\sin i & \sin(\Omega_e t)\cos(\Omega_e t)(1-\cos i) \\ \sin i\cos(\Omega_e t) & \cos i & -\sin i\sin(\Omega_e t) \\ \sin(\Omega_e t)\cos(\Omega_e t)(1-\cos i) & \sin(\Omega_e t)\sin i & 1-\sin^2(\Omega_e t)(1-\cos i) \end{bmatrix}\mathbf{e}_g \tag{2.19}$$

where $\Omega_e t = t = 0$ at the ascending node.

2.7 *Equatorial Normal Yaw Steering Function*

In some cases yaw steering to equatorial normal is desired. Then the body basis is displaced from the orbital basis as

$$\mathbf{e}_b = A_3(\phi_3)\mathbf{e}_2 = A_3(\phi_3)\mathbf{C}\mathbf{e}_g \ . \tag{2.20}$$

Taking $\mathbf{u}_b$ as a body pitch unit vector, the yaw steering angle can be found by requiring the equatorial plane component of this to vanish in $\mathbf{e}_g$. Accordingly,

$$\mathbf{u}_b = \mathbf{e}_b^T[0,1,0]^T = \mathbf{e}_g^T C^T A_3^T(\phi_3)[0,1,0]^T \ , \tag{2.21}$$

and

$$\mathbf{u}_b \cdot \mathbf{e}_g^T[1,0,0]^T = -\sin\phi_3[1-\cos^2(\Omega_e t)(1-\cos i)] + \cos\phi_3[\sin i\cos(\Omega_e t)] = a(t)\sin\phi_3 + b(t)\cos\phi_3 = 0 \ . \tag{2.22}$$

Solving, the ideal yaw steering profile is

$$\phi_3(t) = \mathrm{Tan}^{-1}\{b(t)/a(t)\} \approx i\cos(\Omega_e t) \ \ ; \text{i small.} \tag{2.23}$$

---

[1] Though rotation matrices are useful for analytical studies, a vector based computational alternative is sometimes better for numerical studies. To rotate the scalar components r_o in basis $\mathbf{e}_o$ of $\mathbf{r} = \mathbf{e}_o^T r_o = \mathbf{e}_n^T r_n$, to the components r_n in the new basis, assume two orthogonal vectors $\mathbf{x}$ and $\mathbf{z}$ with components known in $\mathbf{e}_o$ and known to lie along two coordinate axes in $\mathbf{e}_n$ are available or can be constructed. Then create orthogonal unit vectors in the new basis as $\mathbf{u}_x = \mathbf{x}/|\mathbf{x}|$, $\mathbf{u}_z = \mathbf{z}/|\mathbf{z}|$, and $\mathbf{u}_y = \mathbf{u}_z \times \mathbf{u}_x$. Then in the new system $\mathbf{r} = \mathbf{e}_n^T[\mathbf{u}_x \cdot \mathbf{r}, \mathbf{u}_y \cdot \mathbf{r}, \mathbf{u}_z \cdot \mathbf{r}]^T$, noting the $\mathbf{u}$ are the rows of the direction cosine matrix.

2.8 *Transformation From Right Ascension-Declination to Local Horizontal Azimuth-Elevation*

We wish to express a unit vector **u** expressed in right ascension-declination coordinates in terms of azimuth (Az) and elevation (El) in local horizontal coordinates Earth fixed coordinates at longitude λ and latitude γ. Azimuth is the angle from north in the horizontal plane (about the 1-axis) and elevation is the rotation about the 2-axis, such that the 3-axis of $\mathbf{e}_{lh}$ is directed to the target. Let θ_g be sideral time and a unit vector directed to a target at right ascension α and declination δ be

$$\mathbf{u} = \mathbf{e}_c^T[1,\,0,\,0]^T = \mathbf{e}_i^T A_3^T(\alpha)A_2^T(\delta)[1,\,0,\,0]^T = \mathbf{e}_{lh}^T A_2(-\gamma)A_3^T(\alpha-\lambda-\theta_g(t))A_2^T(\delta)[1,\,0,\,0]^T \tag{2.24}$$

$$= \mathbf{e}_{lh}^T\begin{bmatrix}\cos\gamma\cos(\alpha-\lambda-\theta_g(t))\cos\delta - \sin\gamma\sin\delta \\ \sin(\alpha-\lambda-\theta_g(t))\sin\delta \\ -\sin\gamma\cos(\alpha-\lambda-\theta_g(t))\cos\delta - \cos\gamma\sin\delta\end{bmatrix} = \mathbf{e}_{lh}^T A_1^T(Az)A_2^T(El)\begin{bmatrix}0\\0\\1\end{bmatrix} = \mathbf{e}_{lh}^T\begin{bmatrix}\sin El\\ -\sin Az\cos El\\ \cos Az\cos El\end{bmatrix} = \mathbf{e}_{lh}^T\begin{bmatrix}u_1\\u_2\\u_3\end{bmatrix}.$$

Then elevation and azimuth are found as

$$\sin El = u_1\;;\;\; \cos El = \sqrt{u_2^2+u_3^2} \tag{2.25}$$

$$\sin Az = u_2/\sqrt{u_2^2+u_3^2}\;;\;\; \cos Az = u_3/\sqrt{u_2^2+u_3^2}\;.$$

2.9 *Transformation From Orbit Position and Velocity,* **r** and **v**, *to Classical Orbital Elements*

The construction of classical orbital elements from position and velocity vectors uses vector basis definitions from Sect. 2.0 and draws some from the presentation of Ref.11 page 61, though we use 21st century vector mathematics. The satellite position **r** and velocity **v** vectors are with respect to an inertial geocentric-equatorial basis such as $\mathbf{e}_i$ having 1-axis toward Aries and 3-axis north. Let $\mathbf{e}_{en}$ be an equatorial basis with 3-axis north and 1-axis aligned with the line of nodes directed toward the ascending node. Then

$$\mathbf{e}_{en} = A_3(\Omega)\mathbf{e}_i = \begin{bmatrix}\cos\Omega & \sin\Omega & 0\\ -\sin\Omega & \cos\Omega & 0\\ 0 & 0 & 1\end{bmatrix}\mathbf{e}_i\;. \tag{2.26a}$$

and an intermediate orbit plane normal basis also having 1-axis at the ascending node is

$$\mathbf{e}_{on} = A_1(i)\mathbf{e}_{en} = \begin{bmatrix}1 & 0 & 0\\ 0 & \cos i & \sin i\\ 0 & -\sin i & \cos i\end{bmatrix}\mathbf{e}_{en}\;. \tag{2.26b}$$

Define **r** and **v** in the equatorial inertial basis as

$$\mathbf{r} = \mathbf{e}_i^T[r_1, r_2, r_3]^T;\; \mathbf{v} = \mathbf{e}_i^T[v_1, v_2, v_3]^T\;, \tag{2.27}$$

and resultant momentum

$$\mathbf{h} = \mathbf{r}\times\mathbf{v} = \mathbf{e}_i^T[h_1, h_2, h_3]^T = \mathbf{e}_{en}^T[h_1\cos\Omega + h_2\sin\Omega, h_2\cos\Omega - h_1\sin\Omega, h_3]^T = \mathbf{e}_{en}^T[\bar{h}_1,\,\bar{h}_2,\,\bar{h}_3]^T \tag{2.28}$$

$$= \mathbf{e}_{on}^T[h_1\cos\Omega + h_2\sin\Omega,\,(h_2\cos\Omega - h_1\sin\Omega)\cos i + h_3\sin i,\,h_3\cos i - (h_2\cos\Omega - h_1\sin\Omega)\sin i]$$

$$= \mathbf{e}_{on}^T[\bar{h}_1, \bar{h}_2\cos i + \bar{h}_3\sin i,\,\bar{h}_3\cos i - \bar{h}_2\sin i]^T = \mathbf{e}_{on}^T[0,\,0,\,h]^T\;.$$

Noting that both **r** and **v** lie in the orbit plane, the fundamental assumption to developing classical elements form position and velocity is that momentum **h** is perpendicular to the orbit plane.

Semi-major Axis, a

The semi-major parameter, and eccentricity are adopted directly from Ref. 3, pg 20-26.

$$p = h^2/\mu = a(1-e^2)\;, \tag{2.29}$$

also noting $r_a = p/(1-e)$; $r_p = p/(1+e)$.

Orbit Eccentricity, e [3]

$$\mathbf{e} = \mathbf{v}\times\mathbf{h}/\mu - \mathbf{r}/|\mathbf{r}| = \frac{1}{\mu}\left[\left(v^2 - \frac{\mu}{r}\right)\mathbf{r} - (\mathbf{r}\cdot\mathbf{v})\mathbf{v}\right];\; e = |\mathbf{e}|\;. \tag{2.30}$$

Longitude of Ascending Node, Ω

The angle in the equatorial plane from Aries to the ascending node, Ω, is found by equating the 1-axis component on momentum in the orbit plane to zero as follows

$$0 = \bar{h}_1 = h_1 \cos\Omega + h_2 \sin\Omega \Rightarrow \frac{h_1 \cos\Omega}{\sqrt{h_1^2 + h_2^2}} + \frac{h_2 \sin\Omega}{\sqrt{h_1^2 + h_2^2}} = \sin A \cos\Omega + \cos A \sin\Omega = \sin(A + \Omega) = 0 \Rightarrow A = -\Omega \qquad (2.31a)$$

whence

$$\sin\Omega = -h_1/\sqrt{h_1^2 + h_2^2};\ \cos\Omega = h_2/\sqrt{h_1^2 + h_2^2}\ . \qquad (2.31b)$$

Orbit Inclination, i

This found by equating the 2-axis component of momentum in the orbit plane to zero, using functions of Ω from (6b)

$$0 = \bar{h}_2 \cos i + \bar{h}_3 \sin i = (h_2 \cos\Omega - h_1 \sin\Omega)\cos i + h_3 \sin i = \sqrt{h_1^2 + h_2^2}\cos i + h_3 \sin i = 0 \qquad (2.32a)$$

$$\Rightarrow \frac{\sqrt{h_1^2 + h_2^2}\cos i}{h} + \frac{h_3 \sin i}{h} = \sin A \cos i + \cos A \sin i = \sin(A + i) = 0 \Rightarrow A = -i \qquad (2.32b)$$

whence

$$\sin i = -\sqrt{h_1^2 + h_2^2}/h;\ \cos i = h_3/h\ . \qquad (2.32c)$$

Argument of Perigee, ω

The unit vector directed to the ascending node is $\mathbf{n} = \mathbf{e}_{en}^T[1, 0, 0]^T = \mathbf{e}_i^T[\cos\Omega, \sin\Omega, 0]^T$, and argument of perigee is the angle between $\mathbf{n}$ and $\mathbf{e}$, as

$$\cos\omega = [\mathbf{n}\cdot\mathbf{e}]/e = \frac{-(e_1 h_2 - e_2 h_1)}{e\sqrt{h_1^2 + h_2^2}}\ . \qquad (2.33)$$

True Anomaly, ν

True anomaly is the angle between perigee at the vector $\mathbf{e}$ and $\mathbf{r}$, thus

$$\cos\nu = [\mathbf{e}\cdot\mathbf{r}]/e|\mathbf{r}|\ . \qquad (2.34)$$

2.10 *Transformation From Classical Orbital Elements to Orbit* **r** *and* **v**

An orbital coordinate basis with 3-axis north and 1-axis directed from Earth center to perigee is denoted $\mathbf{e}_o$ and related to the Earth fixed equatorial inertial system $\mathbf{e}_i$ as

$$\mathbf{e}_o = A_3(\omega)A_1(i)A_3(\Omega)\mathbf{e}_i \Rightarrow \mathbf{e}_o^T = \mathbf{e}_i^T A_3^T(\Omega)A_1^T(i)A_3^T(\omega)\ . \qquad (2.35)$$

Instantaneous orbit radius $r = |\mathbf{r}|$ is obtained as

$$r = p/(1 + e\cos\nu) = [a(1 - e^2)]/(1 + e\cos\nu)\ . \qquad (2.36a)$$

Then

$$\mathbf{r} = \mathbf{e}_o^T r[\cos\nu, \sin\nu, 0]^T = \mathbf{e}_i^T A_3^T(\Omega)A_1^T(i)A_3^T(\omega) r[\cos\nu, \sin\nu, 0]^T\ . \qquad (2.36b)$$

The radial and tangential components of satellite orbital velocity given by Ref. 2, Eq. 3.3 and 3.4 are

$$V_R = \sqrt{\mu/p}(e\sin\nu);\ V_T = \sqrt{\mu/p}(1 + e\cos\nu) \qquad (2.37a)$$

while sequentially in the perigee directed orbital basis $\mathbf{e}_o$ and the inertial geocentric-equatorial basis $\mathbf{e}_i$,

$$\mathbf{v} = \mathbf{e}_o^T[V_R\cos\nu - V_T\sin\nu,\ V_R\sin\nu + V_T\cos\nu,\ 0]^T \qquad (2.37b)$$

$$= \mathbf{e}_i^T A_3^T(\Omega)A_1^T(i)A_3^T(\omega)[V_R\cos\nu - V_T\sin\nu,\ V_R\sin\nu + V_T\cos\nu,\ 0]^T\ .$$

[1] $\mathbf{x} = \mathbf{e}_i^T[1, 0, 0]^T$; $\mathbf{y} = \mathbf{e}_i^T[0, 1, 0]^T$; $\mathbf{z} = \mathbf{e}_i^T[0, 0, 1]^T$ and $\mathbf{h} = \mathbf{r}\times\mathbf{v}$; $\mathbf{n} = \mathbf{z}\times\mathbf{h}/|\mathbf{h}|$; where $\mathbf{h}$ is orbit normal, $\mathbf{n}$ points to ascending node, and $\mathbf{e}$ points to perigee with magnitude equal to eccentricity, all independent of satellite position in time around the orbit in the Kepler model. If $\mathbf{e} = 0$ set $\mathbf{e} = n$, or is equirotial orbit set $\mathbf{e} = \mathbf{x}$.

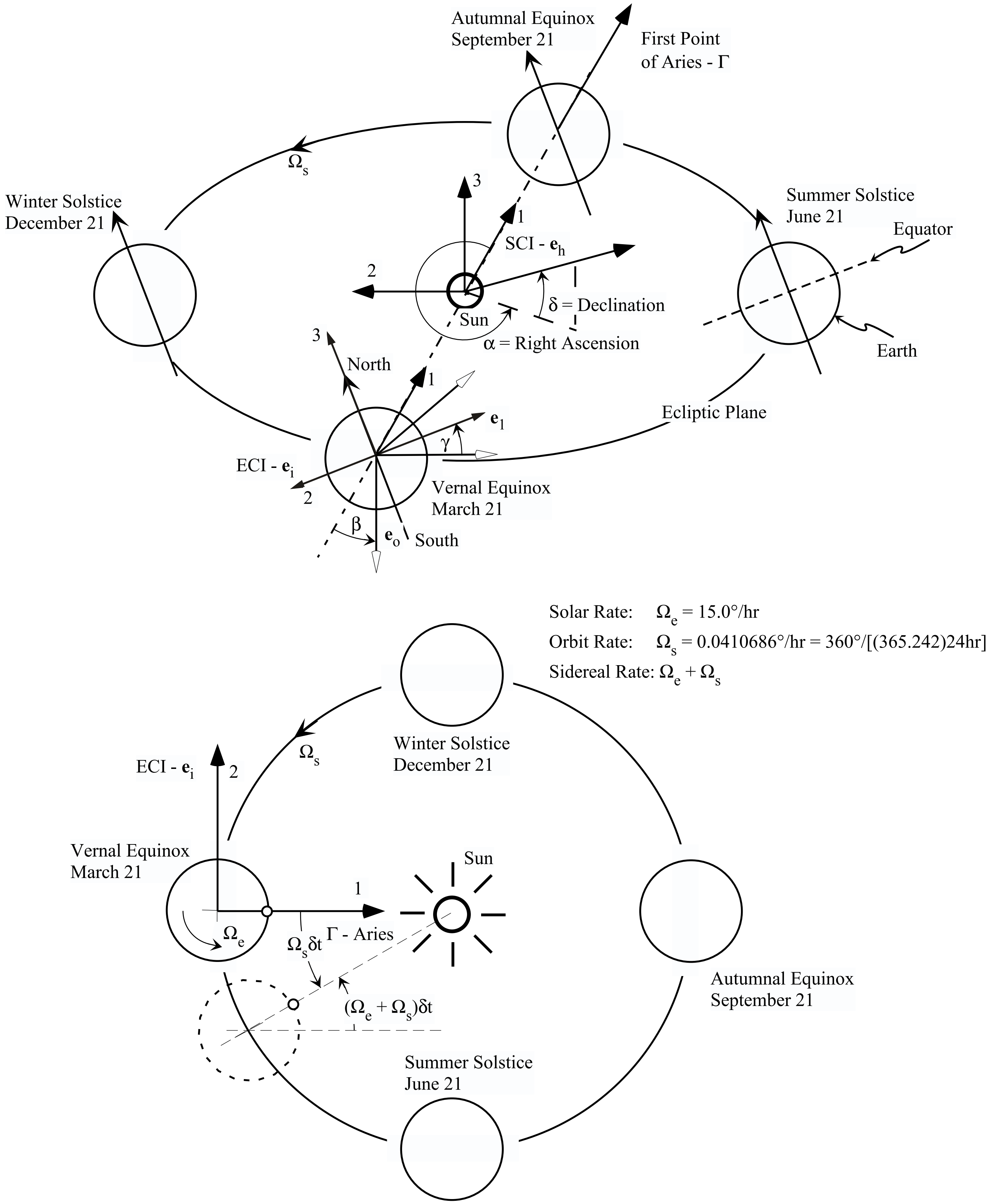

Figure 2.1 Earth-Sun Seasonal Geometry on the Ecliptic Plane.

3.0 Orbit Change Obtained From an Arbitrary Velocity Impulse

We wish to apply an impulsive velocity increment with direction, magnitude, and time or true anomaly of application arbitrary and obtain the new orbital elements. The two body solution of this problem is derived below.

3.1 In Plane ΔV

First the in plane velocity increments are treated. From Ref. 1, Eqs 3.73, 27, 264, and 265

$$p = a(1 - e^2) = r_p r_a/a;\; a = (r_p + r_a)/2 \tag{3.1}$$

$$r = p/(1 + e\cos v);\; e = 1 - r_p/a = r_a/a - 1 \tag{3.2}$$

$$\dot r = \sqrt{\mu/p}(e\sin v) = V_R \tag{3.3}$$

$$r\dot v = \sqrt{\mu/p}(1 + e\cos v) = V_T \tag{3.4}$$

where p is the semimajor parameter, r is instantaneous orbit radius, and $\dot r$, $r\dot v$, are respectively velocity components parallel and normal to r in the orbit plane. The Earth gravitational constant squared $\mu = \beta^2 r_e = [250.50(\mathrm{nm})^{3/2}/\mathrm{sec}]^2 = [631.35(\mathrm{km})^{3/2}/\mathrm{sec}]^2$. A nautical mile is 6076.11 ft(1.8520 km)[4]. Substituting p from (3.2) into (3.3) and (3.4), squaring, and rearranging the resultant two equations, and solving for e and v gives the result

$$e^2 = \xi^2 + r\dot r^2/\mu\xi + r\dot r^2/\mu = \xi^2 + rV_R^2/\mu\xi + rV_R^2/\mu \tag{3.5}$$

$$v = \mathrm{sgn}(\dot r)\mathrm{Cos}^{-1}(\xi/e) \tag{3.6}$$

where

$$\xi = (r\dot v)^2 r/\mu - 1 = (V_T)^2 r/\mu - 1\ . \tag{3.7}$$

Hence, given orbital elements a, e, and v, these can be used in (3.1) through (3.4) to get radial and normal in plane velocity increment components. These values are then altered by the in plane velocity components and used in (3.5) through (3.7) to compute new values of e and v. Eqs. 3.1 and 3.2 then give a for the new orbit. At this point we have three new orbit elements e, v, and a. The period of the orbit is given as $P = 2\pi a^{3/2}/\sqrt{\mu} = 2\pi a^{3/2}/[\beta\sqrt{r_e}]$.

Next we calculate the effect on parameters i, Ω, ω. Let $\mathbf{e}_i$ denote an inertial basis and $\mathbf{e}_o$ an orbit plane basis with 1-axis at perigee and 3-axis normal to the orbit plane. We use sub o to denote the above elements before the velocity increment is added. Then

$$\mathbf{e}_o = A_3(\omega_o)A_1(i_o)A_3(\Omega_o)\mathbf{e}_i = \begin{bmatrix} \cos\omega_o & \sin\omega_o & 0 \\ -\sin\omega_o & \cos\omega_o & 0 \\ 0 & 0 & 1 \end{bmatrix}\begin{bmatrix} 1 & 0 & 0 \\ 0 & \cos i_o & \sin i_o \\ 0 & -\sin i_o & \cos i_o \end{bmatrix} A_3(\Omega_o)\mathbf{e}_i\ . \tag{3.8}$$

Let $\mathbf{e}_1$ be a basis with 3-axis along the 3-axis of $\mathbf{e}_o$ and 1-axis directed to the orbiting body. Then

$$\mathbf{e}_1 = A_3(v_o)\mathbf{e}_o = A_3(v_o)A_3(\omega_o)A_1(i_o)A_3(\Omega_o)\mathbf{e}_i\ . \tag{3.9}$$

Now let $\mathbf{e}_2$ be the orbit plane basis for the new orbit, i.e., same as $\mathbf{e}_o$ for the old orbit. Thus,

$$\begin{aligned}\mathbf{e}_2 &= A_3(-v)\mathbf{e}_1 = A_3(-v)A_3(v_o)A_3(\omega_o)A_1(i_o)A_3(\Omega_o)\mathbf{e}_i \\ &= A_3(\omega_o + v_o - v)A_1(i_o)A_3(\Omega_o)\mathbf{e}_i = A_3(\omega)A_1(i)A_3(\Omega)\mathbf{e}_i\ .\end{aligned} \tag{3.10}$$

Evaluating the last two forms in (3.10) yields a new argument of perigee of

$$\omega = \omega_o - (v - v_o)\ , \tag{3.11}$$

while longitude of the ascending node and inclination are unchanged.

3.1.1 *Small In Plane Velocity Impulses*

For a circular orbit $e = \xi = 0$ and the radial and tangential velocity at every point are respectively $V_R = 0$ and $V_T = \sqrt{\mu/p} = \sqrt{\mu/a} = \sqrt{\mu/r}$. Then, using (3.5), for a radial velocity impulse δV_R,

[3] For general reference, $r_e = 3441.7\ \mathrm{nm} = 6373.9\ \mathrm{km}$, and geosynchronous orbit radius is $r_o = 22,766.85\ \mathrm{nmi} = 42,164.17\ \mathrm{km}$. Some interesting velocities: Point on surface of Earth, $v_g = 903.5\ \mathrm{nm/hr}$, satellite in circular orbit at Earth surface, $v_{oe} = 15,357.5\ \mathrm{nm/hr} = 17v_g$, satellite in geostatonary orbit, $v_{og} = 5,972.9\ \mathrm{nm/hr}$, $\Delta V = 4,884.2\ \mathrm{nm/hr}$ to raise circular Earth radius apogee to geostationary. Earth escape velocity $v_\infty = 11.2\ \mathrm{km/sec} = 21,770.8\ \mathrm{nm/hr}$; Sun escape velocity $7.9\ \mathrm{km/sec} = 15,356\ \mathrm{nm/hr}$. For the moon: $\mu_m = [70.02(\mathrm{km})^{3/2}/\mathrm{sec}]^2$.

$$\delta e^2 = (r/\mu)\dot{r}^2 = (r/\mu)\delta V_R^2 = [\delta V_R/V_T]^2$$

and

$$v = \mathrm{sgn}(\dot{r})\mathrm{Cos}^{-1}(0) = 90^o \mathrm{sgn}(\delta V_R) \ ,$$

so the true anomaly at the maneuver location becomes $\pm 90^o$, the radius p at this point does not change, and by (3.4) we observe that the radial maneuver both raises apogee and lowers perigee.

For a tangential maneuver δV_T in the circular orbit case, noting that $\xi = 0 \Rightarrow (r/\mu) = 1/V_T^2$, and expanding $(V_T + \delta V_T)^2$ in (3.7) gives

$$\delta e = \delta\xi \approx 2\delta V_T V_T (r/\mu) = 2\delta V_T/V_T$$

and

$$v = \mathrm{Cos}^{-1}[\mathrm{sgn}(\delta V_T)] = \begin{cases} 0^o \ ; \ \delta V_T > 0 \\ 180^o \ ; \ \delta V_T < 0 \end{cases}$$

hence, this velocity increment either raises an apogee or lowers a perigee on the opposite side of the orbit. The respective circular orbit geometry effects are pictured on Figure 3.1.

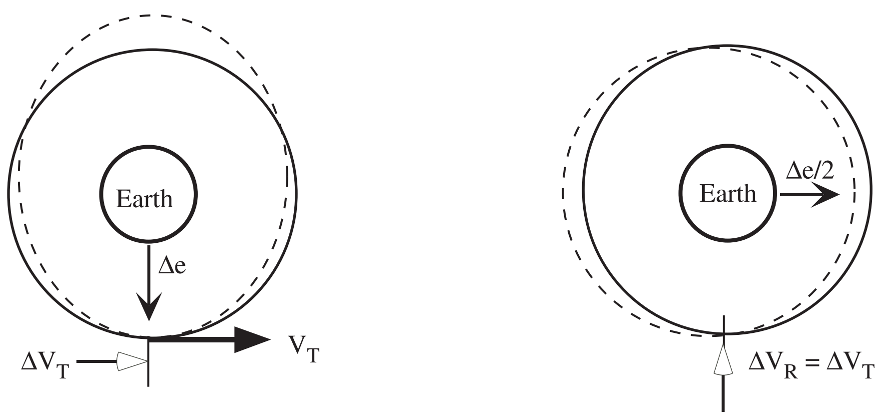

Figure 3.1 Influence of Tangential and Radial Velocity Impulse on Orbit.

For the general case

$$\xi = \xi_o + \delta\xi = \{V_T + \delta V_T\}^2 r_o/\mu - 1 \approx \xi_o + 2\delta V_T V_T r_o/\mu$$

$$\begin{aligned} e^2 &= [\xi_o + \delta\xi]^2 + \{r[V_R + \delta V_R]^2/\mu\}[\xi_o + \delta\xi] + \{r[V_R + \delta V_R]^2/\mu\} \\ &\approx \xi_o^2 + \{rV_R^2/\mu\}\xi_o + \{rV_R^2/\mu\} + 2\delta\xi\xi_o + \{2r\delta V_R V_R/\mu\}\xi_o + \{rV_R^2/\mu\}\delta\xi + \{2r\delta V_R V_R/\mu\} \\ &\approx e_o^2 + 2\delta\xi\xi_o + \{2r\delta V_R V_R/\mu\}\xi_o + \{rV_R^2/\mu\}\delta\xi + \{2r\delta V_R V_R/\mu\} \ . \\ &\approx \begin{cases} e_o^2 + 2\delta\xi\xi_o + \{rV_R^2/\mu\}\delta\xi \ ; \ \delta V_R = 0 \\ e_o^2 + \{2r\delta V_R V_R/\mu\}\xi_o + \{2r\delta V_R V_R/\mu\} \ ; \ \delta V_T = 0 \end{cases} . \end{aligned}$$

3.1.2 *Circular Orbit Raising Velocity Increments*

An initial circular orbit of radius r_o is assumed. Then we determine the velocity impulse required to raise apogee by Δr and one half orbit later to raise perigee by Δr to obtain a new circular orbit of radius $r + \Delta r$. The three orbits of the sequence are depicted on Figure 3.2. Initial velocity is (using the vis-viva equation from Ref. 1)

$$V_1 = \beta\sqrt{\mu(r_e/r_o)} \tag{3.12}$$

where $\beta = 25936$ ft/sec, $\mu \approx 1$, and $r_e = 3441.7$ nm is earth radius. Velocity on the new elliptical orbit at perigee is given as

$$V_2 = V_1\sqrt{2[1 - 1/(2 + \Delta r/r_o)]} \approx V_1[1 + \Delta r/4r_o] \Rightarrow \Delta r = \frac{r_o[(V_2/V_1)^2 - 1]}{[1 - (V_2/V_1)^2/2]} \approx 4r_o[V_2/V_1 - 1] \ . \tag{3.13}$$

This and subsequent approximations are for $\Delta r \ll r_o$. Velocity at apogee on the elliptical orbit is

$$V_3 = V_1\sqrt{2/(1 + \Delta r/r_o) - 1/(1 + \Delta r/2r_o)} \approx V_1[1 - 3\Delta r/4r_o] \,, \tag{3.14}$$

while circular orbit velocity at radius $r_o + \Delta r$ is

$$V_4 = V_1\sqrt{1/(1 + \Delta r/r_o)} \approx V_1[1 - \Delta r/2r_o] \,. \tag{3.15}$$

The resultant velocity increments are

$$\Delta V_1 = V_2 - V_1 = V_1\{\sqrt{2[1 - 1/(2 + \Delta r/r_o)]} - 1\} \approx V_1\Delta r/4r_o \tag{3.16a}$$

$$\Delta V_2 = V_4 - V_3 = V_1\{\sqrt{1/(1 + \Delta r/r_o)} - \sqrt{2/(1 + \Delta r/r_o) - 1/(1 + \Delta r/2r_o)}\} \approx \Delta V_1 \,. \tag{3.16b}$$

Orbit period is given by

$$P = 2\pi a^{3/2}/[K\sqrt{\mu}] \,, \tag{3.17}$$

where $K = 1.5016 \times 10^4 (\mathrm{nm})^{3/2}/\mathrm{min}$, and a is the semi-major axis(respectively r_o, $r_o + \Delta r/2$, and $r_o + \Delta r$).

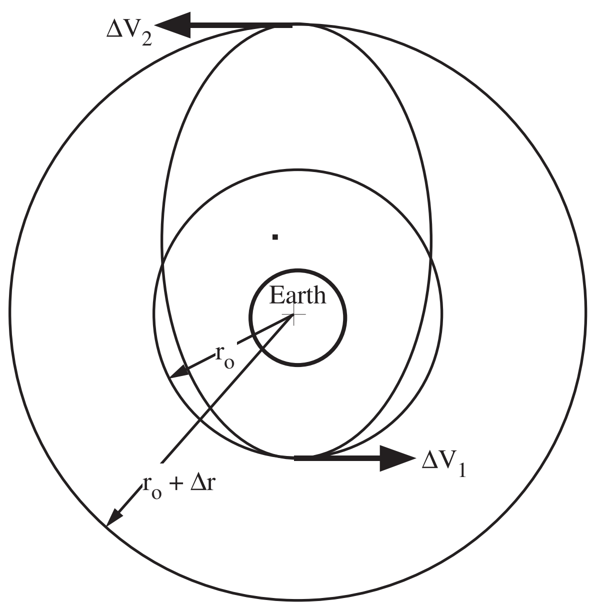

Figure 3.2 In Plane Circular Orbit Raising Geometry.

3.2 Out of Plane ΔV

Assume first that for arbitrary ΔV the in plane component has been used as detailed above to determine a new intermediate orbit due to its effect. Figure 3.3. shows the effect of the out of plane velocity increment. Note that since the velocity change is impulsive, r cannot change and it must lie in both the old and the new orbit planes. From the geometry of Figure 3.3. It is deduced that the radial normal velocity component is rotated through angle

$$\tan\xi = \Delta V/r\dot{v} \tag{3.18}$$

where $r\dot{v}$ is the radial normal velocity component after accounting for the in plane velocity change discussed in the preceding section. In addition, the normal component is lengthened from $r\dot{v}$ to $[(r\dot{v}) + \Delta V^2]$. This will alter parameters a, e, and v. Computation of the effect can be combined with the in plane effect above, but one must use the intermediate $r\dot{v}$ in (3.18).

It remains only to calculate the effect of ξ on parameters i, ω, Ω. Translating from the inertial basis $\mathbf{e}_i$ to the final orbit plane basis, denoted $\mathbf{e}_2$,

$$\mathbf{e}_2 = A_3(-v)A_1(\xi)A_3(v)A_3(\omega')A_1(i_o)A_3(\Omega_o)\mathbf{e}_i \tag{3.19}$$

$$= A_3(-v)A_1(\xi)A_3(v + \omega')A_1(i_o)A_3(\Omega_o)\mathbf{e}_i = A_3(\omega)A_1(i)A_3(\Omega)\mathbf{e}_i \,,$$

where v is the final value of true anomaly and ω' is the intermediate argument of perigee obtained by taking into

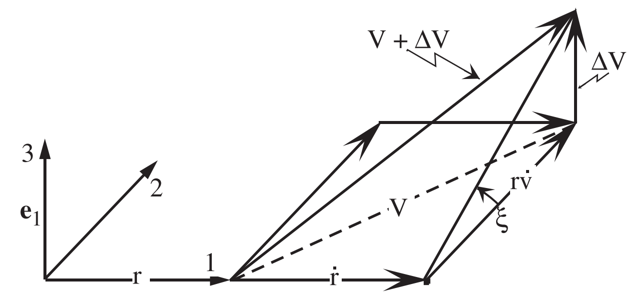

Figure 3.3 Geometry Showing Addition of Out of Plane ΔV.

account the original in plane ΔV and the radial normal velocity augmentation due to the out of plane ΔV. Equating three of the matrix elements from opposite sides of (3.19)

$$b_{33} = \cos\xi\cos i_o - \sin\xi\sin i_o\cos(v + \omega') = \cos i \tag{3.20}$$

$$b_{23} = \sin i_o[\sin v\sin(v + \omega') + \cos\xi\cos v\cos(v + \omega')] + \cos v\cos i_o\sin\xi = \sin i\cos\omega \tag{3.21}$$

$$b_{32} = \sin\xi[\sin\Omega_o\sin(v + \omega') - \cos i_o\cos\Omega_o\cos(v + \omega')] - \cos\Omega_o\sin i_o\cos\xi = -\sin i\cos\Omega\ . \tag{3.22}$$

Here b_{ij} denote elements of the matrix coefficients of (3.19). We solve respectively for i, ω, and Ω from the above three equations.

3.3 Circular Orbit Station Change Maneuvers(Rendezvous[5])

A satellite A is assumed in geostationary orbit while requiring a station change to an alternate station longitude. The situation is depicted on Figure 3.4 where the desired orbital longitude station is indicated by S_1. In the absence of a maneuver both A and S have period $P_o = (2\pi)/\Omega_o$. One approach is to increase the period of A to $P_A = P_o + \Delta\theta/\Omega_o$ by application of a positive tangential velocity ΔV. As A proceeds through the subsequent orbit, the station longitude S moves through $2\pi + \Delta\theta$ to meet A, at which point the negative velocity increment is introduced to synchronize with longitude S. Alternately, time to station can be traded off with ΔV magnitude by allowing multiple orbits to reach the station. To gain some quantitative insight, consider $\Delta\theta = 30^o$, applied to a geostationary orbit with $P_e = 2\pi/\Omega_e \approx 24$ hrs, for which we must add ≈ 2 hours to the drift over n orbits. Solving $P = 2\pi a^{3/2}/\sqrt{\mu}$, where $a = (2r_o + \Delta r)/2$,

$$\Delta r = 2[P_A\sqrt{\mu}/2\pi]^{2/3} - 2r_o = 2\{[P_e + (\Delta\theta/\Omega_e)/n]\sqrt{\mu}/2\pi\}^{2/3} - 2r_o = 2495.8\ \text{nm}\ .$$

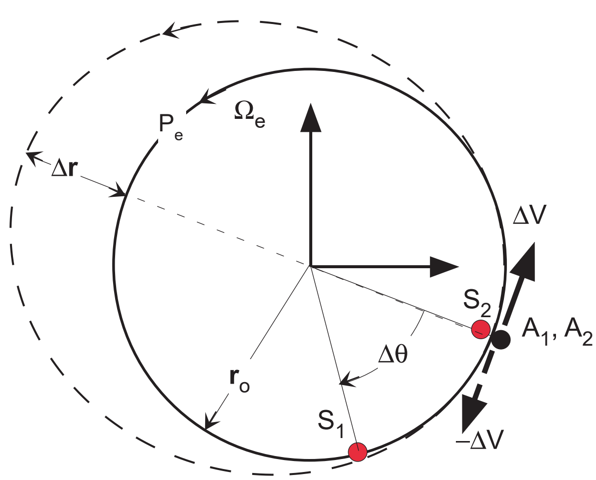

Figure 3.4. Circular Orbit Station Change Scenario with Elliptical Drift.

Then from Eq.3.13 above, using $V_1 = 10080.9$ ft/sec, and noting that an equal velocity increment is required to

[4] Rendezvous of an active approach satellite with a passive target satellite is equivalent to the station change of the active satellite to a new station in the same orbit or a new orbit. Both are just the transition of the approach satellite at a given time and true anomaly in a new orbit.

recircularize at the end of the drift period, we get $2\Delta V = 517.2$ ft/sec. This is quite a large number, of order several years of typical north-south stationkeeping velocity increment. If correct, one might like to take several days in the station change, e.g. one day added to the station change gains a year of operational time! Exploring quantitively

$$\text{Drift Time}(\Delta\theta = 30^o) = \left\{\begin{matrix} 1(P_e + 2/1) \\ 2(P_e + 2/2) \\ 3(P_e + 2/3) \\ (n/\Omega_e)[2\pi + \Delta\theta/n] \end{matrix}\right\} \text{hrs} \Rightarrow \Delta r = \left\{\begin{matrix} 2495.8 \\ 1256.2 \\ 839.4 \\ --- \end{matrix}\right\} \text{nm} \Rightarrow 2\Delta V = \left\{\begin{matrix} 517.2 \\ 268.9 \\ 181.6 \\ --- \end{matrix}\right\} \text{ft/sec} .$$

Finally, for a 1^o station change in 24 hrs and 4 min, we get $\Delta r = 84.3$ nm and $2\Delta V = 18.6$ ft/sec.

In the example the satellite A is ahead of the target longitude station. A parallel scenario applies by lowering a perigee in orbit A and drifting in the opposite direction if A is behind S_1. Also similar developments for any circular orbit. For significant drifts a Hohmann transfer to a new circular orbit might be traded against the above for time to station and propellant impulse purposes. Station changes in elliptical orbits appear more complex. In any initial orbit raising station acquisition scenario requirements for both should be considered and integrated into a mission plan.

An alternate approach is to circularize the drift orbit with two velocity impulses as illustrated on Figure 3.5, using a minimum of two orbits to effect the station change. For the two orbit case the apogee raising increment Δr is solved from

$$2[P_1/2 + P_2/2] = 2[P_e + \Delta\theta/(2\Omega_e)] = \frac{2\pi}{\sqrt{\mu}}[(r_o + \Delta r/2)^{3/2} + (r_o + \Delta r)^{3/2}] .$$

After solving this for Δr, the first apogee raising ΔV_1 and subsequent perigee raising to circularize ΔV_2 velocity increments come form Eq. 3.16a and b as ΔV_2 and ΔV_3.

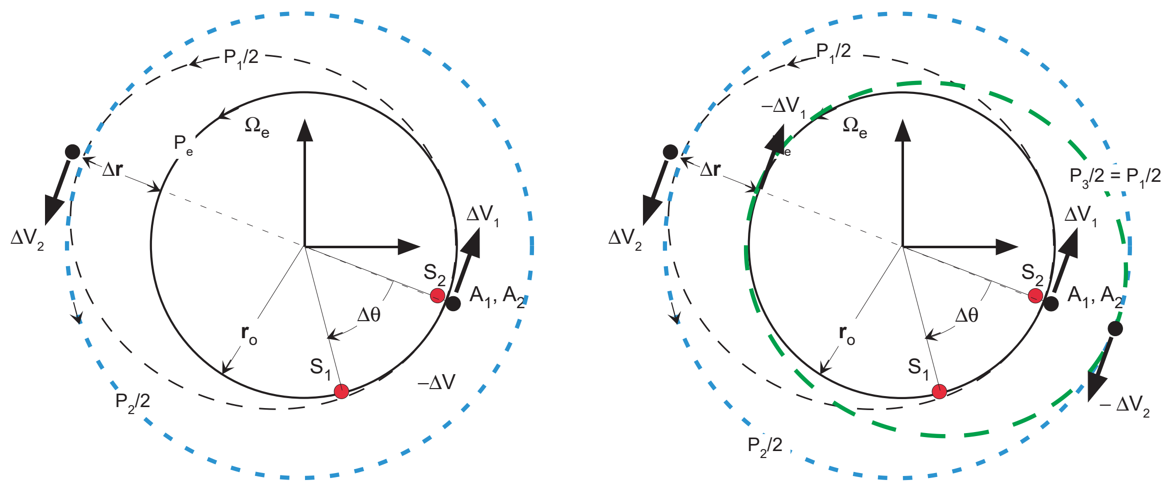

(a) $2[P_1/2 + P_2/2] = (2)2\pi/\Omega_e + \Delta\theta/\Omega_e$

(b) $2P_1/2 + P_2/2 = (3/2)2\pi/\Omega_e + \Delta\theta/\Omega_e$

Figure 3.5. Circular Orbit Station Change Scenario with Elliptical-Circular Drift.

Following through with the $\Delta\theta = 30^o$ example above, we get $\Delta r = 836.8$ nm with $\Delta V_1 = 90.6$ ft/sec, $\Delta V_2 = 89.8$ ft/sec and interm orbit periods of P_1 and P_2 1475.8 min and 1516.0 min respectively. Hence, for the two orbit 30^o station change the total velocity change is $2[\Delta V_1 + \Delta V_2] = 360.8$ ft/sec. At about 30% larger, this does not compare favorably with the two elliptical orbit change requiring 268.9 ft/sec above. For a two circular orbit 1^o station change we get 12 ft/sec, comparable to the total impulse above with a two elliptical orbit period station change.

3.4 Orbit Intersections, Constellations, and Collisions

Orbit intersection points are of frequent interest. For near impulsive orbit changes the change is made at the intersection of two orbits, usually required at a specific location and time. Rendezvous are another example. A constellation of satellites will generally involve multiple orbit intersection points. A popular constellation geometry, the Walker Constellation[6], is characterized by n equal radius circular orbit planes with m equally spaced satellites and results in n(n-1) orbit intersection points. Also collisions, or avoiding them, involves intersection of two orbits.

The instantaneous radius to a satellite is expressed, Eq. 2.36b repeated here for convenience, in Earth centered inertial basis $\mathbf{e}_i$ with classical Keplerian elements, r the instantaneous orbit radius magnitude and ν true anomaly as

$$\mathbf{r} = \mathbf{e}_o^T r[\cos\nu,\ \sin\nu,\ 0]^T = \mathbf{e}_i^T A_3^T(\Omega) A_1^T(i) A_3^T(\omega) r[\cos\nu,\ \sin\nu,\ 0]^T\ . \tag{2.36b}$$

Expanding

$$\mathbf{r} = \mathbf{e}_i^T r \begin{bmatrix} \cos\Omega & -\sin\Omega & 0 \\ \sin\Omega & \cos\Omega & 0 \\ 0 & 0 & 1 \end{bmatrix} \begin{bmatrix} 1 & 0 & 0 \\ 0 & \cos i & -\sin i \\ 0 & \sin i & \cos i \end{bmatrix} \begin{bmatrix} \cos\omega & -\sin\omega & 0 \\ \sin\omega & \cos\omega & 0 \\ 0 & 0 & 1 \end{bmatrix} \begin{bmatrix} \cos\nu \\ \sin\nu \\ 0 \end{bmatrix} = \mathbf{e}_i^T r \begin{bmatrix} \cos\Omega\cos(\omega+\nu) - \sin\Omega\cos i\sin(\omega+\nu) \\ \sin\Omega\cos(\omega+\nu) + \cos\Omega\cos i\sin(\omega+\nu) \\ \sin i\sin(\omega+\nu) \end{bmatrix}. \tag{3.23}$$

The radius can be written $r = p/(1 + e\cos\nu)$ with p the semimajor parameter $2r_a r_p/(r_a + r_p)$.

Consider two satellites in circular orbits of equal radius and longitude of ascending nodes Ω_1, Ω_2, and for $e = 0$, choose $\omega = 0$. Equating the two radii in the last form of 3.23

$$r[\cos\Omega_1\cos\nu_1 - \sin\Omega_1\cos i_1\sin\nu_1] = r[\cos\Omega_2\cos\nu_2 - \sin\Omega_2\cos i_2\sin\nu_2] \tag{3.24a}$$

$$r[\sin\Omega_1\cos\nu_1 + \cos\Omega_1\cos i_1\sin\nu_1] = r[\sin\Omega_2\cos\nu_2 + \cos\Omega_2\cos i_2\sin\nu_2] \tag{3.24b}$$

$$r\sin i_1\sin\nu_1 = r\sin i_2\sin\nu_2\ . \tag{3.24c}$$

Let

$$\cos A_1 = \frac{\cos\Omega_1}{\sqrt{\sin^2\Omega_1\cos^2 i_1 + \cos^2\Omega_1}} = \frac{\cos\Omega_1}{D_1}\ ;\ \sin A_1 = \frac{\sin\Omega_1\cos i_1}{D_1}\ ‘$$

$$\cos B_1 = \frac{\sin\Omega_1}{\sqrt{\cos^2\Omega_1\cos^2 i_1 + \sin^2\Omega_1}} = \frac{\sin\Omega_1}{E_1}\ ;\ \sin B_1 = \frac{\cos\Omega_1\cos i_1}{E_1}\ ‘$$

and similarly define A_2, D_2, B_2, E_2, all of the upper case quantities known, such that 3.24a, b becomes

$$D_1[\cos A_1\cos\nu_1 - \sin A_1\sin\nu_1] = D_1\cos(A_1+\nu_1) = D_2\cos(A_2+\nu_2) \tag{3.25a}$$

$$E_1[\cos B_1\cos\nu_1 + \sin B_1\sin\nu_1] = E_1\cos(B_1-\nu_1) = E_2\cos(B_2-\nu_2) \tag{3.25b}$$

$$\nu_1 = \mathrm{Cos}^{-1}\{(D_2/D_1)\cos(A_2+\nu_2)\} - A_1 \tag{3.26a}$$

$$\nu_1 = -\mathrm{Cos}^{-1}\{(E_2/E_1)\cos(B_2-\nu_2)\} + B_1 \tag{3.26b}$$

subtracting, the orbit #2 true anomaly at the intersection is the solution of

$$f(\nu_2) = \mathrm{Cos}^{-1}\{(D_2/D_1)\cos(A_2+\nu_2)\} + \mathrm{Cos}^{-1}\{(E_2/E_1)\cos(B_2-\nu_2)\} - (A_1+B_1) = 0\ ,$$

and from 3.24c

$$\sin\nu_1 = (\sin i_2/\sin i_1)\sin\nu_2 = \sin\{\mathrm{Cos}^{-1}\{(D_2/D_1)\cos(A_2+\nu_2)\} - A_1\}$$

This transcendental equation is some effort, involving tedious resolving square root sign, and trigonometric function angle ambiguities to match a solution. Hence, we save it and move on to the later recognized vector solution following. Further, this applies to the limited case of circular orbits only.

Orbit Intersection - Another Approach

Consider the orbit momentum vector $\mathbf{h} = \mathbf{r}\times\mathbf{v}$, a vector normal to the orbit plane at all times. The cross product of momentum vectors of two orbits defines a vector normal to both, hence, in both orbit planes along unit vector $\mathbf{u}$. For equal radius $\mathbf{r}$ circular orbits, known to intersect, that intersection must be along unit vector $\mathbf{u}$ as

$$\mathbf{r} = |\mathbf{r}|\frac{\mathbf{h}_1\times\mathbf{h}_2}{|\mathbf{h}_1\times\mathbf{h}_2|} = |\mathbf{r}|\frac{(\mathbf{r}_1\times\mathbf{v}_1)\times(\mathbf{r}_2\times\mathbf{v}_2)}{|(\mathbf{r}_1\times\mathbf{v}_1)\times(\mathbf{r}_2\times\mathbf{v}_2)|} = |\mathbf{r}|\mathbf{u}\ . \tag{3.27}$$

For more general orbits the common radius of intersection must still be found. As the direction of $\mathbf{h}$ is constant in time, any $\mathbf{r}$ and $\mathbf{v}$ suffices to compute $\mathbf{u}$, but for general orbits $\mathbf{r}_1(t) = \mathbf{r}_2(t)$ must be found.

[5] J. G. Walker, Satellite Constellations," *Journal of the British Interplanetary Society*, vol 37, pp. 559-572, 1984.

Expanding from Ref. 2, Eq. 3.36 and 2.37

$$\mathbf{h} = \mathbf{r}\times\mathbf{v} = \mathbf{e}_o^T\begin{bmatrix} r\cos\nu \\ r\sin\nu \\ 0 \end{bmatrix}\times\mathbf{e}_o^T\begin{bmatrix} V_R\cos\nu - V_T\sin\nu \\ V_R\sin\nu + V_T\cos\nu \\ 0 \end{bmatrix} = rV_T\mathbf{e}_o^T\begin{bmatrix} 0 \\ 0 \\ 1 \end{bmatrix} = \sqrt{\mu a(1-e^2)}\mathbf{e}_o^T\begin{bmatrix} 0 \\ 0 \\ 1 \end{bmatrix}. \tag{3.28}$$

This basis, $\mathbf{e}_o$, is the basis of the applicable orbit, so transforming to the inertial frame $\mathbf{e}_i$ for two respective orbits with the rotations of Eq. 1 above

$$\mathbf{u} = \frac{\mathbf{h}_1\times\mathbf{h}_2}{|\mathbf{h}_1\times\mathbf{h}_2|} = \mathbf{e}_i^T\begin{bmatrix} \sin\Omega_1\sin i_1 \\ -\cos\Omega_1\sin i_1 \\ \cos i_1 \end{bmatrix}\times\mathbf{e}_i^T\begin{bmatrix} \sin\Omega_2\sin i_2 \\ -\cos\Omega_2\sin i_2 \\ \cos i_2 \end{bmatrix} = \mathbf{e}_i^T\begin{bmatrix} \cos\Omega_2\sin i_2\cos i_1 - \cos\Omega_1\sin i_1\cos i_2 \\ \sin\Omega_2\sin i_2\cos i_1 - \sin\Omega_1\sin i_1\cos i_2 \\ \sin(\Omega_2-\Omega_1)\sin i_1\sin i_2 \end{bmatrix}. \tag{3.29}$$

To compute the true anomaly of intersect for orbit #1 of a pair compute

$$|\mathbf{r}_1(\nu)\times u| = |\mathbf{r}_1(\nu)|\sin\theta \tag{3.30}$$

with $\theta = \delta\nu = \nu - \nu_i$, where ν_i is the true anomaly that places $\mathbf{r}_1(\nu_i)$ at $\mathbf{u}$ on the line common to the two orbit planes where an intresection may occur. Repeating the calculation for orbit #2, its radius must equal that of #1 for an intersection. Sometimes there will be intersections in both positive and negative directions along $\mathbf{u}$. Intersections manifest in several varieties:

1) Orbits in the same plane have 0, or 2 intersections and $\mathbf{h}_1\times\mathbf{h}_2 = 0$ so intersections must be found by another means. Perhaps by numerical over the two true anomaly variables to find equal radai. Eq. 3.25 above.
2) Circular orbits pairs in different planes have 0 or 2 intersections, the latter if and only if they are same radius.
3) General orbit pairs other than 1) above may have 0, 1, or 2 intersections.
4) Real orbit intersection points may migrate or vanish over time with disturbances applied. Thus to search for rendezvous or collisions it is probably nesessary to perform a time simulation with disturbances models included.

Consider further the same plane case of 1) above. We assert without proof that $\mathbf{h}_1\times\mathbf{h}_2 = 0$ requires that $\Omega_1 = \Omega_2 = i_1 = i_2$, and all taken zero will not alter the solution. In this case we can both generalize and simplify Eq. 3.24 to

$$r_1(\nu_1)\cos(\omega_1+\nu_1) = \left[\frac{p_1}{(1+e_1\cos\nu_1)}\right]\cos(\omega_1+\nu_1) = r_2(\nu_2)\cos(\omega_2+\nu_2) = \left[\frac{p_2}{(1+e_2\cos\nu_2)}\right]\cos(\omega_2+\nu_2) \tag{3.31a}$$

$$r_1(\nu_1)\sin(\omega_1+\nu_1) = \left[\frac{p_1}{(1+e_1\cos\nu_1)}\right]\sin(\omega_1+\nu_1) = r_2(\nu_2)\sin(\omega_2+\nu_2) = \left[\frac{p_2}{(1+e_2\cos\nu_2)}\right]\sin(\omega_2+\nu_2)\ . \tag{3.31b}$$

We suggest a small value of i_2 may yield an initial guess for a numerical solution, still to be confirmed.

4.0 Transformation From Classical Elements (i, Ω, ω, T) to Longitude Latitude Coordinates

Let $\mathbf{e}_i$ be an ECI inertial basis with 1-axis earth-to-sun pointed at the vernal equinox and 3-axis north and let $\mathbf{e}_a$ be this basis rotated about the 3-axis such that its 1-axis is at the ascending node. Let $\mathbf{e}_1$ be the orbit normal basis with 1-axis along the orbit radius and 3-axis orbit normal, and finally let $\mathbf{e}_2$ be $\mathbf{e}_a$ rotated in longitude λ and latitude δ such that $\mathbf{e}_1$, $\mathbf{e}_2$ have the same local vertical 1-axis and the 3-axis of $\mathbf{e}_2$ is north. Both $\mathbf{e}_1$, $\mathbf{e}_2$ have 2-3 planes local horizontal. We denote the satellite right ascension as $\alpha = \Omega + \lambda$. Then the following transformations obtain.

$$\mathbf{e}_a = A_3(\Omega)\mathbf{e}_i \tag{4.1}$$

$$\mathbf{e}_1 = A_3(\omega + v)A_1(i)\mathbf{e}_a \tag{4.2}$$

$$\mathbf{e}_2 = A_2(-\delta)A_3(\lambda)\mathbf{e}_a \;. \tag{4.3}$$

To relate longitude and latitude to classical angles we observe that a unit vector along the l-axis of both $\mathbf{e}_1$ and $\mathbf{e}_2$ is identical, i.e., $\mathbf{e}_1^T[1, 0, 0]^T = \mathbf{e}_2^T[1, 0, 0]^T$. Transforming this vector to $\mathbf{e}_a$ using both (4.2) and (4.3) and equating terms yields,

$$\sin\lambda = \sin(\alpha - \Omega) = \sin(\omega + v)\cos i/\cos\delta = \tan\delta/\tan i \tag{4.4a}$$

$$\cos\lambda = \cos(\alpha - \Omega) = \cos(\omega + v)/\cos\delta \tag{4.4b}$$

$$\sin\delta = \sin(\omega + v)\sin i \;. \tag{4.5}$$

These results are obtained on page 1-5 of Ref. 2. For the singular case of $i = 0$, $\delta = 0$, and $\lambda = \omega + v$. Note that λ here is the satellite longitude with respect to the ascending node rather than the Greenwich meridian. To fix both the ascending node and the satellite with respect to the earth, the sidereal time θ_g (angle from Aries to the Greenwich meridian) must be given. The earth sidereal rate is $\Omega_e = 7.2921159 \times 10^{-5}$ rad/sec, and

$$\theta_g(t) = \theta_g(T) + \Omega_e(t - T) \;, \tag{4.6}$$

where T is some reference time. In the classical elements T is the time of perigee passage and we must then relate $(t - T)$ to true anomaly v through Kepler's Equation (1.1) and the transformation (1.2) from v to eccentric anomaly E. Thus, given T and t, or v, we can determine the remaining quantity and $\theta_g(t)$. Then the ascending node and satellite east longitudes with respect to the Greenwich meridian are respectively

$$\Omega' = \Omega - \theta_g(t) \tag{4.7}$$

$$\lambda' = \Omega + \lambda - \theta_g(t) \;. \tag{4.8}$$

Next we wish to obtain the azimuth and flight path angles β and γ as defined by Figure 4.1 and Ref. 1 p 140. The azimuth angle β is simply 90° minus the 1-axis rotational displacement between the $\mathbf{e}_1$ and $\mathbf{e}_2$ bases described above. A unit vector along the 2-axis of $\mathbf{e}_1$, in the orbit plane and normal to the radius is

$$\mathbf{u} = \mathbf{e}_1^T[0, 1, 0]^T = \mathbf{e}_2^T[0, \sin\beta, \cos\beta]^T \;. \tag{4.9}$$

Transforming $\mathbf{u}$ to $\mathbf{e}_a$ using the transforms of both (4.2) and (4.3), and equating terms gives azimuth angle as

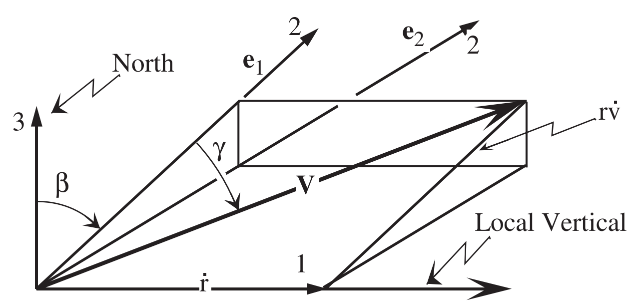

Figure 4.1 Azimuth Angle β and Flight Path Angle γ.

$$\cos\beta = \cos(\omega + v)\sin i/\cos\delta \;. \tag{4.10}$$

The flight path angle we accept as given in Refs. 1 and 2, i.e.,

$$\tan\gamma = e\sin v/(1 + e\cos v) \ . \tag{4.11}$$

Here azimuth β is the angle from north to the projection of the orbit velocity on the local horizontal. In Ref. 2 azimuth β' is differently defined as the angle from north to the total velocity vector. It is easily shown using geometry from Figure 4.1 that

$$\sin\beta' = \sqrt{\sin^2\beta\cos^2\gamma + \sin^2\gamma} \ , \tag{4.12}$$

while Ref. 2 relates β' to inclination and latitude as

$$\sin\beta' = \cos i/\cos\delta \ . \tag{4.13}$$

5.0 Sidereal Time Computation

Sidereal time is defined as the angle from Aries to the Greenwich meridian, i.e., $\mathbf{e}_e = A_3(\theta_g)\mathbf{e}_i$. The rules for computation of this angle given universal time UT or GMT[1] are here extracted from Ref. 1 without derivation. The desired angle is denoted

$$\theta_g(t) = \theta_g(T) + \Omega_e(t - T) \ , \tag{5.1}$$

where

$$\Omega_e = [1 + 1/365.24219879] \text{ revolutions/day} = 7.2921159\times10^{-5} \text{ rad/sec} = 15.0410687^o\text{/hour} \tag{5.2}$$

is the earth mean sidereal rate. Given time T = UT = GMT, one must first convert this to the Julian Day JD using Table 1.7, p. 19 (from Ref. 1) or equivalent. Because Julian days change at noon an example computation is given. Consider t = June 19, 1991 at 2:32 pm. The portion of June 19 will be accounted for in (32) using the Ω_e term so we need to obtain JD for T = June 19, 1991. The day 0 number on Table 1.7 is the Julian day at noon of the last day of the preceding month. Thus, the Julian day at the beginning of June 19, 1991 (0000hrs) is JD = 2448408 + 0.5 + 18 = 2448426.5 days. This is converted to its corresponding fraction of the 20th century by subtracting the 1900 JD and dividing by the days in a century, i.e.,

$$T_u = [JD - 2415020.0]/36525 = 0.91462012 \text{ centuries} \ . \tag{5.3}$$

Finally, the sidereal time is obtained as

$$\theta_g(T) = 99.6909833 + 36000.7689T_u + 0.00038708T_u^2 = 266.71899^o \ . \tag{5.4}$$

The sidereal time at 2:32 pm becomes $\theta_g(t) = 266.71899 + 218.59686 - 360. = 125.31585^o$.

6.0 Tracking Station Satellite Visibility

Here we consider a ground tracking station at longitude λ_s and latitude δ_s on the earth surface. The locations of a number of specific stations are listed below on Table 1. The station location in longitude-latitude coordinates is written

$$\mathbf{r}_s = \mathbf{e}_e^T r_e[\cos\lambda_s\cos\delta_s,\ \sin\lambda_s\cos\delta_s,\ \sin\delta_s]^T \tag{6.1}$$

where $\mathbf{e}_e$ is earth fixed with 3-axis north and l-axis at the Greenwich meridian. The satellite longitude λ' and latitude δ have been expressed earlier in terms of sidereal time and the classical orbit parameters. Thus, we denote the satellite position as

$$\mathbf{r}_o = \mathbf{e}_e^T r_o[\cos\lambda'\cos\delta,\ \sin\lambda'\cos\delta,\ \sin\delta]^T \tag{6.2}$$

$$= \mathbf{e}_1^T r_o[1, 0, 0]^T = \mathbf{e}_i^T A_3^T(\Omega)A_1^T(i)A_3^T(\omega)A_3^T(v)r_o[1, 0, 0]^T = \mathbf{e}_i^T A_3^T(\Omega)A_1^T(i)A_3^T(\omega + v)r_o[1, 0, 0]^T$$

$$= \mathbf{e}_i^T r_o\begin{bmatrix}\cos\Omega\cos(\omega + v) - \cos i\sin\Omega\sin(\omega + v)\\ \sin\Omega\cos(\omega + v) + \cos i\cos\Omega\sin(\omega + v)\\ \sin i\sin(\omega + v)\end{bmatrix}$$

where we have completed the extra expansion in classical orbital angles for future reference. Now the satellite is line-of-sight visible when $\mathbf{r}_o - \mathbf{r}_s$, the vector from the ground station to the satellite, is within 90^o of the vertical. Let

[1] GMT − PST = 8 hrs; GMT − PDT = 7 hrs.

β denote the angle from the ground station local vertical to $\mathbf{r}_o - \mathbf{r}_s$. Then the visibility constraint is mathematically

$$0 < \cos\beta = \mathbf{r}_s \cdot [\mathbf{r}_o - \mathbf{r}_s]/[|\mathbf{r}_s||\mathbf{r}_o - \mathbf{r}_s|] = [\mathbf{r}_s \cdot \mathbf{r}_o - |r_s|^2]/[|\mathbf{r}_s||\mathbf{r}_o - \mathbf{r}_s|] \tag{6.3}$$

$$= \{r_o[\cos\delta_s \cos\delta\cos(\lambda' - \lambda_s) + \sin\delta_s \sin\delta] - r_e\}/|\mathbf{r}_o - \mathbf{r}_s| \,.$$

Constraints on the ground antenna may preclude its going all the way down to the horizon and set some lower limit on β and $\cos\beta$.

For a circular orbit of radius r_o and a ground station in the orbit plane which can see down to angle η above the horizon, the ground station will have visibility over the orbital arc δv given by

$$\cos(\Delta v/2) = (r_e/r_o)\cos^2\eta + \sin\eta\{1 - [(r_e/r_o)\cos\eta]^2\}^{1/2} \,. \tag{6.4}$$

While the constraint for line-of-sight visibility is given by (6.3), additional constraints may exist for visibility of a particular satellite antenna. For example, on a spinning satellite an omni-directional antenna usually has a field of view that excludes a cone around each end of the spin axis. In this case the antenna is visible from the ground station when the line-of-sight vector, $\mathbf{r}_o - \mathbf{r}_s$, is sufficiently close to 90^o from the spin axis, i.e.,

$$a > |\cos\nu| = |\mathbf{u} \cdot [\mathbf{r}_o - \mathbf{r}_s]|/|\mathbf{r}_o - \mathbf{r}_s| \tag{6.5}$$

where a is some positive limit defining omni antenna beamwidth, $\mathbf{u}$ is a unit vector along the spin axis, and (6.3) and (6.5) must simultaneously hold.

Table 1. Satellite Tracking Station Locations.

Station	Latitude geodetic deg N	Longitude deg W	Altitude ft
Spring Creek, NY	40.65361	73.88917	20.
Fillmore, CA	34.40610	118.89280	1015.
Andover, ME	44.63240	-289.29980	918.
Paumalu, Hawaii	21.67340	-201.96320	508.
Fucino, Italy	41.97580	-13.60110	2182.
Carnarvon, Australia	-24.86940	-113.70280	115.
Tangua, Brazil	-22.981	-317.21544	116.
Guaratiba, Brazil	-22.9981	43.60636	-18.
Zamengoe, Cameroon	3.94390	-11.44580	2696.
Pleumeur Bodou, France	48.78472	-336.48611	253.
Yamaguchi, Japan	34.21292	-131.55953	621.
Allen Park, Canada	44.174	80.94	
Edmonton, Canada	53.3	114.1	
Lake Cowichen, Canada	48.71	124.07	
KSC, Fla.	28.31	80.54	
Kourou, F. Guiana	5.2358	52.7747	-16.
Castle Rock, CO	39.2772	104.8069	
Hawley, PA	41.2751	75.1300	919.
Glenwood, NJ	41.2	74.5	
Jakarta, Indonesia	-6.4089	253.0394	
Jatiluhur, Indonesia	-6.523897	252.5876	
Daan Magot, Indonesia	-6.45192	253.24634	
Langkawi, Malaysia	6.36849	260.18262	
Three Peaks, CA			
Norfolk SCS, VA	36.56	76.2675	10.
Stockton SCS, CA	37.94166	121.35139	22.
Hawaii SCS	21.52333	157.9975	900.
Guam SCS	13.58149	215.15279	500
Altair, Marshall Is.	9.3975	192.5209	206.
Millstone, MA	42.6174	71.49109	404.
Belrose, Australia	-33.7170	208.7884	748.
Perth, Australia	-31.8813	244.0602	79.
Ixtapalapa, Mexico	19.3953	99.1612	7447.4
Chilworth, England	50.9667	1.4167	
Stanley, Hong Kong	22.1987	245.7832	367.
Tai Po, Hong Kong	22.4530	245.8123	-42.4
White Sands, N. M.(TDRS)	32.37	106.47	
Xi Chang, China	28.245	-102.03	
Baikonur, Russia	45.6	-63.4	
Nittedal, Norway	60.1	-10.8	
Hartebeesthock, So Africa			

7.0 Sun Position in an Earth Centered Inertial (ECI) Basis

Let $\mathbf{e}_h$ be a basis with 1-axis Earth-to-Sun pointed at Aries, 1-2 plane in the ecliptic with 3-axis North. Then, the earth-to-sun vector in this is system is

$$\mathbf{s} = \mathbf{e}_h^T A_3(-\bar{\phi})[1, 0, 0]^T = \mathbf{e}_h^T[\cos\bar{\phi}, \sin\bar{\phi}, 0]^T \tag{7.1}$$

where $\bar{\phi}$ is the mean longitude in the ecliptic of the sun, nominally $\phi = 0$ at the vernal equinox (Mar. 21), and is given by

$$\bar{\phi} = \Omega_s[t - t_o] = (0.985647^o/\text{day})[t - t_o] = \Omega_s[t - t_o] = (1.99106 \times 10^{-7}\text{rad/sec})[t - t_o] \ , \tag{7.2a}$$

with $t = t_o$ at the vernal equinox of 1965. The mean longitude is perturbed by eccentricity of the earth's orbit about the sun ($e = 0.0167$). The perturbation from mean position can be more than 4^o and changing at 0.12^o day. The correction E, known as the equation of time, gives the true longitude as

$$\phi = \bar{\phi} - E \tag{7.2b}$$

where E has been approximated by Neufeld as

$$E = -102.5 \sin\bar{\phi} - 430.0 \cos\bar{\phi} + 596.4 \sin 2\bar{\phi} \text{ (seconds)} \tag{7.3}$$

$$E = -0.427 \sin\bar{\phi} - 1.79 \cos\bar{\phi} + 2.49 \sin 2\bar{\phi} \text{ (degrees)}$$

This approximation to E reduces the error in ϕ to less than $\pm 0.25^o$. The ECI system, denoted by $\mathbf{e}_i$, has 1-axis earth-to-sun pointed along the vernal equinox and is rotated $\phi_h = \beta_e = -23.44384^o \approx -23.5^o$ (obliquity of the ecliptic) about the 1-axis. Thus,

$$\mathbf{s} = \mathbf{e}_h^T[1, 0, 0]^T = \mathbf{e}_i^T A_1(-23.5^o)A_3(-\phi)[1, 0, 0]^T = \mathbf{e}_i^T[\cos\phi, \cos(23.5^o)\sin\phi, \sin(23.5^o)\sin\phi]^T \tag{7.4}$$

$$= \mathbf{e}_i^T[\cos\phi, 0.917 \sin\phi, 0.398 \sin\phi]^T = \mathbf{e}_i^T[\bar{s}_1, \bar{s}_2, \bar{s}_3]^T \ .$$

The right ascension and declination of the sun in $\mathbf{e}_i$ are respectively,

$$\sin\alpha_s = \frac{\cos(23.5^o)\sin\phi}{\sqrt{\cos^2\phi + \cos^2(23.5^o)\sin^2\phi}} \ ; \ \cos\alpha_s = \frac{\cos\phi}{\sqrt{\cos^2\phi + \cos^2(23.5^o)\sin^2\phi}} \tag{7.5a}$$

$$\sin\delta_s = \sin(23.5^o)\sin\phi \ ; \ \cos\delta_s = \sqrt{\cos^2\phi + \cos^2(23.5^o)\sin^2\phi} \ . \tag{7.5b}$$

The sun vector in $\mathbf{e}_i$ may then be expressed

$$\mathbf{s} = \mathbf{e}_i^T[\cos\alpha_s \cos\delta_s, \sin\alpha_s \cos\delta_s, \sin\delta_s]^T \ , \tag{7.6}$$

and the sun aspect angle λ to any other target vector $\mathbf{u}$ with right ascension and declination α, δ is

$$\cos\lambda = \mathbf{u} \cdot \mathbf{v} = \cos\delta \cos\delta_s \cos(\alpha - \alpha_s) + \sin\delta \sin\delta_s \ . \tag{7.7}$$

7.1 *Angle From the Orbit Plane*

Let $\mathbf{u}$ be the earth-to-sun vector having right ascension and declination α, δ in inertial basis $\mathbf{e}_i$ which is explicit as

$$\mathbf{u} = \mathbf{e}_i^T A_3(-\alpha)A_2(\delta)[1, 0, 0]^T = \mathbf{e}_i^T[\cos\alpha \cos\delta, \sin\alpha \cos\delta, \sin\delta]^T \ . \tag{7.8}$$

We wish to determine the angle of this vector from an orbit plane described by classical elements Ω and i. In a basis with 3-axis orbit normal

$$\mathbf{u} = \mathbf{e}^T A_1(i)A_3(\Omega)A_3(-\alpha)A_2(\delta)[1, 0, 0]^T = \mathbf{e}^T A_1(i)A_3(\Omega - \alpha)A_2(\delta)[1, 0, 0]^T \tag{7.9}$$

$$= \mathbf{e}^T \begin{bmatrix} \cos(\Omega - \alpha)\cos\delta \\ \sin i \sin\delta - \cos i \sin(\Omega - \alpha)\cos\delta \\ \cos i \sin\delta + \sin i \sin(\Omega - \alpha)\cos\delta \end{bmatrix} = \mathbf{e}^T[u_1, u_2, u_3]^T$$

$$= \mathbf{e}^T A_1(i)A_3(\Omega)A_1(-23.5^o)A_3(-\phi)[1, 0, 0]^T = \mathbf{e}^T A_1(i)A_3(\Omega)[\cos\phi, \cos(23.5^o)\sin\phi, \sin(23.5^o)\sin\phi]^T$$

$$= \mathbf{e}^T \begin{bmatrix} \cos\Omega\cos\phi + \cos(23.5^o)\sin\Omega\sin\phi \\ [\cos i\cos\Omega\cos(23.5^o) + \sin i\sin(23.5^o)]\sin\phi - [\cos i\sin\Omega]\cos\phi \\ -[\sin i\cos\Omega\cos(23.5^o) - \cos i\sin(23.5^o)]\sin\phi - [\sin i\sin\Omega]\cos\phi \end{bmatrix} \to \mathbf{e}^T \begin{bmatrix} \cos\phi \\ \cos(i - 23.5^o)\sin\phi \\ -\sin(i - 23.5^o)\sin\phi \end{bmatrix}; \ \Omega \to 0$$

$$= \mathbf{e}^T \begin{bmatrix} (1/2)[1 - \cos(23.5^o)]\cos(\Omega + \phi) + (1/2)[1 + \cos(23.5^o)]\cos(\Omega - \phi) \\ -(1/2)\cos i[1 - \cos(23.5^o)]\sin(\Omega + \phi) - (1/2)\cos i[1 + \cos(23.5^o)]\sin(\Omega - \phi) + \sin i\sin(23.5^o)\sin\phi \\ -(1/2)\sin i[1 + \cos(23.5^o)]\sin(\Omega + \phi) - (1/2)\sin i[1 - \cos(23.5^o)]\sin(\Omega - \phi) + \cos i\sin(23.5^o)\sin\phi \end{bmatrix}.$$

The desired angle μ, of $\mathbf{u}$ from the orbit plane is

$$\mu = \mathrm{Sin}^{-1}[u_3] = \mathrm{Tan}^{-1}[u_3/\sqrt{u_1^2 + u_2^2}] \ . \tag{7.10}$$

The last expansion of $\mathbf{u}$ shows three frequency components in u_3 that might be expected to show up in the sun angle μ. By some means that has been lost, we have guessed that the sun angle approximates

$$\hat{\mu}(t) = \beta_e \sin[\Omega_s t + \psi_s] + i\sin[(\dot{\Omega} - \Omega_s)t + \psi_r]$$

and this yields results quite close to (7.10). $\dot{\Omega}$ is nodal regression rate, and ψ_s, ψ_r are phase adjustments.

7.2 *Solar Navigation*

Normally three dimensional navigation, determination of position with respect to some inertial point, would require two bodies such as two stars. However, navigation from a point on the Earth's surface means one coordinate (elevation) is assumed known and position can be determined by two angles to the sun and knowledge of time. Following the Earth fixed coordinate notation of Eq.2.6 with east longitude and north latitude λ, γ and local horizontal coordinate basis designation $\mathbf{e}_{lh}$,

$$\mathbf{e}_i^T = \mathbf{e}_e^T A_3(\theta_g(t)) = \mathbf{e}_{lh}^T A_2(-\gamma) A_3(\lambda + \theta_g(t)) \tag{7.11}$$

so the unit vector from Earth center to the sun may be written in local horizontal coordinates of a point on Earth as

$$\mathbf{s} = \mathbf{e}_{lh}^T A_2(-\gamma) A_3(\lambda + \theta_g(t))[\cos\alpha_s\cos\delta_s, \sin\alpha_s\cos\delta_s, \sin\delta_s]^T = \mathbf{e}_{lh}^T[s_1, s_2, s_3]^T \tag{7.12}$$

$$= \mathbf{e}_{lh}^T \begin{bmatrix} \cos\gamma & 0 & \sin\gamma \\ 0 & 1 & 0 \\ -\sin\gamma & 0 & \cos\gamma \end{bmatrix} \begin{bmatrix} \cos(\lambda + \theta_g(t)) & \sin(\lambda + \theta_g(t)) & 0 \\ -\sin(\lambda + \theta_g(t)) & \cos(\lambda + \theta_g(t)) & 0 \\ 0 & 0 & 1 \end{bmatrix} \begin{bmatrix} \cos\alpha_s\cos\delta_s \\ \sin\alpha_s\cos\delta_s \\ \sin\delta_s \end{bmatrix}$$

$$= \mathbf{e}_{lh}^T \begin{bmatrix} \cos\gamma & 0 & \sin\gamma \\ 0 & 1 & 0 \\ -\sin\gamma & 0 & \cos\gamma \end{bmatrix} \begin{bmatrix} \cos\delta_s\cos(\lambda + \theta_g(t) - \alpha_s) \\ -\cos\delta_s\sin(\lambda + \theta_g(t) - \alpha_s) \\ +\sin\delta_s \end{bmatrix} = \mathbf{e}_{lh}^T \begin{bmatrix} \cos\gamma\cos\delta_s\cos(\lambda + \theta_g(t) - \alpha_s) + \sin\gamma\sin\delta_s \\ -\cos\delta_s\sin(\lambda + \theta_g(t) - \alpha_s) \\ -\sin\gamma\cos\delta_s\cos(\lambda + \theta_g(t) - \alpha_s) + \cos\gamma\sin\delta_s \end{bmatrix}.$$

Following the definition of azimuth, Az, and elevation, El of Eq. 2.25

$$\sin El = s_1/\sqrt{s_1^2 + s_2^2 + s_3^2} = s_1; \ \cos El = \sqrt{s_2^2 + s_3^2}/\sqrt{s_1^2 + s_2^2 + s_3^2} = \sqrt{s_2^2 + s_3^2} \tag{7.13a}$$

$$\sin Az = s_2/\sqrt{s_2^2 + s_3^2} = s_2/\cos El; \ \cos Az = s_3/\sqrt{s_2^2 + s_3^2} = s_3/\cos El \ . \tag{7.13b}$$

Given the time of year, epoch, α_s and δ_s are known, Eq. 7.5, and the time of day determines θ_g. Hence, with measurements of Az and El to the sun, one can solve for longitude and latitude λ and γ, completing the navigation solution. Strictly, one needs to use the sun vector from the navigation point obtained by adding the Earth center to sun vector to the position vector from Earth center of the observation point, which incidentally is unknown! However, since Earth radius is so much smaller than the distance to the sun the maximum error is less than $\varepsilon \le \tan^{-1} r_e/R_s = 0.12^o$. Navigating from another star the maximum error is totally negligible. Conversely, if this is significant, or if navigating with respect to a closer body like the moon or an Earth satellite, Earth radius should be included and perhaps modified by the geodetic flat Earth model.

At sun rise or set $El = \sin El = s_1 = 0$ yielding $s_2^2 + s_3^2 = 1$ and solving from s_1

$$\cos(\lambda + \theta_g(t) - \alpha_s) = -\tan\gamma\tan\delta_s$$

then substituting in s_2,

$$s_2^2 = \cos^2\delta_s(1 - \tan^2\gamma\tan^2\delta_s) = \cos^2\delta_s\,\frac{(\cos^2\gamma\cos^2\delta_s - \sin^2\gamma\sin^2\delta_s)}{\cos^2\gamma\cos^2\delta_s} = \frac{\cos^2\gamma\cos^2\delta_s - \sin^2\gamma\sin^2\delta_s}{\cos^2\gamma}$$

giving the unique value of sun azimuth at sunset (or rise) Az_0,

$$\sin Az_0 = s_2 = \frac{\sqrt{\cos^2\gamma\cos^2\delta_s - \sin^2\gamma\sin^2\delta_s}}{\cos\gamma} = \frac{\sqrt{\cos^2\gamma[\cos^2\phi + \cos^2(23.5)\sin^2\phi] - \sin^2\gamma[\sin^2(23.5)\sin^2\phi]}}{\cos\gamma}\ .$$

At the equinoxes $\delta_s = 0$ and $\phi = \pm\pi/2$, $\sin Az_0 = \pm 1$ and $Az_0 = \pm\pi/2 = \pm 90^o$, i.e. due East or West. Alternately,

$$\sin Az_0 = s_2 = \pm\cos\delta_s\sqrt{1 - \tan^2\gamma\tan^2\delta_s}$$

vanishes yielding at $Az_0 = 0^o, 180^o$ at latitude $\gamma = \pm(90 - 23.5)^o$ on the artic circle(s) at solstices when $\delta_s = \pm 23.5^o$ and $\le (90 - 23.5)^o$ for lower latitudes. Qualitatively, the artic circle has one day per year, the solstice, of no sunset (or sunrise) while higher altitudes have multiple days of continual sun or dark, the number increasing with latitude. To compute the time of sunset, denoting this particular value of $\theta_g(t)$ as $\bar\theta_g(t_0)$,

$$\bar\theta_g(t_0) = \mathrm{Sin}^{-1}[-s_2/\cos\delta_s] - \lambda + \alpha_s = \pm\mathrm{Sin}^{-1}[\sqrt{1 - \tan^2\gamma\tan^2\delta_s}] - \lambda + \alpha_s\ .$$

To complete the navigation solution we must solve for longitude and latitude λ and γ in terms of the measurements Az and El. It is presumed that local time of day $\theta_g(t)$ is known along with time of year ϕ, which defines α_s, δ_s, also known. From 7.13, $s_2 = \sin Az\cos El$, leads simply equating to s_2 in 7.12 as

$$\lambda + \theta_g(t) = \mathrm{Sin}^{-1}[-s_2/\cos\delta_s] + \alpha_s = \mathrm{Sin}^{-1}[-\sin Az\cos El/\cos\delta_s] + \alpha_s\ . \tag{7.14a}$$

Then manipulating s_1

$$s_1 = \sin El = \cos\gamma\cos\delta_s\cos(\lambda + \theta_g(t) - \alpha_s) + \sin\gamma\sin\delta_s = A\sin\gamma + B\cos\gamma$$

$$= \sqrt{A^2+B^2}\left[\frac{A}{\sqrt{A^2+B^2}}\sin\gamma + \frac{B}{\sqrt{A^2+B^2}}\cos\gamma\right] = \sqrt{A^2+B^2}[\sin\gamma\cos\alpha + \cos\gamma\sin\alpha] = \sqrt{A^2+B^2}\sin(\gamma+\alpha)$$

where

$$\sin\alpha = \frac{B}{\sqrt{A^2+B^2}} = \frac{\cos\delta_s\cos(\lambda + \theta_g(t) - \alpha_s)}{\sqrt{\sin^2\delta_s + \cos^2\delta_s\cos^2(\lambda + \theta_g(t) - \alpha_s)}}\ ;\ \cos\alpha = \frac{A}{\sqrt{A^2+B^2}} = \frac{\sin\delta_s}{\sqrt{\sin^2\delta_s + \cos^2\delta_s\cos^2(\lambda + \theta_g(t) - \alpha_s)}}$$

giving

$$\gamma = \mathrm{Sin}^{-1}[s_1/\sqrt{A^2+B^2}] - \alpha = \mathrm{Sin}^{-1}[\sin El/\sqrt{A^2+B^2}] - \alpha \tag{7.14b}$$

$$= \mathrm{Sin}^{-1}\left[\frac{\sin El}{\sqrt{\sin^2\delta_s + \cos^2\delta_s\cos^2(\lambda + \theta_g(t) - \alpha_s)}}\right] - \mathrm{Tan}^{-1}[(\cos\delta_s/\sin\delta_s)\cos(\lambda + \theta_g(t) - \alpha_s)]$$

$$= \mathrm{Sin}^{-1}\left[\frac{\sin El}{\sqrt{1 - \sin^2 Az\cos^2 El}}\right] - \mathrm{Tan}^{-1}[(\cos\delta_s/\sin\delta_s)\{1 - \sqrt{\sin^2 Az\cos^2 El/\cos^2\delta_s}\}]\ .$$

In evaluation of these we find frequent examples of inverse trigonometric function ambiguity leading to $\pm 180^o$ or $\pm 360^o$ modulo in the result. Presumably in any practical case the navigator knows what hemisphere he is on, hence enough is known about λ, γ to compensate.

Frequently for analytical purposes it is desirable to pursue vector based solutions over the trigonometric. To that end and as a check on the preceding the following alternate is developed. Eq. 7.12 can be equivalently written

$$\mathbf{s} = \mathbf{e}_{lh}^T\begin{bmatrix}\cos\gamma[\bar s_1\cos(\lambda + \theta_g(t)) + \bar s_2\sin(\lambda + \theta_g(t))] + \bar s_3\sin\gamma \\ \bar s_2\cos(\lambda + \theta_g(t)) - \bar s_1\sin(\lambda + \theta_g(t)) \\ -\sin\gamma[\bar s_1\cos(\lambda + \theta_g(t)) + \bar s_2\sin(\lambda + \theta_g(t))] + \bar s_3\cos\gamma\end{bmatrix} = \mathbf{e}_{lh}^T\begin{bmatrix}s_1\\ s_2\\ s_3\end{bmatrix}. \tag{7.15}$$

Noting

$$s_2 = \sqrt{\bar{s}_1^2 + \bar{s}_2^2}[\sin\xi\cos(\lambda + \theta_g(t)) - \cos\xi\sin(\lambda + \theta_g(t))] = \sqrt{\bar{s}_1^2 + \bar{s}_2^2}\sin(\xi - \lambda - \theta_g(t)) \; ,$$

having defined

$$\sin\xi = \bar{s}_2/\sqrt{\bar{s}_1^2 + \bar{s}_2^2}; \; \cos\xi = \bar{s}_1/\sqrt{\bar{s}_1^2 + \bar{s}_2^2} \; .$$

so that

$$\lambda + \theta_g(t) = -\mathrm{Sin}^{-1}\left[\frac{s_2}{\sqrt{\bar{s}_1^2 + \bar{s}_2^2}}\right] + \xi = -\mathrm{Sin}^{-1}\left[\frac{s_2}{\sqrt{\bar{s}_1^2 + \bar{s}_2^2}}\right] + \mathrm{Tan}^{-1}[\bar{s}_2/\bar{s}_1] \tag{7.16a}$$

$$= -\mathrm{Sin}^{-1}\left[\frac{s_2}{\sqrt{\bar{s}_1^2 + \bar{s}_2^2}}\right] + \mathrm{Sin}^{-1}\left[\frac{\bar{s}_2}{\sqrt{\bar{s}_1^2 + \bar{s}_2^2}}\right] = -\mathrm{Sin}^{-1}\left[\frac{s_2\sqrt{\bar{s}_1^2} - \bar{s}_2\sqrt{\bar{s}_1^2 + \bar{s}_2^2 - s_2^2}}{\bar{s}_1^2 + \bar{s}_2^2}\right]$$

$$= -\mathrm{Sin}^{-1}\left[\frac{\sin \mathrm{Az}\cos \mathrm{El}}{\sqrt{\cos^2\phi + \cos^2(23.5^o)\sin^2\phi}}\right] + \mathrm{Tan}^{-1}\left[\frac{\cos(23.5^o)\sin\phi}{\cos\phi}\right] = \mathrm{Sin}^{-1}[-\sin \mathrm{Az}\cos \mathrm{El}/\cos\delta_s] + \alpha_s \; .$$

Next, multiplying s_1 and s_3 of 7.15 by $\sin\gamma$ and $\cos\gamma$ respectively, and adding produces

$$\bar{s}_3 = s_1\sin\gamma + s_3\cos\gamma = \sqrt{s_1^2 + s_3^2}[\sin\gamma\cos\sigma + \cos\gamma\sin\sigma] = \sqrt{s_1^2 + s_3^2}\sin(\gamma + \sigma)$$

$$\sin\sigma = s_3/\sqrt{s_1^2 + s_3^2}; \; \cos\sigma = s_1/\sqrt{s_1^2 + s_3^2}$$

$$\gamma = \mathrm{Sin}^{-1}[\bar{s}_3/\sqrt{s_1^2 + s_3^2}] - \sigma = \mathrm{Sin}^{-1}\left[\frac{\bar{s}_3}{\sqrt{s_1^2 + s_3^2}}\right] - \mathrm{Sin}^{-1}\left[\frac{s_3}{\sqrt{s_1^2 + s_3^2}}\right] = \mathrm{Sin}^{-1}\left[\frac{\bar{s}_3\sqrt{s_1^2} - s_3\sqrt{s_1^2 + s_2^2 - \bar{s}_3^2}}{s_1^2 + s_3^2}\right] \tag{7.16b}$$

$$= \mathrm{Sin}^{-1}\left[\frac{\sin(23.5^o)\sin\phi}{\sqrt{\sin^2 \mathrm{El} + \cos^2 \mathrm{Az}\cos^2 \mathrm{El}}}\right] - \mathrm{Tan}^{-1}[\cos \mathrm{Az}\cos \mathrm{El}/\sin \mathrm{El}] \; .$$

$$= \mathrm{Sin}^{-1}\left[\frac{\sin(23.5^o)\sin\phi}{\sqrt{1 - \sin^2 \mathrm{Az}\cos^2 \mathrm{El}}}\right] - \mathrm{Tan}^{-1}[\cos \mathrm{Az}\cos \mathrm{El}/\sin \mathrm{El}] \; .$$

$$\frac{d\lambda}{d\theta_g} = 1; \; \frac{d\lambda}{d\phi} = \frac{d\alpha_s}{d\phi} = \frac{\cos(23.5^o)\cos^2\alpha_s}{\cos^2\phi} = \frac{\cos(23.5^o)}{\cos^2\phi + \cos^2(23.5^o)\sin^2\phi} \le 1/\cos(23.5^o) = 1.09$$

8.0 Orbit Perturbations

8.1 Earth Gravitational Orbit Perturbations

The nonspherical mass distribution (oblateness) of the earth, Ref. 10 page 318, produces gravitational forces that are a function of position. In Ref. 1 page 366 or Ref. 3 page 62 the first order secular orbit perturbations are derived as:

Anomalistic Period: $P = 2\pi/n$; $n_o = \sqrt{\mu/a^3} = 2\pi/P_o$

$$n = n_o[1 + (3/2)J_2 r_e^2 a^{-2}\{1 - e^2\}^{-3/2}\{1 - (3/2)\sin^2 i\}] \tag{8.1}$$

$$= n_o[1 + 6.60624 \times 10^4 a^{-2}\{1 - e^2\}^{-3/2}\{1 - (3/2)\sin^2 i\}]$$

$$= n_o[1 + 1.92361 \times 10^4 a^{-2}\{1 - e^2\}^{-3/2}\{1 - (3/2)\sin^2 i\}] = n_o;\ i = \mathrm{Sin}^{-1}\{\sqrt{2/3}\} \approx 54.7^o\ .$$

Regression of Nodes:

$$\Omega = \Omega_o - \dot{\Omega}(t - t_o) \tag{8.2}$$

$$= \Omega_o - \{(3/2)J_2\sqrt{\mu} r_e^2 a^{-7/2}(1 - e^2)^{-2}\cos i\}(t - t_o)$$

$$= \Omega_o - \{2.06474 \times 10^{14} a^{-7/2}(1 - e^2)^{-2}\cos i\}(t - t_o)$$

$$= \Omega_o - \{2.383114 \times 10^{13} a^{-7/2}(1 - e^2)^{-2}\cos i\}(t - t_o)\ .$$

Advance of Perigee:

$$\omega = \omega_o + \dot{\Omega}\{[2 - (5/2)\sin^2 i]/\cos i\}(t - t_o)\ . \tag{8.3}$$

The numerical values use $\mu = [631.35\,\mathrm{km}^{3/2}/\mathrm{sec}]^2 = [250.26\,\mathrm{nm}^{3/2}/\mathrm{sec}]^2$ and $J_2 = 1.08263 \times 10^{-3}$. The first numerical coefficient requires a in km while the second requires a in nautical miles. $\dot{\Omega}$ is in degrees/day.

8.1.1 *Sun Synchronous Orbit*

If the product of terms in a, e, and i in the nodal regression rate expression is $-4.7737 \times 10^{-15}\mathrm{km}^{-7/2}$ the regression rate will be 0.9856^o/day and the orbit will be fixed with respect to the sun and with respect to time of day (Ref. 3 page 68).

8.1.2 *Molniya Orbit*

It can be seen that in the last equation if $i = \mathrm{Sin}^{-1}[\sqrt{4/5}] = 63.435^o$ the perigee is fixed. This orbit with 12 hour period and argument of perigee $\omega = 270^o$ was chosen for the Russian Molniya communications satellites (1965) to cover the high latitude polar regions and thus has become known as the Molniya orbit. The argument of perigee is fixed regardless of its absolute position and the period.

8.2 Triaxiality of Earth's Gravitational Potential (E-W Stationkeeping)

Because the earth gravitational potential varies as one moves around an equatorial circumference, tangential perturbing accelerations alter the orbit of a geosynchronous satellite. The earth shape can be thought of as elliptical and the resultant longitudinal motion can be likened to the angular motion of a frictionless pendulum. Although this effect is probably small with regard to most orbits, for a geostationary satellite located far from a stable null it can be the dominant east-west perturbation and requires stationkeeping to maintain the satellite in the desired bounds. Other important east-west perturbations are solar acceleration (discussed below) and error induced by the much larger inclination stationkeeping maneuvers.

Assuming the drift rate of a satellite is initialized at zero with the satellite at the edge of a stationkeeping deadband $\Delta\lambda$ farthest from the stable node λ_o, the longitude is approximated in the neighborhood of the station λ_1 by

$$\lambda(t) = \lambda_1 - \Delta\lambda + (\nu/2)[\sin 2(\lambda_1 - \lambda_o)]t^2; \Rightarrow \begin{cases}\lambda(0) = \lambda_1 - \Delta\lambda \\ \lambda(\Delta t) = \lambda_1 + \Delta\lambda\end{cases} \Rightarrow \Delta t = 2\sqrt{\Delta\lambda/[\nu \sin 2(\lambda_1 - \lambda_o)]} \tag{8.4}$$

where $\lambda_o = (106^o \pm 6^o\mathrm{W}$ and $286^o \pm 6^o\mathrm{W})$ are the stable node locations, and $\nu = 9\tilde{J}_{22}[r_e\Omega_e/r_o]^2 = 1.7 \times 10^{-3}\mathrm{deg/day}^2$. r_o, r_e are respectively orbit and earth radius, Ω_e is earth rate, and $\tilde{J}_{22} = 3.65 \times 10^{-6}$ approximates the equatorial ellipticity coefficient in the Bessel function representation of the earth gravitational function (Ref. 6 and 7).

The time Δt is the time to drift one way across a control deadband $2\Delta\lambda$, yielding a round trip maneuver interval

$$2\Delta t = 4\sqrt{\Delta\lambda/[\nu\sin 2(\lambda_1 - \lambda_o)]} \ge 4\sqrt{\Delta\lambda/\nu} = 4\sqrt{(0.05^o)/[1.7\times 10^{-3}]^o/\text{day}^2} = 21.7\ \text{days}; \begin{cases} \lambda_1 = \lambda_o \pm\pi/4 \\ \Delta\lambda = 0.05^o \end{cases} . \qquad (8.5)$$

For a single δV impulse, in geostationary orbit, the semimajor axis δa and incremental velocity change δV are related as $\delta a = 2r_o(\delta V/V)$, and implicitly differentiating $P = 2\pi a^{3/2}/\sqrt{\mu} = 2\pi/(\Omega_s + \Omega_e)$, longitude drift rate is[1]

$$\delta\dot{\lambda} = -[(3/2)\delta a/a](\Omega_s + \Omega_e) = -[3\delta V/V](\Omega_s + \Omega_e) \Rightarrow \delta V = -(1/3)\delta\dot{\lambda}V/(\Omega_s + \Omega_e) \qquad (8.6)$$

For geosynchronous velocity, $V = 10080.9$ ft/sec, deadband $\Delta\lambda = 0.05^o$, and $\nu = [1.7\times 10^{-3}]^o/\text{day}^2$, giving

$$\dot{\lambda}(\Delta t) = [\nu\sin 2(\lambda_1 - \lambda_o)]\Delta t = 2\sqrt{\Delta\lambda[\nu\sin 2(\lambda_1 - \lambda_o)]} \le 2\sqrt{\Delta\lambda\nu} \qquad (8.7a)$$

$$= (180/\pi)2\sqrt{(\pi/180)(0.05^o)(\pi/180)([1.7\times 10^{-3}]^o/\text{day}^2)} = 0.018^o/\text{day}$$

$$\delta V = -(2/3)\sqrt{\Delta\lambda[\nu\sin 2(\lambda_1 - \lambda_o)]}[V/(\Omega_s + \Omega_e)] \le -(2/3)\sqrt{\Delta\lambda\nu}[V/(\Omega_s + \Omega_e)] \qquad (8.7b)$$

$$\le -[(1/3)(0.018^o/\text{day})/(360^o/\text{day})](10080.9\ \text{ft/sec}) = 0.172\ \text{ft/sec}$$

One must impart twice this velocity impulse in order to stop the satellite and reverse the drift direction at the same initial speed. Hence, approximate maximum yearly velocity impulse is[2]

$$\Delta V = 2[(365\ \text{day/year})/(2\Delta t)]\delta V = 2[(365\ \text{day/year})/(2\Delta t)](2/3)\sqrt{\Delta\lambda[\nu\sin 2(\lambda_1 - \lambda_o)]}[V/(\Omega_s + \Omega_e)] \qquad (8.7c)$$

$$= [365\ \text{day/year}](1/3)\nu\sin 2(\lambda_1 - \lambda_o)[V/(\Omega_s + \Omega_e)] \le [365\ \text{day/year}](1/3)\nu[V/(\Omega_s + \Omega_e)] = 5.77\ \text{ft/sec/year} = 1.76\ \text{m/sec/year} .$$

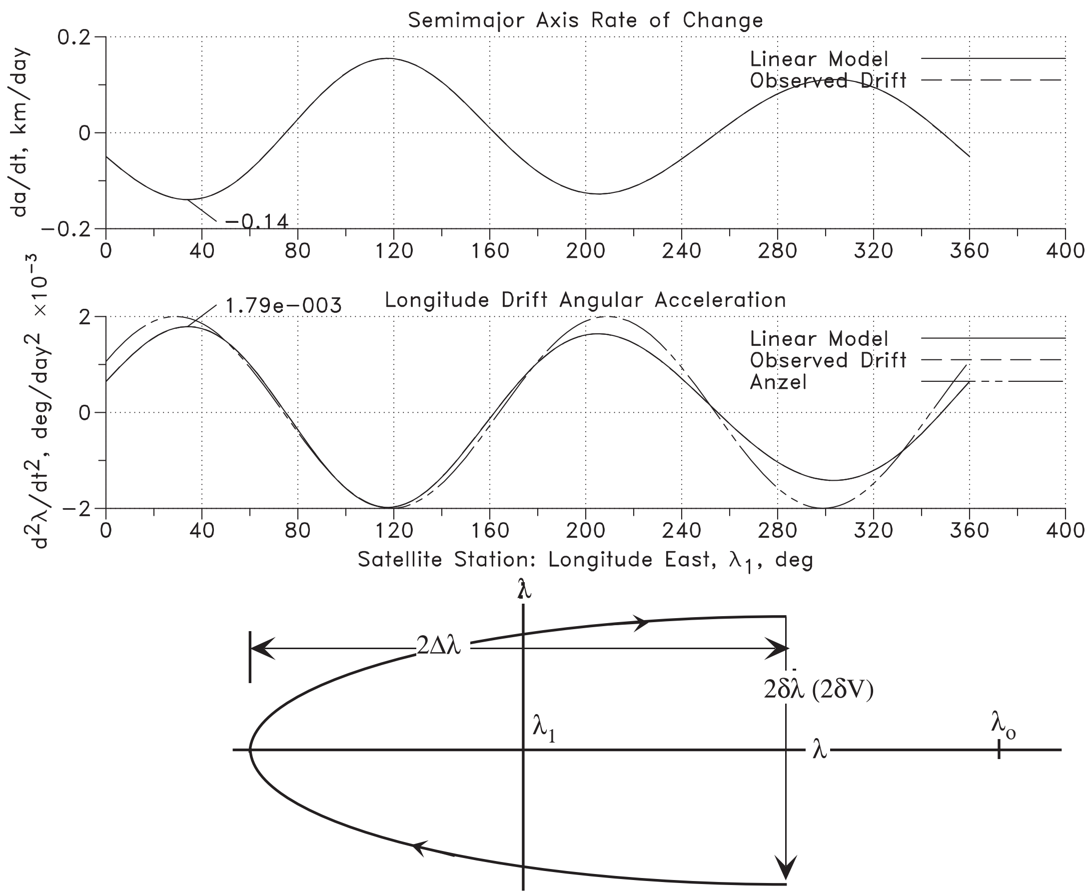

Figure 8.1 Oblateness Gravitational Acceleration and Typical E-W Stationkeeping Pattern.

---

[1] $P = 2\pi a^{3/2}/\sqrt{\mu} \Rightarrow \dfrac{\partial P}{\partial a} = 2\pi(3/2)a^{1/2}/\sqrt{\mu} = (3/2)P/a$; $P = 2\pi/\Omega_e \Rightarrow \dfrac{\partial P}{\partial \Omega_e} = -2\pi/\Omega_e^2 = -P/\Omega_e$

[2] This can vary at worst case points by ± 0.3 m/sec/year when higher order gravity terms are included.

8.3 Sun and Moon Gravitational Perturbations(N-S Stationkeeping)

The gravitational attraction of the sun and moon induce secular and periodic changes in inclination of an earth orbiting spacecraft. This gives rise to need for North-South Stationkeeping or orbit inclination correction of a geosynchronous satellite. In Ref. 2 the first order drift rate is obtained as

$$\dot{\boldsymbol{\beta}} = \mathbf{e}_i^T[0.132\sin\{\Omega_m(t-t_o)\} + 0.29\sin\{2\Omega_s(t-t_o)\},\ 0.852 + 0.098\cos\{\Omega_m(t-t_o)\} - 0.29\cos\{2\Omega_s(t-t_o)\},\ 0]^T \text{ deg/year} \quad (8.8)$$

where $\boldsymbol{\beta}$ is orbit inclination, Ω_s is Earth rate about the Sun, $\Omega_m = \Omega_s/18.6$ is the 18.6 year phase of the moon rate. The reference epoch is t_o = March 22, 1969; 0000 hrs (JD = 2440302.5), and the twice Earth orbit rate terms peak 45.67 days after each equinox. Figure 2.1 shows the Earth at the four seasonal points on the ecliptic. The pole of the moon's orbit is displaced about 5.15 deg from the pole of the ecliptic and precesses around the latter with the noted 18.6 year period. The predominant inclination drift is the secular term above induced by the gravity of the sun. As an example, Figure 8.2 shows Earth-Satellite-Sun geometry at Winter Solstice when the right ascension of the sun is 270 deg. The gravitational acceleration of the sun at noon and midnight is indicated on the sketch. At noon when the satellite is closest to the sun the gravitational acceleration, **a**, is larger, and in particular the orbit normal components at noon and midnight integrate to an equivalent Southward impulse at noon, while the effects at dawn and dusk have equal and opposite canceling effect. This induces an ascending node at 90 deg right ascension in the satellite orbit. A similar sketch at an equinox shows that orbit normal components of sun gravitational acceleration at 6 am and 6 pm are equal and opposite in sign, tending again to rotate the orbit about the 90 deg right ascension axis. More generally, at all times of year the sun gravitational pull induces an ascending node near 270^o, fixed inertially and therefore rotating through all hours of the satellite day. As can be seen from the drift rate expression above, the moon has only a small perturbing effect ($\approx \pm 9^o$) on the described dominant sun effect.

North-South stationkeeping is performed by inducing a velocity increment at the proper node to cancel the sun and moon effects. For North accelerating thrusters the maneuver is near the descending node at 270 deg right ascension and for South accelerating thrusters it is near 90 deg. Another consequence of the derivation is that maneuver time at the satellite progresses through 24 hours over one year so a maneuver can occur at any hour. Further, in eclipse or equinox seasons the maneuvers are near 6 am or 6 pm, so a N-S maneuver is never required during eclipse. Using synchronous orbit velocity of V_s = 10,060 ft/sec, the required annual stationkeeping velocity increment varies between 132 and 167 ft/sec with an average value of 150 ft/sec.

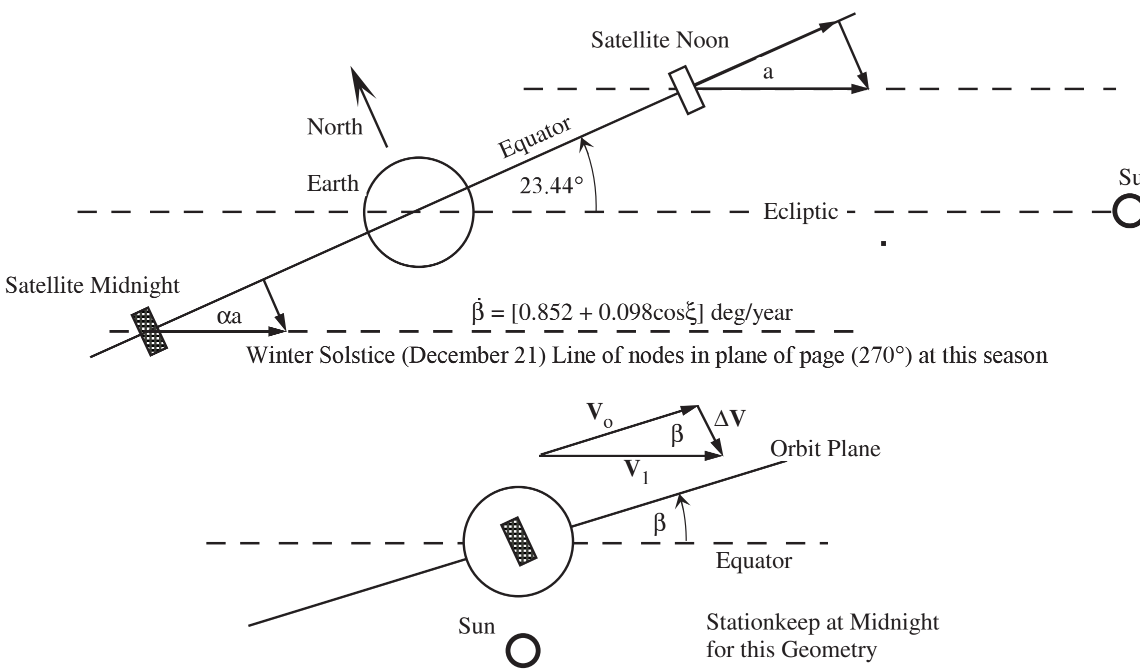

Figure 8.2 Earth-Satellite-Sun Geometry at Winter Solstice (December 21).

8.4 Orbit Perturbation Induced by Solar Pressure Acceleration

Acceleration due to solar radiation pressure integrates to a velocity change in a spacecraft, and hence alters its orbit. The pressure varies as distance squared from the sun, and at earth (1 AU) is $(1+\mu\gamma)1\mu lb/m^2$ where μ is the reflectance coefficient, μ = 1 for 100% reflection, and γ is the diffusivity coefficient, γ = 1 for specular reflection. For earth orbit the solar acceleration can be separated into orbit normal and in plane components. The orbit normal component has vanishing net effect over one orbit. The in plane component along the sun line is essentially inertially fixed and tends to gradually alter the eccentricity and shift the line of apsides of an orbit. For a circular orbit, the in plane acceleration will alter eccentricity by inducing a perigee at dusk and an apogee at dawn as depicted below on Figure 8.3[3]. The perturbation can be controlled by executing a single radial velocity maneuver of magnitude ΔV_R outward at noon or inward at midnight. Alternately it can be corrected by two tangential maneuvers of magnitude $\Delta V_T = \Delta V_R/4$ each, increasing velocity at dawn and decreasing it at dusk.

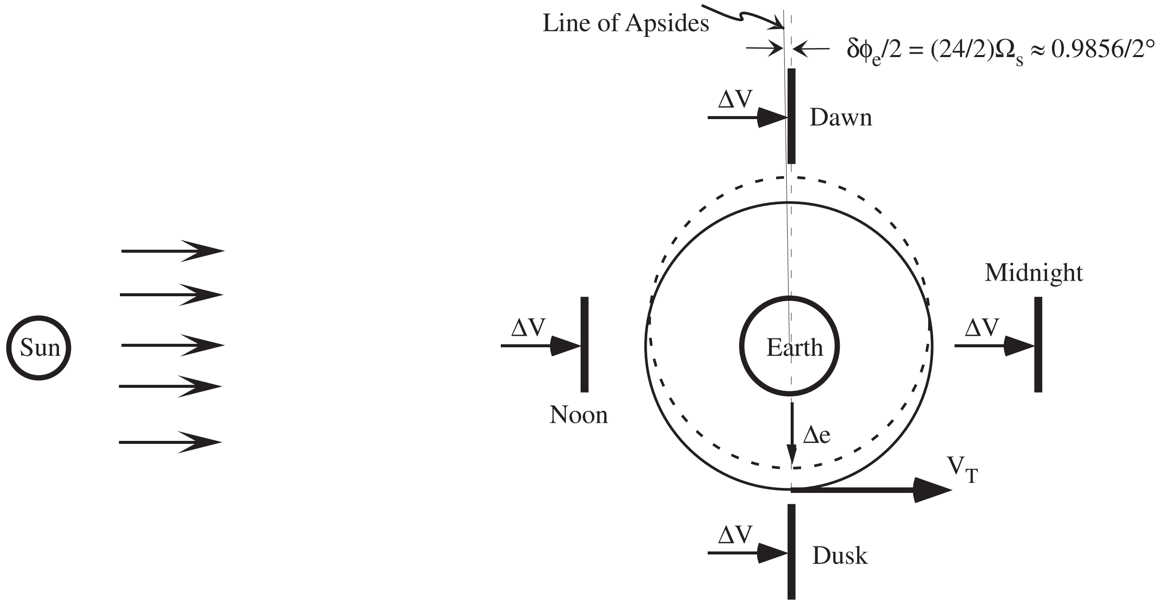

a) Solar radiation force b) Influence of solar radiation force on orbit

$\Delta e = (3/2)[\Delta T/V_T][F/m] = (3/2)[(2\pi/\Omega_o)/V_T][F/m]$; per orbit

$\Delta V_T = \Delta e[V_T/2] = (3/4)\Delta T[F/m]$; per orbit

Typical Spacecraft:

$$\Delta V_T = (3/4)\Delta T[\alpha PA/m] = \Delta V_R/2$$
$$= (3/4)[86400 \text{ sec}][(1\ \mu lb/m^2))(70\ m^2)/(100 \text{ slug})]$$
$$= 0.045 \text{ ft/sec/day} \Rightarrow 16.5 \text{ ft/sec/year}$$

Figure 8.3 Effect of Solar Radiation Pressure on Orbit Must be Nulled by Noon or Midnight Radial ΔV_R.

Notes:
- Acceleration component normal to orbit plane alters inclination, but has zero effect over an orbit.
- Acceleration component at dawn lowers perigee at dusk Δe/3.
- Acceleration component at dusk raises apogee at dawn Δe/3.
- Acceleration component at noon lowers perigee at dusk Δe/6.
- Acceleration component at midnight raises apogee at dawn Δe/6.
- Total effect over one orbit is equal lowering of perigee at dusk and raising of apogee at dawn for total Δe.

Over multiple orbits the acceleration effect accumulates, both increasing eccentricity and rotating the line of apsides. For near-circular orbits the six classical elements are conveniently replaced by three 2-vectors, eccentricity,

[3] The eccentricity 2-vector is in the orbit plane with magnitude e and directed from apogee to perigee, viz. $\mathbf{e} = \mathbf{e}_o^T e[1, 0]$.

inclination, and longitude (argument of perigee and mean anomaly)[4]. Beginning with a perfect orbit, over the first solar day, the small eccentricity δe is induced with line of apsides at inertial angle at half the earth orbit travel from the starting location, $\delta\phi_e/2 = (24\text{hr})/2)\Omega_s = 0.9856^o/2$. On each subsequent day the change is constant in magnitude while advanced in angle by $\delta\phi_e$, close to 1^o, or on the nth day the added vector eccentricity is δe at angle $(n-1/2)\delta\phi_e$. Since only the magnitude of one orbit (daily) change depends on spacecraft parameters, the accumulation over n days is otherwise dependent only on sidereal rate Ω_s for geostationary orbit as

$$\Delta e = \delta e \sum_{i=1}^{n} \begin{bmatrix} \cos(i-1/2)\delta\phi_e \\ \sin(i-1/2)\delta\phi_e \end{bmatrix}; \ .\ n,\ |\Delta e|/\delta e.\ \phi_e \approx \begin{cases} 1,\ 1.00,\ 0.4928^o \\ 14,\ 13.97,\ 6.9^o \\ 30,\ 29.67,\ 14.78^o \\ 183,\ 116.26,\ 90.19^o \\ 365,\ 0.2425,\ 179.9^o \end{cases}. \tag{8.8}$$

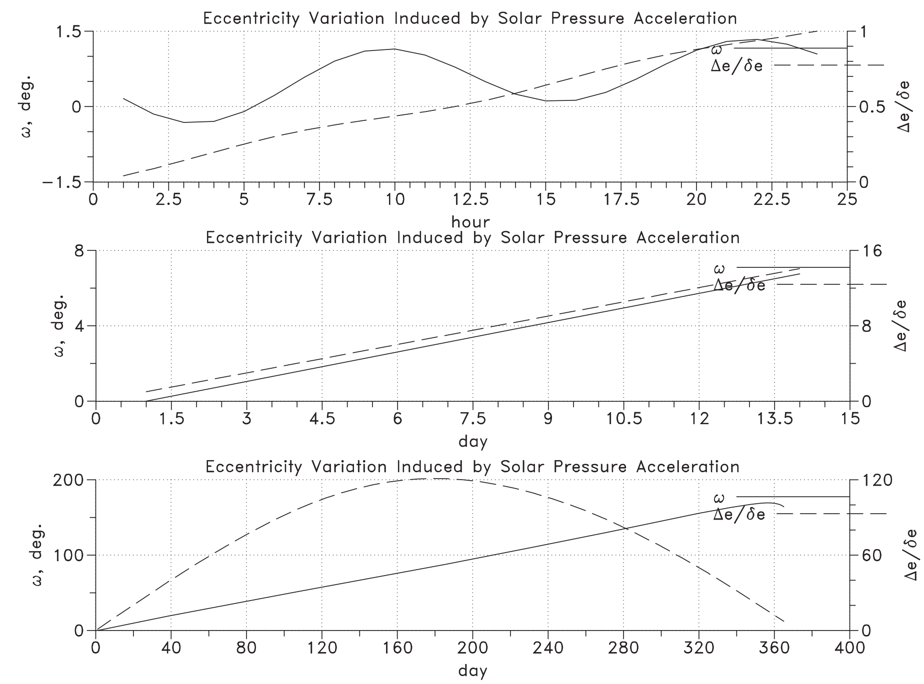

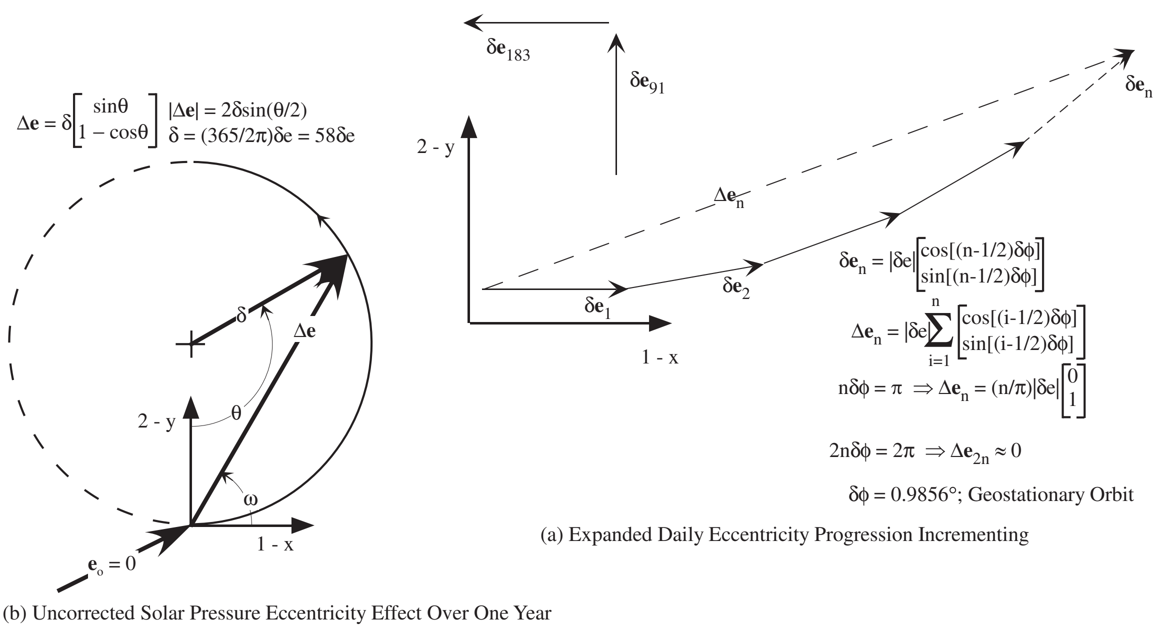

(a) Expanded Daily Eccentricity Progression Incrementing

(b) Uncorrected Solar Pressure Eccentricity Effect Over One Year

Figure 8.4 Path of Eccentricity Vector due to Solar Pressure Acceleration in Geostationary Orbit.

9.0 AMF ΔV Doppler Shift Derivation

9.1 *Radial* ΔV *Calculation*

Consider a ground station at latitude δ and longitude λ with respect to a spacecraft as depicted by Figure 9.1. Let $\mathbf{e}_o$ be a vector basis with 3-axis North and l-axis in the equatorial plane directed from the earth center to the spacecraft cm. The orbit radius vector is

$$\mathbf{r}_o = \mathbf{e}_o^T r_o [1, 0, 0]^T$$

and a vector from earth center to the ground station is

$$\mathbf{r}_s = \mathbf{e}_o^T r_e [\cos\delta\cos\lambda, \cos\delta\sin\lambda, \sin\delta]^T .$$

We wish the component of velocity change colinear with the ground station to spacecraft line of sight, i.e., the vector

$$\mathbf{r}_o - \mathbf{r}_s = \mathbf{e}_o^T [r_o - r_e\cos\delta\cos\lambda, -r_e\cos\delta\sin\lambda, -r_e\sin\delta]^T .$$

To first order for synchronous orbit injection at the transfer orbit ascending node the velocity change $\mathbf{\Delta V}$ can be expressed

$$\mathbf{\Delta V} = \mathbf{e}_o^T [0, V_s - V_t\cos\theta_i, -V_t\sin\theta_i]^T$$

where $V_s = 10,088$ ft/sec and $V_t = 5,280$ ft/sec are respectively drift orbit and transfer orbit perigee velocity magnitudes and θ_i is transfer orbit inclination. Drift orbit inclination is assumed negligible.

The desired radial velocity component is then obtained as

$$\Delta V_n = [\mathbf{r}_o - \mathbf{r}_s] \cdot \mathbf{\Delta V}/|\mathbf{r}_o - \mathbf{r}_s| = -r_e[(V_s - V_t\cos\theta_i)\cos\delta\sin\lambda - V_t\sin\theta_i\sin\delta]/|\mathbf{r}_o - \mathbf{r}_s|$$

where

$$|\mathbf{r}_o - \mathbf{r}_s|^2 = r_o^2 + r_e^2 - 2r_o r_e\cos\delta\cos\lambda .$$

9.2 *Frequency Shift*

Let V_1, V_2 be the radial components of velocity positive away from the ground station before and after AMF. Then the doppler shift is

$$\Delta f = f_2 - f_1 = f_o[1/(1 + V_2/c) - 1/(1 + V_1/c)] \approx f_o[(1 - V_2/c) - (1 - V_1/c)] = -f_o(V_2 - V_1)/c = -f_o\Delta V/c ,$$

where $c = 3 \times 10^8$ m/sec $= 9.84 \times 10^8$ ft/sec is the speed of light and f_o is the down link frequency.

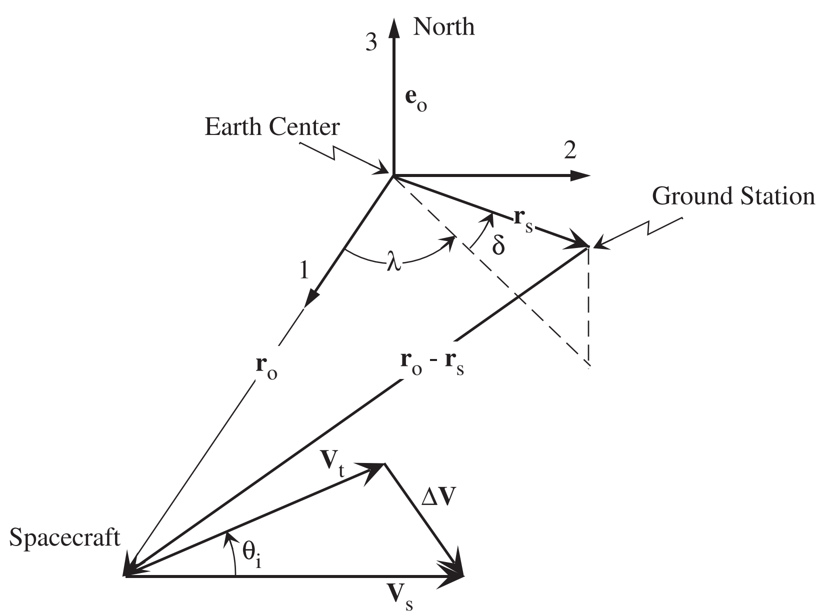

Figure 9.1 Geometry of AMF ΔV and Doppler Frequency Shift Analysis.

10.0 Satellite Ground Track

10.1 *Ground Track of the Sub-Satellite Point (Yaw Axis)*

We develop in this section the trajectory on the earth surface of the subsatellite point of an orbiting satellite in standard earth longitude latitude coordinates. Eq. 10 transforms from an inertial basis (ECI) $\mathbf{e}_i$ to an orbit reference frame $\mathbf{e}_o$ and (11) completes the transformation to a frame $\mathbf{e}_1$ rotating with true anomaly of spacecraft motion having 1-axis earth center to spacecraft directed and 3-axis north. Hence, a unit vector through the subsatellite point is given by

$$\mathbf{u} = \mathbf{e}_1^T[1, 0, 0]^T = \mathbf{e}_o^T A_3^T(v)[1, 0, 0]^T = \mathbf{e}_i^T A_3^T(\Omega)A_1^T(i)A_3^T(\omega + v)[1, 0, 0]^T \ . \qquad (10.1)$$

An earth fixed basis $\mathbf{e}_e$ is related to $\mathbf{e}_i$ as

$$\mathbf{e}_e = A_3(\Omega_e t)\mathbf{e}_i \ , \qquad (10.2)$$

where Ω_e is earth inertial (sidereal) rate, so that the satellite directed unit vector in earth fixed coordinates is

$$\mathbf{u} = \mathbf{e}_e^T A_3(\Omega_e t)A_3^T(\Omega)A_1^T(i)A_3^T(\omega + v)[1, 0, 0]^T = \mathbf{e}_e^T A_3(\Omega_e t - \Omega)A_1^T(i)A_3^T(\omega + v)[1, 0, 0]^T \ . \qquad (10.3)$$

To study just the shape of the ground track trajectory and ignoring lesser orbit perturbations such as nodal regression and perigee drift we can set $\Omega = \omega = 0$, and get

$$\mathbf{u} = \mathbf{e}_e^T A_3(\Omega_e t)A_1^T(i)A_3^T(v)[1, 0, 0]^T = \mathbf{e}_e^T \begin{bmatrix} \cos v \cos \Omega_e t + \sin v \cos i \sin \Omega_e t \\ -\cos v \sin \Omega_e t + \sin v \cos i \cos \Omega_e t \\ \sin v \sin i \end{bmatrix} = \mathbf{e}_e^T [u_1, u_2, u_3]^T \ . \qquad (10.4)$$

Note first that for $i = 0$, $v = \Omega_e t$, the result reduces to $\mathbf{u} = \mathbf{e}_e^T[1, 0, 0]^T$, the *geostationary* case. Defining symbols and noting their relationship to $\mathbf{u}$,

$$\lambda = \mathrm{Tan}^{-1}[u_2/u_1] \approx u_2 \ ; \ \text{longitude} \qquad (10.5a)$$

$$\gamma = \mathrm{Tan}^{-1}[u_3/\sqrt{u_1^2 + u_2^2}] \approx u_3 \ ; \ \text{latitude} \qquad (10.5b)$$

$$= \mathrm{Tan}^{-1}[(\sin v \sin i)/(\cos^2 v + \sin^2 v \cos^2 i)^{1/2}] \ .$$

Taking only $v = \Omega_e t$, provides the *geosynchronous* case as

$$\mathbf{u} = \mathbf{e}_e^T \begin{bmatrix} \cos^2 \Omega_e t + \cos i \sin^2 \Omega_e t \\ (\cos i - 1)\sin\Omega_e t \cos \Omega_e t \\ \sin i \sin \Omega_e t \end{bmatrix} \approx \mathbf{e}_e^T \begin{bmatrix} 1 \\ -(i^2/4)\sin 2\Omega_e t \\ i \sin \Omega_e t \end{bmatrix} ; \ \text{small } i \ . \qquad (10.6a)$$

This yields peak longitude and latitude errors of $u_2 = \lambda = i^2/4$ and $u_3 = \gamma = i$ respectively. The inclination and small angle ground track trajectory are illustrated on Figure 10.1. Small angle pointing errors seen from the spacecraft are altered by the factor $1/(r_o/r_e - 1) = 0.178$.

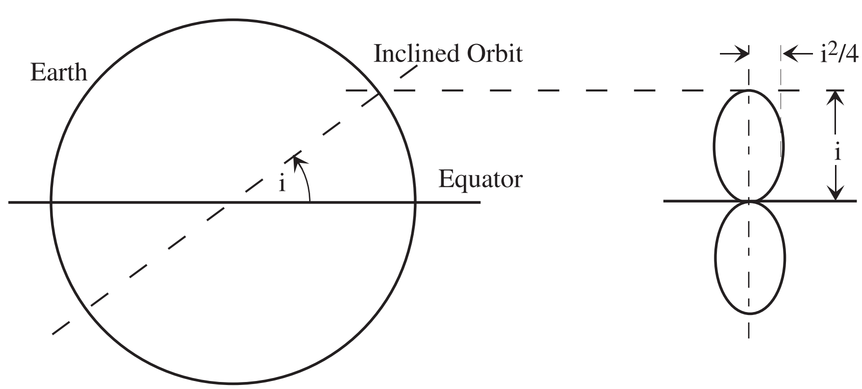

Figure 10.1 Geosynchronous Inclination and Ground Track Geometry.

10.2 *Ground Track Induced by Eccentricity*

Consider the in-plane deviation from mean anomaly M of true anomaly v for a circular orbit induced by variation in eccentricity e. Not very interesting in general, but for a geosynchrouous orbit this results in a small East-West drift over the orbit. Differentiating mean anomaly implicitly in Kepler's Equation and substituting in terms of true anomaly from (1.2a)

$$\frac{dM}{de} = 0 = \frac{d}{de}[E - e\sin E] = (1 - e\cos E)\frac{dE}{de} - \sin E \Rightarrow \frac{dE}{de} = \frac{\sin E}{(1 - e\cos E)} = \frac{\sin v}{\sqrt{1 - e^2}}\ .$$

Then implicitly differentiating cosE or a similar operation with sinE leads after tedious manipulation and substitution to

$$\frac{d}{de}\cos E = -\sin E\frac{dE}{de} = \frac{d}{de}\left[\frac{\cos v + e}{1 + e\cos v}\right] \Rightarrow \frac{dv}{de} = \frac{[2 + e\cos v]\sin v}{[1 - e^2]}\ . \tag{10.6b}$$

At the apoapsides mean anomaly, M, and true anomaly, v, are in sync, while at 90^o past perigee v is ahead (East drift) of M while at $M = 270^o$, v lags behind (West drift).

10.3 *Ground Track of an Arbitrary Spacecraft Axis in Arbitrary Orbit*

In this section we shall investigate the ground track of an arbitrary line or axis fixed in the spacecraft body (or fixed in the orbital basis $\mathbf{e}_1$) with perfect attitude control. We define the axis by the point that intersects the earth surface in an unperturbed equatorial orbit. A unit vector from the spacecraft to earth center has been developed above as $\mathbf{u}$. Using this, the position vector is obtained by multiplying by the orbit radius r_o as

$$\mathbf{r}_o(v, e, \omega, i, \Omega) = \mathbf{e}_1^T r_o(v, e)[1, 0, 0]^T = \mathbf{e}_o^T A_3^T(v) r_o(v, e)[1, 0, 0]^T = \mathbf{e}_i^T A_3^T(\Omega) A_1^T(i) A_3^T(\omega + v) r_o(v, e)[1, 0, 0]^T$$

$$= \mathbf{e}_e^T A_3(\Omega_e t) A_3^T(\Omega) A_1^T(i) A_3^T(\omega + v) r_o(v, e)[1, 0, 0]^T\ , \tag{10.7}$$

while a vector from earth center to a point at longitude, latitude λ_s, δ_s respectively is

$$\mathbf{r}_s = \mathbf{e}_e^T r_e[\cos\lambda_s \cos\delta_s, \sin\lambda_s \cos\delta_s, \sin\delta_s]^T = \mathbf{e}_i^T r_e A_3^T(\Omega_e t)[\cos\lambda_s \cos\delta_s, \sin\lambda_s \cos\delta_s, \sin\delta_s]^T \tag{10.8}$$
$$= \mathbf{e}_o^T r_e A_3(\omega) A_1(i) A_3(\Omega) A_3^T(\Omega_e t)[\cos\lambda_s \cos\delta_s, \sin\lambda_s \cos\delta_s, \sin\delta_s]^T$$
$$= \mathbf{e}_1^T r_e A_3(v + \omega) A_1(i) A_3(\Omega) A_3^T(\Omega_e t)[\cos\lambda_s \cos\delta_s, \sin\lambda_s \cos\delta_s, \sin\delta_s]^T\ .$$

Referring to the geometric sketch in Figure 10.2, we wish to define a vector $\mathbf{r}_t$ in spacecraft body coordinates $\mathbf{e}_b$ that nominally points to a designated point $\mathbf{r}_s$ on the earth surface. Assuming perfect attitude control where the pitch axis is normal to the orbit plane and the yaw axis remains nadir pointed it will be adequate to treat $\mathbf{r}_t$ as fixed in the orbital basis $\mathbf{e}_1$. Hence, we can write $\mathbf{r}_t$ as

$$\mathbf{r}_t = \mathbf{r}_s - \mathbf{r}_o(0) = \mathbf{e}_e^T r_e[\cos\lambda_s \cos\delta_s, \sin\lambda_s \cos\delta_s, \sin\delta_s]^T - \mathbf{e}_1^T r_o[1, 0, 0]^T \tag{10.9}$$

and transform to orbital basis $\mathbf{e}_1$ as

$$\mathbf{r}_t = \mathbf{e}_1^T r_e A_3(v) A_3(\omega) A_1(i) A_3(\Omega) A_3^T(\Omega_e t)[\cos\lambda_s \cos\delta_s, \sin\lambda_s \cos\delta_s, \sin\delta_s]^T - \mathbf{e}_1^T r_o[1, 0, 0]^T \tag{10.10}$$
$$= \mathbf{e}_1^T r_e A_3(\Omega_o t + v_o) A_3(\omega) A_1(i) A_3(\Omega) A_3^T(\Omega_e t)[\cos\lambda_s \cos\delta_s, \sin\lambda_s \cos\delta_s, \sin\delta_s]^T - \mathbf{e}_1^T r_o[1, 0, 0]^T$$
$$= \mathbf{e}_1^T r_e A_3(\Omega_e t) A_3(\omega) A_1(i) A_3(\Omega) A_3^T(\Omega_e t)[\cos\lambda_s \cos\delta_s, \sin\lambda_s \cos\delta_s, \sin\delta_s]^T - \mathbf{e}_1^T r_o[1, 0, 0]^T\ ,$$

where we have sequentially restricted v to a circular orbit, $\dot{v} = \Omega_o$ and geosynchronous orbit $\dot{v} = \Omega_e$. This is a vector, to be taken fixed in the spacecraft body, that points to the designated point on the earth surface at $\mathbf{r}_s$ when the spacecraft body attitude is perfectly aligned with orbital basis $\mathbf{e}_1$ and at some selected instant in time or equivalently true anomaly. At least for geosynchronous orbits it suits our present purpose and simplifies the derivation to define $\mathbf{r}_t$ with $\Omega = i = \omega = 0$ which yields

$$\mathbf{r}_t = \mathbf{e}_1^T r_e[\cos\lambda_s \cos\delta_s, \sin\lambda_s \cos\delta_s, \sin\delta_s]^T - \mathbf{e}_1^T r_o[1, 0, 0]^T = \mathbf{e}_1^T r_e[\cos\lambda_s \cos\delta_s - r_o/r_e, \sin\lambda_s \cos\delta_s, \sin\delta_s]^T\ . \tag{10.11}$$

Using this definition for the body fixed pointing vector, say a beacon null, it transforms back to $\mathbf{e}_1$ as

$$\mathbf{r}_t = \mathbf{e}_b^T r_e[\cos\lambda_s \cos\delta_s - r_o/r_e, \sin\lambda_s \cos\delta_s, \sin\delta_s]^T = \mathbf{e}_1^T A_b^T A_a^T(\phi_1, \phi_2, \phi_3) r_e[\cos\lambda_s \cos\delta_s - r_o/r_e, \sin\lambda_s \cos\delta_s, \sin\delta_s]^T \tag{10.12}$$

where A_a, A_b are the body attitude transformations of (2.11) and (2.12).

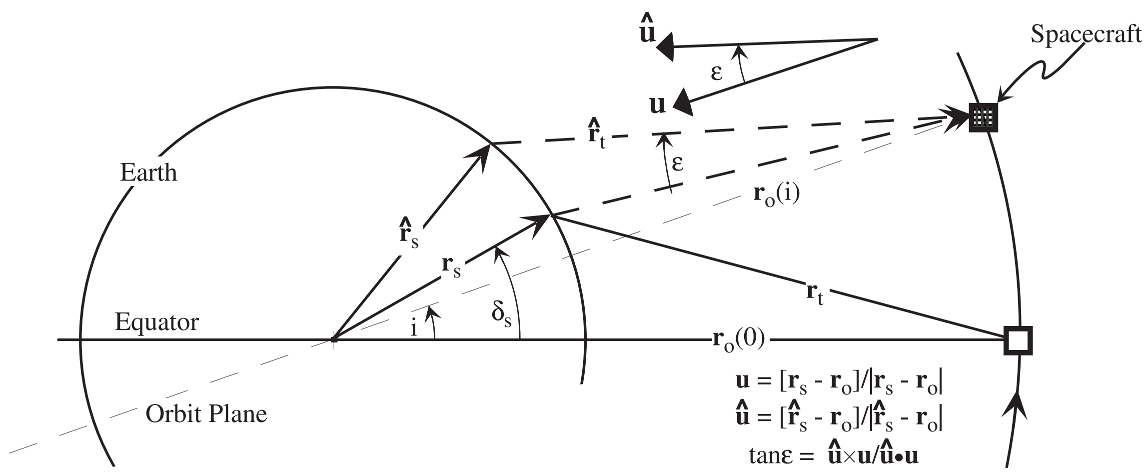

Figure 10.2 General Three Dimensional Pointing or Ground Track Geometry.

Now this vector, fixed in the spacecraft body and in the ideally pointed orbital basis, varies in the earth basis as a function of orbit orientation and spacecraft position in orbit. Rotating back to the earth fixed basis for arbitrary orbit parameters

$$\hat{\mathbf{r}}_t = \mathbf{e}_e^T r_e A_3(\Omega_e t)A_3^T(\Omega)A_1^T(i)A_3^T(\omega)A_3^T(v)[\cos\lambda_s \cos\delta_s - r_o/r_e,\ \sin\lambda_s\cos\delta_s,\ \sin\delta_s]^T \tag{10.13}$$

Again for geosynchronous orbits we take $\Omega = \omega = 0$ and $v = \Omega_e t$, but this time $i \neq 0$,

$$\hat{\mathbf{r}}_t = \mathbf{e}_e^T r_e A_3(\Omega_e t)A_1^T(i)A_3^T(\Omega_e t)[\cos\lambda_s \cos\delta_s - r_o/r_e,\ \sin\lambda_s\cos\delta_s,\ \sin\delta_s]^T \tag{10.14}$$

Next, we require a vector from the spacecraft to the original desired target point on the earth at $\mathbf{r}_s$, given by

$$\tilde{\mathbf{r}}_t = \mathbf{r}_s - \mathbf{r}_o(i) = \mathbf{r}_s - \mathbf{e}_1^T r_o[1,0,0]^T = \mathbf{r}_s - \mathbf{e}_e^T r_o A_3(\Omega_e t)A_3^T(\Omega)A_1^T(i)A_3^T(\omega)A_3^T(v)[1,0,0]^T \tag{10.15}$$

$$= \mathbf{e}_e^T r_e[\cos\lambda_s\cos\delta_s,\ \sin\lambda_s\cos\delta_s,\ \sin\delta_s]^T - \mathbf{e}_e^T r_o A_3(\Omega_e t)A_1^T(i)A_3^T(\Omega_e t)[1,0,0]^T$$

Then we denote with $\hat{\mathbf{u}}$ the general unit vector from the spacecraft to the earth point as

$$\hat{\mathbf{u}} = \frac{\hat{\mathbf{r}}_t}{|\hat{\mathbf{r}}_t|} = \hat{\mathbf{u}}(\Omega_e t, \Omega, i, \omega, v, \lambda_s, \delta_s) = \mathbf{e}_e^T[\hat{u}_1, \hat{u}_2, \hat{u}_3]^T\ . \tag{10.16a}$$

In like fashion for simplicity of notation we drop the ˜ and write

$$\mathbf{u} = \frac{\tilde{\mathbf{r}}_t}{|\tilde{\mathbf{r}}_t|} = \mathbf{u}(\Omega_e t, \Omega, i, \omega, v, \lambda_s, \delta_s) = \mathbf{e}_e^T[u_1, u_2, u_3]^T\ . \tag{10.16b}$$

The ground track of an axis $\mathbf{u}$ for a geostationary orbit having $i = 0$ and $v = \Omega_e t$ is a point and one way to describe the ground track of the same axis $\hat{\mathbf{u}}$ in a spacecraft in the more general orbit is to compute the angle(s) between these two unit vectors. This is perhaps most usefully done as 'azimuth' and 'elevation' or pitch (ε_3) and roll (ε_1) angles in the true spacecraft orbit plane basis $\mathbf{e}_1$ as these are representative of the attitude steering angles required to point at the fixed ground track point despite the perturbation. In terms of the unit vector components

$$\sin\varepsilon_3 = \mathbf{e}_e^T\frac{[\hat{u}_1, \hat{u}_2, 0]^T}{\sqrt{\hat{u}_1^2+\hat{u}_2^2}} \times \mathbf{e}_e^T\frac{[u_1, u_2, 0]^T}{\sqrt{u_1^2+u_2^2}} = \frac{\hat{u}_1u_2 - \hat{u}_2u_1}{[(\hat{u}_1^2+\hat{u}_2^2)(u_1^2+u_2^2)]^{1/2}} \tag{10.17a}$$

$$\cos\varepsilon_3 = \mathbf{e}_e^T\frac{[\hat{u}_1, \hat{u}_2, 0]^T}{\sqrt{\hat{u}_1^2+\hat{u}_2^2}} \cdot \mathbf{e}_e^T\frac{[u_1, u_2, 0]^T}{\sqrt{u_1^2+u_2^2}} = \frac{\hat{u}_1u_1 + \hat{u}_2u_2}{[(\hat{u}_1^2+\hat{u}_2^2)(u_1^2+u_2^2)]^{1/2}} \tag{10.17b}$$

$$\sin\varepsilon_1 = \mathbf{e}_e^T[0, \sqrt{\hat{u}_1^2+\hat{u}_2^2}, \hat{u}_3]^T \times \mathbf{e}_e^T[0, \sqrt{u_1^2+u_2^2}, u_3]^T = u_3\sqrt{\hat{u}_1^2+\hat{u}_2^2} - \hat{u}_3\sqrt{u_1^2+u_2^2} \tag{10.17c}$$

$$\cos\varepsilon_1 = \mathbf{e}_e^T[0, \sqrt{\hat{u}_1^2+\hat{u}_2^2}, \hat{u}_3]^T \cdot \mathbf{e}_e^T[0, \sqrt{u_1^2+u_2^2}, u_3]^T = \sqrt{\hat{u}_1^2+\hat{u}_2^2}\sqrt{u_1^2+u_2^2} + u_3\hat{u}_3\ . \tag{10.17d}$$

The polar angle between the two is simply given by the vector products

$$\sin\varepsilon = |\hat{\mathbf{u}} \times \mathbf{u}| \; ; \;\; \cos\varepsilon = \hat{\mathbf{u}} \cdot \mathbf{u} \; . \tag{10.18}$$

In some applications it may be useful to compute the earth longitude and latitude errors between $\mathbf{r}_s$ and $\hat{\mathbf{r}}_s$. These attitude angles will describe the ground track or pointing error excursions induced by orbit motion of an arbitrary axis in the spacecraft body when the nominal attitude control system tracks nadir or the subsatellite point with pitch axis (3-axis in $\mathbf{e}_1$) orbit normal.

Expanding the earth point radius with $\Omega = \omega = 0$ produces

$$\hat{\mathbf{r}}_t = \mathbf{e}_e^T r_e \begin{bmatrix} \cos v \cos\Omega_e t + \cos i \sin v \sin\Omega_e t & -\cos v \sin\Omega_e t + \cos i \sin v \cos\Omega_e t & -\sin i \sin v \\ -\sin v \cos\Omega_e t + \cos i \cos v \sin\Omega_e t & \sin v \sin\Omega_e t + \cos i \cos v \cos\Omega_e t & -\sin i \cos v \\ \sin i \sin\Omega_e t & \sin i \cos\Omega_e t & \cos i \end{bmatrix} \begin{bmatrix} \cos\lambda_s \cos\delta_s - r_o/r_e \\ \sin\lambda_s \cos\delta_s \\ \sin\delta_s \end{bmatrix}, \tag{10.19}$$

and

$$\tilde{\mathbf{r}}_t = \mathbf{e}_e^T r_e \begin{bmatrix} \cos\lambda_s \cos\delta_s \\ \sin\lambda_s \cos\delta_s \\ \sin\delta_s \end{bmatrix} - \mathbf{e}_e^T r_o \begin{bmatrix} \cos v \cos\Omega_e t + \cos i \sin v \sin\Omega_e t \\ -\sin v \cos\Omega_e t + \cos i \cos v \sin\Omega_e t \\ \sin i \sin\Omega_e t \end{bmatrix} . \tag{10.20}$$

This can easily be generalized to specific orbit orientation by substituting $\Omega_e t = \Omega_e t - \Omega$ and $v = v + \omega$. Instead, we choose here to particularize it to the geosynchronous orbit by substituting $v = \Omega_e t$, to get

$$\hat{\mathbf{r}}_t = \mathbf{e}_e^T r_e \begin{bmatrix} 1 + (\cos i - 1)\sin^2\Omega_e t & (\cos i - 1)\sin\Omega_e t \cos\Omega_e t & -\sin i \sin\Omega_e t \\ (\cos i - 1)\sin\Omega_e t \cos\Omega_e t & 1 + (\cos i - 1)\cos^2\Omega_e t & -\sin i \cos\Omega_e t \\ \sin i \sin\Omega_e t & \sin i \cos\Omega_e t & \cos i \end{bmatrix} \begin{bmatrix} \cos\lambda_s \cos\delta_s - r_o/r_e \\ \sin\lambda_s \cos\delta_s \\ \sin\delta_s \end{bmatrix}, \tag{10.21}$$

$$\tilde{\mathbf{r}}_t = \mathbf{e}_e^T r_e \begin{bmatrix} \cos\lambda_s \cos\delta_s - (r_o/r_e)[1 + (\cos i - 1)\sin^2\Omega_e t] \\ \sin\lambda_s \cos\delta_s - (r_o/r_e)[(\cos i - 1)\sin\Omega_e t \cos\Omega_e t] \\ \sin\delta_s - (r_o/r_e)[\sin i \sin\Omega_e t] \end{bmatrix} .$$

These give an expansion of $\hat{\mathbf{u}}$ and $\mathbf{u}$ for geosynchronous orbits. The previously derived subsatellite point ground track results by applying this with $\lambda_s = \delta_s = 0$.

Although we now have expressions to compute pointing excursions ε_1, ε_3, this is still perhaps too much information as it computes the angles at every point in time. Instead, it seems desirable to compute just the maximum excursions of each. Analytically this appears quite unwieldy, so at least for geosynchronous orbits with limited inclination, say < 30°, we shall apply judgement and guess that the maximum excursions occur at the same points as previously developed to the simpler case of subsatellite pointing, i.e., maximum roll error at the apsides 90° from the node, and maximum pitch error at the four points 45° from the nodes. By our arbitrary selection of $\Omega = \omega = 0$ the node and "perigee" are both at Aries, as is the satellite at t = 0. Choosing the satellite longitude on the earth at Aries also at t = 0 and using λ_s as station longitude with with respect to the satellite longitude, we then get the apsides at $\Omega_e t = \pm 90°$ and the pitch extremes at $\Omega_e t = \pm 45°$ and $180° \pm 45°$. Then

$$\hat{\mathbf{r}}_t = \mathbf{e}_e^T r_e \begin{bmatrix} \cos i & 0 & \mp\sin i \\ 0 & 1 & 0 \\ \pm\sin i & 0 & \cos i \end{bmatrix} \begin{bmatrix} \cos\lambda_s \cos\delta_s - r_o/r_e \\ \sin\lambda_s \cos\delta_s \\ \sin\delta_s \end{bmatrix} = \mathbf{e}_e^T r_e \begin{bmatrix} \cos i[\cos\lambda_s \cos\delta_s - r_o/r_e] \mp \sin i \sin\delta_s \\ \sin\lambda_s \cos\delta_s \\ \pm\sin i[\cos\lambda_s \cos\delta_s - r_o/r_e] + \cos i \sin\delta_s \end{bmatrix}; \;\; \Omega_e t = \pm 90°$$

$$= \mathbf{e}_e^T r_e \begin{bmatrix} \cos i[\cos\delta_s - r_o/r_e] \mp \sin i \sin\delta_s \\ 0 \\ \pm\sin i[\cos\delta_s - r_o/r_e] + \cos i \sin\delta_s \end{bmatrix} = \mathbf{e}_e^T r_e \begin{bmatrix} \cos(\delta_s \pm i) - (r_o/r_e)\cos i \\ 0 \\ \sin(\delta_s \pm i) \mp (r_o/r_e)\sin i \end{bmatrix}; \;\; \Omega_e t = \pm 90° \;, \lambda_s = 0 \tag{10.22}$$

and

$$\hat{\mathbf{u}} = \mathbf{e}_e^T \frac{1}{\sqrt{1 + (r_o/r_e)^2 - 2(r_o/r_e)\cos\delta_s}} \begin{bmatrix} \cos(\delta_s \pm i) - (r_o/r_e)\cos i \\ 0 \\ \sin(\delta_s \pm i) \mp (r_o/r_e)\sin i \end{bmatrix}; \;\; \Omega_e t = \pm 90° \;, \lambda_s = 0 \tag{10.23}$$

Similarly we expand the second vector

$$\tilde{\mathbf{r}}_t = \mathbf{e}_e^T r_e \begin{bmatrix} \cos\lambda_s \cos\delta_s - (r_o/r_e)\cos i \\ \sin\lambda_s \cos\delta_s \\ \sin\delta_s \mp (r_o/r_e)\sin i \end{bmatrix} ;\ \Omega_e t = \pm 90^o \quad = \mathbf{e}_e^T r_e \begin{bmatrix} \cos\delta_s - (r_o/r_e)\cos i \\ 0 \\ \sin\delta_s \mp (r_o/r_e)\sin i \end{bmatrix} ;\ \Omega_e t = \pm 90^o\ ,\ \lambda_s = 0 \tag{10.24}$$

$$\mathbf{u} = \mathbf{e}_e^T \frac{1}{\sqrt{1 + (r_o/r_e)^2 - 2(r_o/r_e)\cos(\delta_s \mp i)}} \begin{bmatrix} \cos\delta_s - (r_o/r_e)\cos i \\ 0 \\ \sin\delta_s \mp (r_o/r_e)\sin i \end{bmatrix} ;\ \Omega_e t = \pm 90^o\ ,\ \lambda_s = 0 \tag{10.25}$$

hence,

$$\tan\varepsilon_1 = \frac{|\hat{\mathbf{u}} \times \mathbf{u}|}{\hat{\mathbf{u}} \cdot \mathbf{u}} = \frac{\pm\sin i + (r_o/r_e)[\sin(\delta_s \mp i) - \sin\delta_s]}{(r_o/r_e)^2 + \cos i - (r_o/r_e)[\cos(\delta_s \mp i) + \cos\delta_s]}\ . \tag{10.26}$$

For the other limiting case where we expect maximum pitch error

$$\hat{\mathbf{r}}_t = \mathbf{e}_1^T \frac{r_e}{2} \begin{bmatrix} (\cos i + 1) & \pm(\cos i - 1) & \mp\sqrt{2}\sin i \\ \pm(\cos i - 1) & (\cos i + 1) & \sqrt{2}\sin i \\ \pm\sqrt{2}\sin i & \sqrt{2}\sin i & \cos i \end{bmatrix} \begin{bmatrix} \cos\lambda_s \cos\delta_s - r_o/r_e \\ \sin\lambda_s \cos\delta_s \\ \sin\delta_s \end{bmatrix} \tag{10.27}$$

$$= \mathbf{e}_e^T \frac{r_e}{2} \begin{bmatrix} 2\cos\lambda_s \cos\delta_s - (r_o/r_e)[\cos i + 1] \\ 2\sin\lambda_s \cos\delta_s \mp (r_o/r_e)[\cos i - 1] \\ 2\sin\delta_s \mp \sqrt{2}(r_o/r_e)[\sin i] \end{bmatrix} ;\ \Omega_e t = \pm 45^o\ .$$

10.4 *Fixed Point Attitude Tracking(Beacon Tracking)*

The above ground track or attitude angles assume attitude control tracking of the subsatellite point, which itself is moving on the earth surface. This would result for example by earth sensor attitude sensing with no supplemental orbit corrections. Another case of significant interest is when a spacecraft beacon sensor tracks an earth fixed beacon, while we are interested in the pointing error excursions of some other axis in the spacecraft body due to orbital motion. In the above we defined the spacecraft axis, say a beacon boresight, by the earth longitude latitude coordinates λ_s, δ_s where this axis intercepts the earth in the absence of orbit perturbation. Hence, the attitude angles may be written as $\varepsilon_1(\lambda_s, \delta_s)$, $\varepsilon_3(\lambda_s, \delta_s)$. In the case of beacon tracking where we wish the pointing excursions of a second point, say λ_t, δ_t while the beacon pointing error is nulled, we denote the residual by $\delta\varepsilon_i$ and compute it as

$$\delta\varepsilon_i = \varepsilon_i(\lambda_t, \delta_t) - \varepsilon_i(\lambda_s, \delta_s)\ . \tag{10.28}$$

10.5 *Doppler Shift Evaluation for Inclined Orbit*

The doppler frequency shift is proportional to the velocity along the line of sight to the radiation source

$$\dot{r} = \frac{d\tilde{\mathbf{r}}_t}{dt} \cdot \frac{\tilde{\mathbf{r}}_t}{|\tilde{\mathbf{r}}_t|}\ . \tag{10.29}$$

The indicated derivative is

$$\frac{d\tilde{\mathbf{r}}_t}{dt} = \mathbf{e}_e^T - r_o\Omega_e \begin{bmatrix} (\cos i - 1)2\sin\Omega_e t \cos\Omega_e t \\ (\cos i - 1)[\cos^2\Omega_e t - \sin^2\Omega_e t] \\ \sin i \cos\Omega_e t \end{bmatrix} = \mathbf{e}_e^T - r_o\Omega_e \begin{bmatrix} (\cos i - 1)\sin 2\Omega_e t \\ (\cos i - 1)\cos 2\Omega_e t \\ \sin i \cos\Omega_e t \end{bmatrix} . \tag{10.30}$$

The dominant term is the 1-axis term

$$\dot{r} \approx -r_o\Omega_e(\cos i - 1)\sin 2\Omega_e t\ . \tag{10.31}$$

11.0 Simple Eclipse Model

Let $\mathbf{r}_o$ and $\mathbf{r}_h = r_h\mathbf{s}$ be vectors respectively from earth center to a spacecraft and the sun, expanded in the same basis $\mathbf{e}_i$ in Eqs. 37 and 44 respectively. Eclipse occurs when the angle ν between the two vectors $-\mathbf{r}_o$ and $\mathbf{r}_h - \mathbf{r}_o$, say

$$\tan\nu = \frac{[\mathbf{r}_h - \mathbf{r}_o]\times\mathbf{r}_o}{|\mathbf{r}_h - \mathbf{r}_o|\cdot|\mathbf{r}_o|} \approx \frac{\mathbf{r}_h\times\mathbf{r}_o}{|\mathbf{r}_h|\cdot|\mathbf{r}_o|} \tag{11.1}$$

is less than the earth chord. Let the earth and sun angular subtense as seen from the spacecraft whose eclipse we are modeling be respectively λ_e, and $\lambda_s = 0.53^o$. Assuming the earth disk as much larger than the sun, we can approximate the earth edge as a straight line passing across the circular sun disk. This should hold for all satellites having orbit radius small compared to the earth-sun distance. Denoting the sun disk radius as r, and a measurement of the visible portion along a diameter normal to the earth edge as r + x, the ratio of eclipsed area A_x to total area $A = \pi r^2$ is

$$A_x/A = \begin{cases} 1\ ;\ \ x/r \le -1 \\ \{r^2[\pi/2 - \mathrm{Sin}^{-1}x/r] - x\sqrt{r^2 - x^2}\}/[\pi r^2] = \{[\pi/2 - \mathrm{Sin}^{-1}x/r] - (x/r)\sqrt{1-(x/r)^2}\}/[\pi]\ ;\ -1 < x/r < 1\ . \\ 0\ ;\ \ x/r \ge +1 \end{cases} \tag{11.2}$$

Then a solar array with normal pointed at angle θ with respect to the sun line will have output current

$$I_P = I_m \cos\theta[1 - A_x/A] \tag{11.3}$$

where I_m is maximum current the panel can produce. Let ξ denote true anomaly referenced to midnight, i.e., at midnight $\xi(t) = 0$. For a circular orbit, for example

$$\xi(t) = \mathrm{mod}[\Omega_o t, 2\pi]\ \varepsilon\ (0, 2\pi)\ . \tag{11.4}$$

Then let

$$\lambda(t) = \begin{cases} \xi(t)\ ;\ \ 0 \le \xi(t) \le \pi \\ \xi(t) - 2\pi\ ;\ \ \pi < \xi(t) < 2\pi \end{cases} = \xi(t) - \pi\{\mathrm{sgn}[\xi(t) - \pi] + 1\}\ \varepsilon\ (-\pi, \pi) \tag{11.5}$$

so that $\lambda(t)$ passes symmetrically through zero at midnight and any eclipse is centered at $\lambda(t) = 0$ with entry and exit symmetrically spaced on each side at $\pm\lambda_e/2$. Then

$$x = (2r/\lambda_s)(|\lambda(t)| - \lambda_e/2) \tag{11.6}$$

We handle the case where the sun is out of the orbit plane by angle β by reducing the earth disk angular subtense accordingly as

$$\sin(\lambda_e/2) = \frac{\sqrt{(r_e/r_o)^2 - \sin^2\beta}}{\cos\beta} \tag{11.7}$$

where r_e, r_o are respectively earth and orbit radius. Note that for non circular orbits r_o is not constant.

For geosynchronous orbit where $\Omega_o = 0.25^o$/min, eclipse seasons are about 40 days in duration when $\beta < 8.2^o$ with maximum eclipse length at equinox of 70 min and average eclipse duration of 53 min.

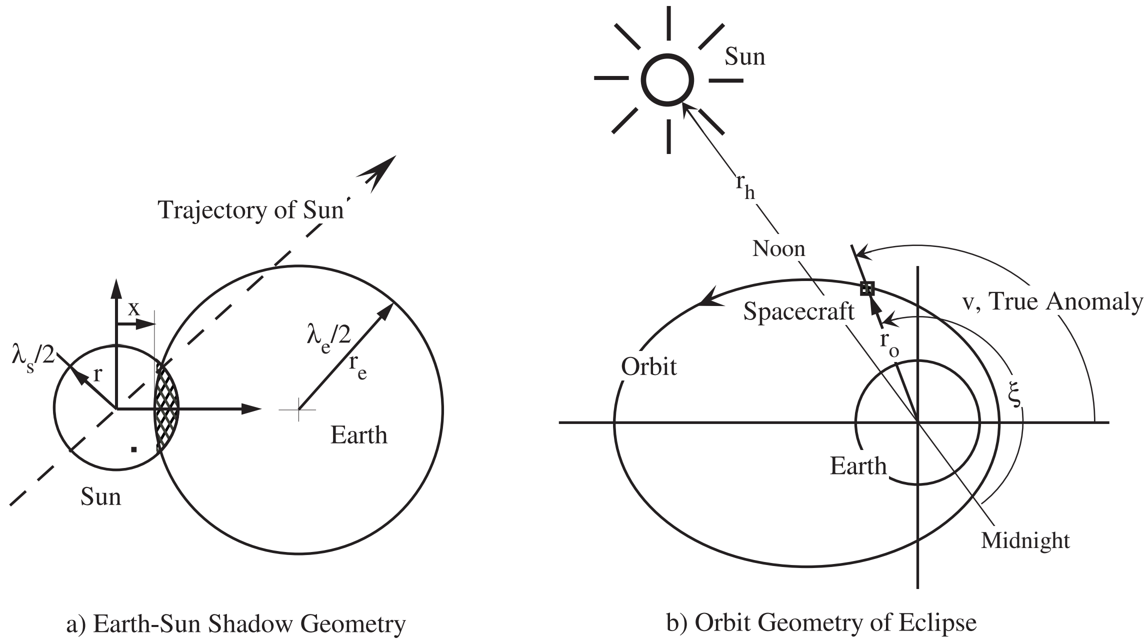

Figure 11.1 Simplified Earth-Sun-Satellite Eclipse Geometry.

12.0 Pointing Errors Induced by Orbit Perturbations

12.1 Orbit Inclination

When an earth-center sensing sensor is used, orbit inclination induces all three of North-South (roll), East-West (pitch), and yaw pointing errors which are cyclic at diurnal frequency for roll and yaw and twice diurnal frequency for pitch. The error geometry is depicted on Figure 12.1. This may be viewed as either a pure inclination or a pure longitude error geometry. For the latter the curved arc viewed as the orbit trajectory, while for the former it is simply the path of the inclination change. A payload offset pointing angle α is assumed to point to the target point a r_2, say at latitude λ. The offset pointing angle and latitude are related by

$$\lambda = \mathrm{Sin}^{-1}\{r_o \sin\alpha/r_e\} - \alpha \approx \alpha\{r_o/r_e - 1\}\ ;\ \ \alpha, \lambda \text{ small} \tag{12.1a}$$

or

$$\alpha = \mathrm{Tan}^{-1}\{\sin\lambda/(r_o/r_e - \cos\lambda)\} \approx \lambda/\{r_o/r_e - 1\}\ ;\ \ \alpha, \lambda \text{ small.} \tag{12.1b}$$

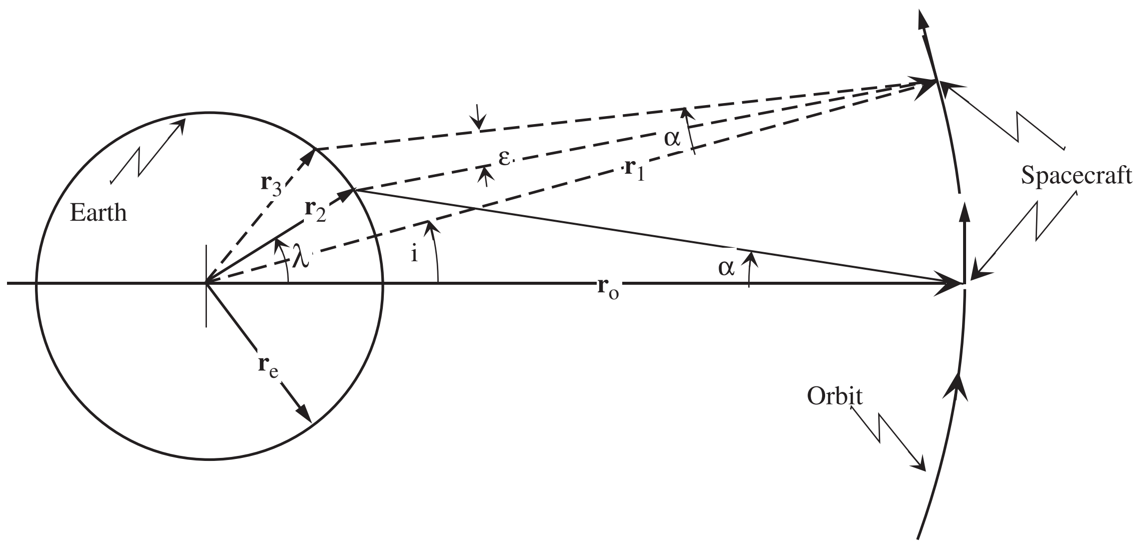

Figure 12.1 Pointing Error Induced by Orbit Perturbation with Earth-Center Pointing Sensor.

In Figure 12.1, i is the orbit inclination angle and ε is the resultant North-South pointing error. We write

$$\mathbf{r}_1 = \mathbf{r}_o[\cos i, \sin i, 0]^T \tag{12.2}$$

$$\mathbf{r}_2 = \mathbf{r}_e[\cos\lambda, \sin\lambda, 0]^T \tag{12.3}$$

$$\mathbf{r}_3 = \mathbf{r}_e[\cos(\lambda + i), \sin(\lambda + i), 0]^T \tag{12.4}$$

while

$$\tan\varepsilon = \frac{|[\mathbf{r}_1 - \mathbf{r}_2]\times[\mathbf{r}_1 - \mathbf{r}_3]|}{|[\mathbf{r}_1 - \mathbf{r}_2]\cdot[\mathbf{r}_1 - \mathbf{r}_3]|} = \frac{\sin i + (r_o/r_e)[\sin(\lambda - i) - \sin\lambda]}{(r_o/r_e)^2 + \cos i - (r_o/r_e)[\cos(\lambda - i) + \cos\lambda]}\ . \tag{12.5}$$

$$\approx \varepsilon \approx \frac{i[1 - (r_o/r_e)\cos\lambda]}{(r_o/r_e)^2 + 1 - (r_o/r_e)[i\sin\lambda + 2\cos\lambda]}\ ;\ \ i \text{ small},$$

$$\approx i/(r_o/r_e - 1)\ ;\ \ i, \lambda \text{ small}.$$

This equation gives the extreme North-South pointing error ε, occurring at the orbit apsides, due to orbit inclination i provided the pitch axis (spin axis) is maintained at orbit normal. A yaw error equal to i will also occur at the orbit nodes. If the spin axis is maintained at equatorial normal the North-South and yaw errors become respectively $\varepsilon + i$ and zero. This attitude is advantageous for a spacecraft with active North-South pointing capability, such as a roll gimbaled payload, to simultaneously minimize both roll and yaw errors. Approximate pointing error expressions for small i, λ are summarized on Table 12.1.

Table 12.1. Pointing Errors Due to Orbit Inclination.

Nominal Attitude	Error		
	Roll	Pitch	Yaw
Orbit Normal	$i/[r_o/r_e - 1] = 0.178\,i$	$(i^2/4)/[r_o/r_e - 1]$	i
Equatorial Normal	$i(r_o/r_e)/[r_o/r_e - 1] = 1.178\,i$	$(i^2/4)/[r_o/r_e - 1]$	0

For the limiting case of λ at a grazing angle, i.e., spacecraft to target point line tangent to the earth disk,

$$\sin\lambda = \sqrt{r_o^2 - r_e^2}/r_o \;;\; \cos\lambda = r_e/r_o \;, \tag{12.6}$$

and

$$\varepsilon \approx -(i^2/2)(r_e/r_o)\sqrt{1 - (r_e/r_o)^2} = i^2/13.4 \;;\; \text{synchronous orbit.} \tag{12.7}$$

The above error was computed assuming a pointing reference, such as an earth sensor, that maintains the spacecraft yaw axis nadir pointed. A related case of interest is when a beacon tracking sensor is used which maintains a spacecraft axis (beacon LOS) pointed at a fixed point on the earth surface. Then, the pointing error at a target point λ_t is computed as the difference between errors introduced at the beacon at say λ_s and the target point, i.e., using (5)

$$\delta\varepsilon = \varepsilon(\lambda_t) - \varepsilon(\lambda_s) \;. \tag{12.8}$$

12.2 Longitude Drift

The geometry of longitudinal drift is identical to Figure 12.1 where α is payload pitch pointing offset, λ is the longitude displacement of the payload target point from the on-station subsatellite point, and i is the satellite longitude drift angle. Thus, the East-West (pitch) pointing error for longitude drift is given by Eq. 5. There are no roll and yaw errors related to longitude drift.

12.3 Roll and Pitch Errors Induced by Yaw Error

A number of trigonometric relations applicable to the spacecraft-earth geometry are summarized on Figure 12.3. At an arbitrary point on the earth surface a yaw attitude error ε_3 introduces roll and pitch pointing errors ε_1, ε_2 as illustrated on Figure 12.2.

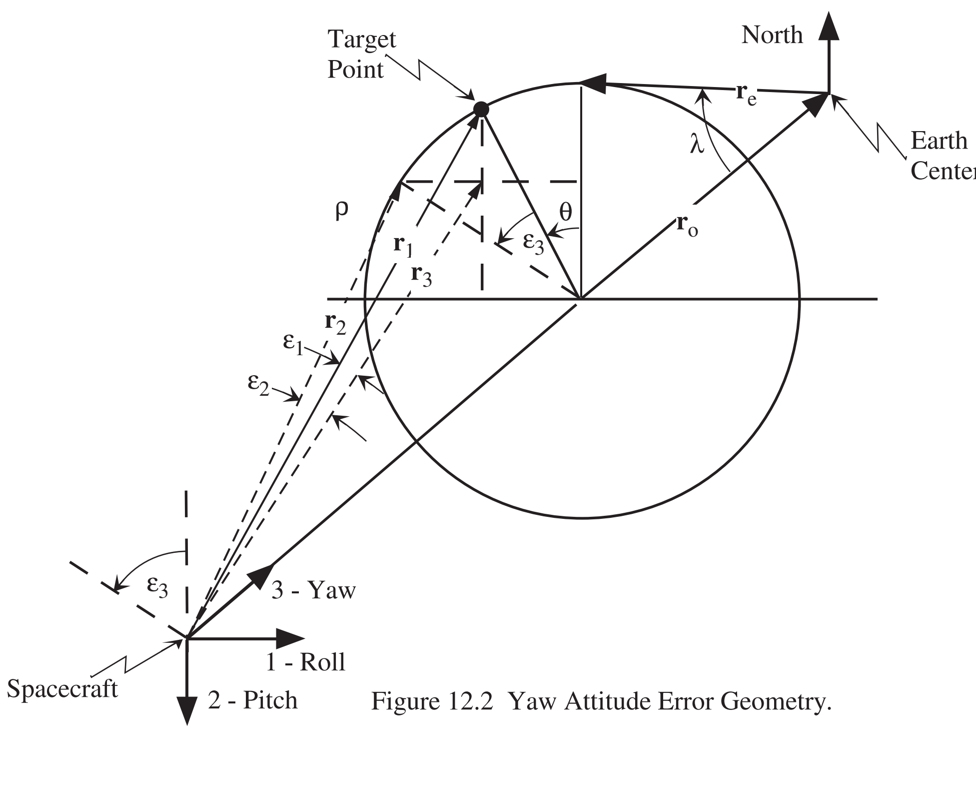

Figure 12.2 Yaw Attitude Error Geometry.

Three position vectors shown and used for calculating roll and pitch errors are

$$r_1 = [-r_e \sin\lambda \sin\theta, -r_e \sin\lambda \cos\theta, r_o - r_e \cos\lambda]^T = [x, y, z]^T \tag{12.9}$$

$$r_2 = [-r_e \sin\lambda \sin(\theta + \varepsilon_3), -r_e \sin\lambda \cos(\theta + \varepsilon_3), r_o - r_e \cos\lambda]^T \tag{12.10}$$

$$r_3 = [-r_e \sin\lambda \sin\theta, -r_e \sin\lambda \cos(\theta + \varepsilon_3), r_o - r_e \cos\lambda]^T . \tag{12.11}$$

With appropriate resolution of the sign ambiguity, the roll error is obtained as

$$\tan\varepsilon_1 = \pm|r_1 \times r_3|/|r_1 \cdot r_3| \tag{12.12}$$

$$= \frac{\pm[\cos(\theta+\varepsilon_3) - \cos\theta] r_e \sin\lambda [(r_e \cos\lambda \sin\theta)^2 + (r_o - r_e\cos\lambda)^2]^{1/2}}{[r_o - r_e\cos\lambda]^2 + [r_e \sin\lambda]^2[\cos\theta\cos(\theta+\varepsilon_3) + \sin^2\theta]}$$

$$\approx \frac{\pm\varepsilon_3 \sin\theta [r_e\sin\lambda][(r_e\cos\lambda\sin\theta)^2 + (r_o - r_e\cos\lambda)^2]^{1/2}}{[r_o - r_e\cos\lambda]^2 + [r_e\sin\lambda]^2} \to \varepsilon_3 (r_e/r_o)\sin\theta \sin\lambda = -(x/r_o)\varepsilon_3 \ ; \ r_e \ll r_o ,$$

$$= \frac{\pm\varepsilon_3 r_e \sin\lambda [(r_e\cos\lambda)^2 + (r_o - r_e\cos\lambda)^2]^{1/2}}{[r_o - r_e\cos\lambda]^2 + [r_e\sin\lambda]^2} \ ; \theta \to 90^o$$

the latter two forms for small ε_3. As $\theta \to 0$,

$$\tan\varepsilon_1 \approx \varepsilon_1 \approx \frac{\pm(\varepsilon_3^2/2) r_e \sin\lambda [r_o - r_e\cos\lambda]}{r_o^2 + r_e^2 - 2r_o r_e \cos\lambda} \ ; \ \theta \to 0 , \tag{12.13}$$

while

$$\tan\varepsilon_1 \approx \varepsilon_1 \approx \frac{\pm\varepsilon_3 r_e \sin\lambda}{\{r_o^2 + r_e^2 - 2r_o r_e\cos\lambda\}^{1/2}} \to \pm\varepsilon_3[r_e/r_o]\sin\lambda \ ; \ r_e/r_o \ll 1, \theta \to 90^o . \tag{12.14}$$

For worst case at the grazing tangent angle

$$\sin\lambda = [1 - (r_e/r_o)^2]^{1/2} \ ; \ \cos\lambda = r_e/r_o \tag{12.15}$$

$$\tan\varepsilon_1 \approx \frac{\pm\varepsilon_3 (r_e/r_o)\sin\theta \{[(r_e/r_o)^2 \sin\theta]^2 + [1 - (r_e/r_o)^2]^2\}^{1/2}}{[1 - (r_e/r_o)^2]^{1/2}} \tag{12.16}$$

$$\approx \frac{\pm\varepsilon_3 (r_e/r_o) \{[(r_e/r_o)^2]^2 + [1 - (r_e/r_o)^2]^2\}^{1/2}}{[1 - (r_e/r_o)^2]^{1/2}} \ ; \theta \to 90^o$$

$$\approx \pm[r_e/r_o]\varepsilon_3 \ ; \ r_e/r_o \ll 1$$

$$= \pm 0.15\, \varepsilon_3 \ ; \ \text{geosynchronous orbit} .$$

Similarly the pitch pointing error is

$$\tan\varepsilon_2 = \pm|r_2 \times r_3|/|r_2 \cdot r_3| \tag{12.17}$$

$$= \frac{\pm[\sin(\theta+\varepsilon_3) - \sin\theta] r_e \sin\lambda [(r_e \sin\lambda \cos(\theta+\varepsilon_3))^2 + (r_o - r_e\cos\lambda)^2]^{1/2}}{[r_o - r_e\cos\lambda]^2 + [r_e\sin\lambda]^2[\sin\theta\sin(\theta+\varepsilon_3) + \cos^2(\theta+\varepsilon_3)]}$$

$$\approx \frac{\pm\varepsilon_3 \cos\theta [r_e\sin\lambda][(r_e\sin\lambda\cos\theta)^2 + (r_o - r_e\cos\lambda)^2]^{1/2}}{[r_o - r_e\cos\lambda]^2 + [r_e\sin\lambda]^2} \to \varepsilon_3 (r_e/r_o)\cos\theta \sin\lambda = -(y/r_o)\varepsilon_3 \ ; \ r_e \ll r_o ,$$

when ε_3 is small. As θ vanishes,

$$\tan\varepsilon_2 \approx \varepsilon_2 \approx \frac{\pm\varepsilon_3 r_e \sin\lambda}{\{r_o^2 + r_e^2 - 2r_o r_e\cos\lambda\}^{1/2}} \to \pm\varepsilon_3[r_e/r_o]\sin\lambda \ ; \ r_e/r_o \ll 1, \theta \to 0^o . \tag{12.18}$$

Maximum pitch error occurs when $\theta \to 0$ for maximum λ and is the same as maximum roll error in (12.16) above.

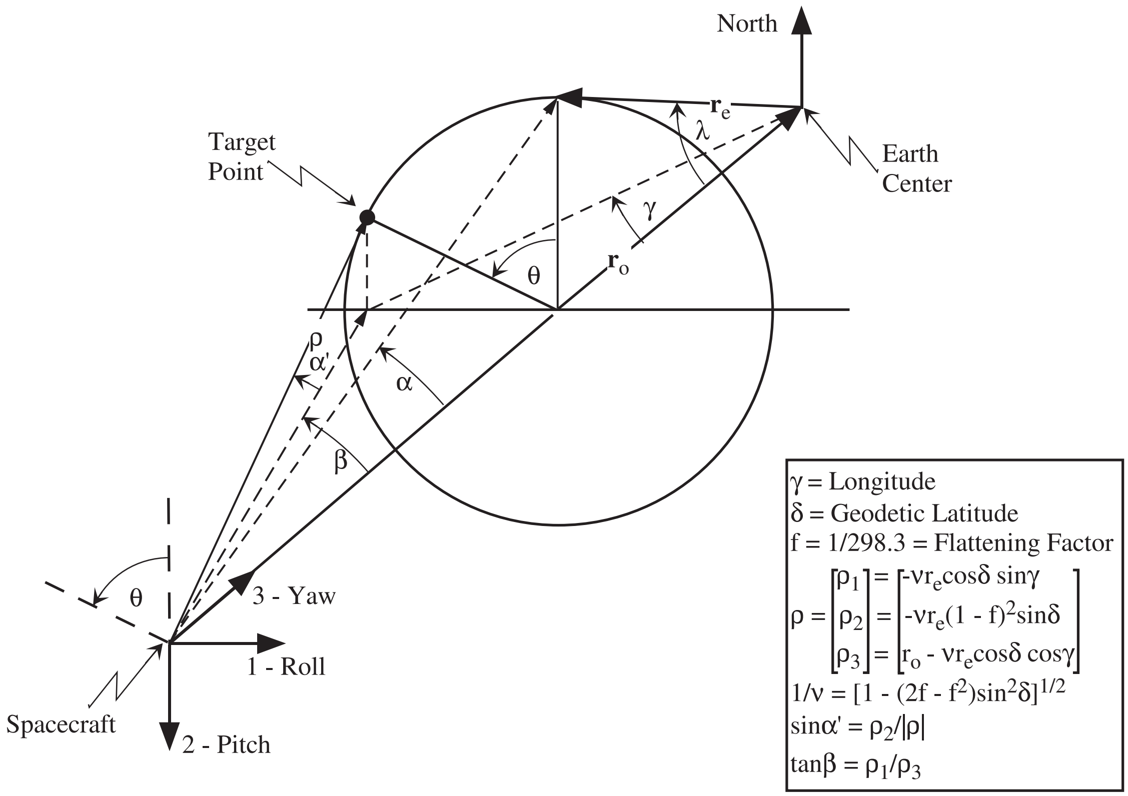

$$\lambda = \mathrm{Sin}^{-1}[(r_o/r_e)\sin\alpha] - \alpha \quad ;\alpha = \mathrm{Tan}^{-1}[r_e\sin\lambda/(r_o - r_e\cos\lambda)]$$
$$\theta = \mathrm{Tan}^{-1}[\sin\gamma/\tan\delta] \quad ;\lambda = \mathrm{Sin}^{-1}\{[1 - (\cos\delta\cos\gamma)^2]^{1/2}\} = \mathrm{Cos}^{-1}[\cos\delta\cos\gamma]$$
$$\delta = \mathrm{Sin}^{-1}[\cos\theta\sin\lambda] \quad ;\gamma = \mathrm{Sin}^{-1}\{\sin\theta\sin\lambda/[1 - (\cos\theta\sin\lambda)^2]^{1/2}\} = \mathrm{Tan}^{-1}[\sin\theta\tan\lambda]$$
$$\theta = \mathrm{Tan}^{-1}[\sin\beta/\tan\alpha'] \quad ;\alpha = \mathrm{Sin}^{-1}\{[1 - (\cos\alpha'\cos\beta)^2]^{1/2}\}$$
$$\alpha' = \mathrm{Sin}^{-1}[\cos\theta\sin\alpha] \quad ;\beta = \mathrm{Sin}^{-1}\{\sin\theta\sin\alpha/[1 - (\cos\theta\sin\alpha)^2]^{1/2}\}$$

Figure 12.3 Spacecraft-Earth Pointing Geometry.

13.0 Four XIPS Orbit Maintenance

The following is the writer's description of the ion thruster mounting geometry and operational plan as defined and patented by Bernie Anzel. The scheme will of course work with any thrusters, but its inefficiency is more tolerable with ion thrusters. One suitable description is to note four XIPS (xenon ion propulsion system) thrusters are mounted with their thrust vectors along the four corner edges of a pyramid whose apex is at the spacecraft center-of-mass and whose base is normal to the nadir line, or the yaw axis. The described geometry is depicted by Figure 1. Each of the thrusters has force components along all three spacecraft axes, roll, pitch, and yaw. Taken as pairs, one pair (say the North pair, $\mathbf{F}_1$ and $\mathbf{F}_4$) has positive orbit normal (pitch) thrust, and opposing tangential (roll) components of thrust. The second pair (South pair $\mathbf{F}_2$ and $\mathbf{F}_3$) has negative pitch thrust and opposing roll. All four thrusters have radial (yaw) thrust with the same sign, although the sign does not matter.

There are fundamentally three orbit perturbation effects, each described briefly elsewhere in this document, to be corrected in geosynchronous orbits: 1) inclination due to sun and moon gravity, 2) eccentricity due to solar radiation acceleration, and 3) longitude drift or period error due to earth's gravitational triaxiality. During any one orbit the two South pointing thrusters will be fired for an interval centered at the ascending node of the orbit and the North pointing thrusters will be fired for an interval about the descending node, such that their respective orbit normal accelerations remove orbit inclination. One way to compensate for solar acceleration is insertion of a radial velocity increment outward at noon or inward at midnight. Alternatively, eccentricity may be corrected by two tangential maneuvers, in opposite directions with respect to orbit velocity, respectively at dawn and dusk. The former will be employed when noon/midnight is near the line of nodes at 90^{o} right ascension (solstices) and the latter when the line of nodes is near dawn/dusk (equinoxes). Compensation for triaxiality requires tangential impulses in the same direction with respect to orbit velocity at two orbit positions separated by 180^{o}, but not fixed to any particular true anomaly or inertial orientation, hence they can be applied at the nodes in conjunction with inclination control. From the preceding we conclude that at any time of year the orbit maintenance corrections can be effected by the application the correct three dimensional velocity increment at the two nodes. This may be accomplished by firing the South thrusting pair, $\mathbf{F}_1$ and $\mathbf{F}_4$ at the ascending node, and the North thrusting pair at the descending node. The total firing time determines the inclination correction, the differential in the sum of firing times on the two sides of the orbit determine a net radial velocity increment, and a differential in firing time of the two individual thrusters at either or both nodes produces one or two tangential impulses in either desired direction.

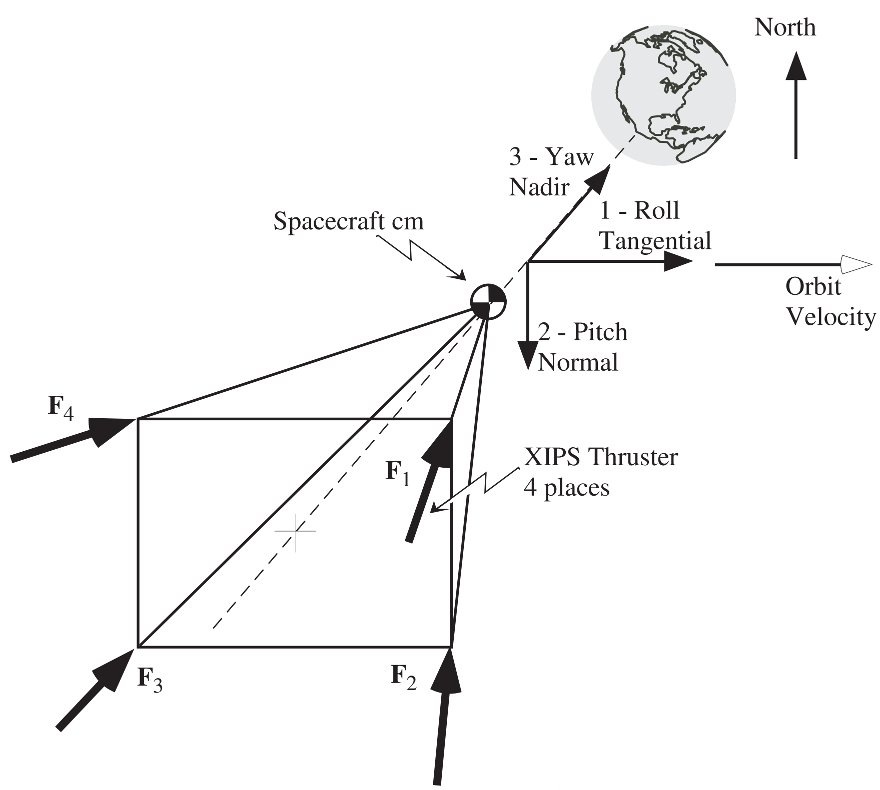

Figure 13.1 Four XIPS Thruster Mounting Geometry.

We remark that the Hughes Galaxy on which XIPS are first being flown has thruster pairs $\mathbf{F}_1$, $\mathbf{F}_4$ and $\mathbf{F}_2$, $\mathbf{F}_3$ essentially in the pitch-yaw plane so they do not provide for a tangential velocity increment. As a result, they are used only to control inclination and the component of eccentricity that is radial at the line of nodes. i.e., the "solstice" component. Triaxiality and the "equinox" component of eccentricity are controlled with chemical thrusters.

If a thruster fails a new degraded operational scenario is introduced. For descriptive purposes say that $\mathbf{F}_4$ fails. Then individual thrusters $\mathbf{F}_1$ and $\mathbf{F}_3$ will be used respectively at the ascending and descending nodes with a time duration to give the required inclination correction and a time differential to produce the necessary tangential velocity increment. The two firings may induce an unwanted radial velocity increment so subsequent eccentricity control is performed by firing $\mathbf{F}_1$ and $\mathbf{F}_3$ for equal time simultaneously, or closely in sequence if simultaneous firing is precluded by the failure, at a point approximately 90^o of true anomaly from the node.

Let the two burns be identified by superscripts a and b, and let F_i^j denote the force component of thruster i along axis j, Δt_i denote the burn duration of thruster i, etc. Then the incremental velocities are

$$\Delta V_n = |F_1^2|\Delta t_1 + |F_2^2|\Delta t_2 + |F_3^2|\Delta t_3 + |F_4^2|\Delta t_4 = \sum |F_i^2|\Delta t_i$$

$$\Delta V_r = \{F_1^3\Delta t_1 + F_4^3\Delta t_4\} - \{F_2^3\Delta t_2 + F_3^3\Delta t_3\}$$

$$\Delta V_t^a = F_1^1\Delta t_1 + F_4^1\Delta t_4$$

$$\Delta V_t^b = F_2^1\Delta t_2 + F_3^1\Delta t_3$$

and in matrix format

$$\begin{bmatrix} \Delta V_n \\ \Delta V_r \\ \Delta V_t^a \\ \Delta V_t^b \end{bmatrix} = \begin{bmatrix} F_1^2 & F_2^2 & F_3^2 & F_4^2 \\ F_1^3 & -F_2^3 & -F_3^3 & F_4^3 \\ F_1^1 & 0 & 0 & F_4^1 \\ 0 & F_2^1 & F_3^1 & 0 \end{bmatrix} \begin{bmatrix} \Delta t_1 \\ \Delta t_2 \\ \Delta t_3 \\ \Delta t_4 \end{bmatrix} .$$

Hence, given the desired velocities it is simple to solve for the firing time. Of course this does not account for the practical realizability of the firing times, e.g., negative values.

It is also possible to displace the thrusters slightly from the cm and dump momentum in the same maneuver. Such displacements will alter the F_i^j slightly and the delivered ΔV. Ultimately, the non-linear problem should be formulated so that a simultaneous solution is obtained for the ΔV and Δh equations for the firing times and the thrust alignment parameters.

Obsidian

Here consider some quantitative values for the Obsidian spacecraft. Using an average daily inclination velocity increment of $\Delta V_n = 150/365.25 = 0.41$ ft/sec, 13 cm, F = 0.004 lb thrusters with a 45^o cant and a 5000 lb spacecraft the sum of daily firing times is

$$\sum_i \Delta t_i = \{m/[(\sin\theta_c)F]\}\Delta V_n = (5000\,\text{lb}/32.2\,\text{ft/sec}^2)/[2\sin 45^o(0.004\,\text{lb})]\}0.41\,\text{ft/sec} = 315\,\text{min} = 6.25\,\text{hrs} .$$

The actual thrusting time will be closer to half this value because when inclination control dominates (tangential components small) two thrusters will usually be on simultaneously. Further, we evaluate the momentum dumping capability. Assume a $\pm 10^o$ range gimbal on the thruster and a 6 ft displacement from the cm. Then the maximum momentum increment is approximately

$$\Delta h_1 = 2(\sin 10^o)6\,\text{ft}(0.004\,\text{lb})[3600(6.25/2)\,\text{sec}] = 94\,\text{ft}-\text{lb}-\text{sec} .$$

Since we expect 1 to 5 ft-lb-sec per day maximum secular roll-yaw momentum and 10 to 20 ft-lb-sec per day of secular pitch momentum, it should not be difficult to dump with the XIPS thrusters.

References:

1. Pedro Escobal, *Methods of Orbit Determination*, John Wiley & Sons, New York, 1965.
2. SCG820092R, *Orbital Dynamics for Synchronous Missions*, B. M. Anzel, March 1982.
3. James R. Wertz, (ed), *Spacecraft Attitude Determination and Control*, D. Reidel, Boston, Mass., 1978.
4. Pocha, J. J., *An Introduction to Mission Design for Geostationary Satellites*, D. Reidel, Boston, Mass., 1987.
5. R. H. Frick and T. B. Garber, "Perturbations of a Synchronous Satellite Due to Triaxiality of the Earth," *Journal of Aerospace Sciences*, September 1962, pp. 1105-1111 and 1144.
6. R. E. Balsam and B. M. Anzel, "Determination of the Pacific Equilibrium Point for a stationary Orbit," *Journal of Spacecraft and Rockets*, No. 4, 1967, pp. 1289-1294.
7. IDC 2281/26, "Motion of the Orbital Plane of Near-Stationary Satellites," R. E. Balsam, March 31, 1966.
8. IDC 2881/3, "Derivation of Equation of Time Approximation," M. Neufeld, October 1, 1965.
9. U. S. Patent 5,443,231, B. M. Anzel, *Method and Apparatus For a Satellite Stationkeeping*, August 22, 1995.
10. Pedro Escobal, *Methods of Astrodynamics*, John Wiley & Sons,
11. Roger R. Bates, Donald D. Mueller & Jerry E. White, *Fundamentals of Astrodynamics*, Dover Publications, Inc., NY, 1971.New York, 1968.
12. Bruce Shuman, Comprehensive library, Malib, of spacecraft mission design and analysis software in fortran.